9-1-2015

EXPERIMENTAL STUDIES OF THE CHEMICAL EFFECTS OF ZINC-BEARING MATERIALS FOLLOWING A LOSS-OF-COOLANT ACCIDENT IN A PRESSURIZED WATER REACTOR

David Allan Pease

David Allan Pease

Candidate

Department of Nuclear Engineering

Department

This thesis is approved, and it is acceptable in quality and form for publication:

Approved by the Thesis Committee:

Dr. Edward D. Blandford, Chairperson

Dr. Kerry J. Howe

Dr. Robert D. Busch

Dr. Jose M. Cerrato

EXPERIMENTAL STUDIES OF THE CHEMICAL EFFECTS OF ZINC-BEARING MATERIALS FOLLOWING A LOSS-OF-COOLANT ACCIDENT IN A PRESSURIZED WATER REACTOR

BY

DAVID ALLAN PEASE

B.S. PHYSICS, UTAH VALLEY UNIVERSITY, 2013
B.S. CHEMISTRY, UTAH VALLEY UNIVERSITY, 2013

THESIS

Submitted in Partial Fulfillment of the
Requirements for the Degree of

Master of Science

Nuclear Engineering

The University of New Mexico
Albuquerque, New Mexico

May, 2015

DEDICATION

I would first like to dedicate this thesis to my wife, Melissa, who has always encouraged my academic and professional dreams, and for making my education a priority throughout our marriage. I also dedicate this to my family; with interests and careers as varied as elementary education, emergency first-response, comparative literature, architecture, aviation, and accounting, I consider myself very fortunate to have the support of such a loving and diverse family. I finally dedicate this to the six best furry friends I could ask for—Margi, Gussi, Sauri, Tip, Zip, and Pip—who always bring excitement and joy into my life and the lives of those closest to me.

ACKNOWLEDGEMENTS

I would like to thank my laboratory team—James, Sterling, Jamison, Chris and Lexy—for the support that I have received in all aspects of the experimental work. I would like to thank Dr. LaBrier and Lana for their contributions; without their involvement, this body of research would not have grown into what it is today.

I would like to thank Dr. Blandford for providing me with the opportunity to join the UNM GSI-191 research group and for helping me grow as an independent research engineer and scientist. I would like to thank Dr. Howe for making time to discuss new developments in my research, and always being a source of inspiration and thought-provoking questions.

This research would not have been possible without the support of Southern Nuclear Operating Company Vogtle Electric Generating Plant.

ABSTRACT

Generic Safety Issue-191 (GSI-191) was developed by the United States Nuclear Regulatory Commission (U.S. NRC) to assess the effect of debris loading on pressurized water reactor (PWR) emergency core cooling systems (ECCS) sump strainers during a Loss-of-Coolant Accident (LOCA). Potential contributors to the debris loading include latent dirt, fiberglass insulation, paints, epoxies, and chemical products which form when containment surfaces interact with the released reactor coolant. Chemical effects experiments have been completed to assess the potential debris loading contributions of zinc-bearing materials found in the containment building. Zinc-bearing materials in containment include galvanized steel and inorganic zinc-coated steel (IOZ).

This research has shown that zinc interacts with post-LOCA containment chemistry to form chemical products including zinc oxide and zinc phosphate, which may become available to transport to the ECCS sump strainers and impair safe operations. A large amount of zinc release from the dissolution of zinc-bearing surfaces in acidic conditions is shown (up to 120 mg/L), and the retrograde solubility of zinc is confirmed, with strong implications during the cool-down phase of a post-LOCA scenario. Zinc phosphate is shown to form rapidly in the chemical environment within post-LOCA containment following the dissolution of containment buffer trisodium phosphate (TSP), and controls the solubility of dissolved zinc (to less than 1 mg/L). The reduction of dissolved zinc concentration from 120 mg/L to less than 1 mg/L through zinc phosphate precipitation may significantly contribute to the debris loading on ECCS sump strainers and increase sump head loss.

Zinc is shown to reduce the corrosion and release from aluminum and iron sources in containment, cathodically shielding those sources and reducing the chemical products of iron and aluminum that contribute to the loading on the ECCS sump strainer. Therefore, while a high release of zinc and the resulting zinc-product precipitation is not favorable for ECCS functionality, zinc is shown to reduce the possible contributions of aluminum corrosion products.

TABLE OF CONTENTS

LIST OF FIGURES XII

LIST OF TABLES XV

CHAPTER 1: INTRODUCTION 1

CHAPTER 2: ZINC PHENOMENOLOGY AND BACKGROUND 6

2.1 Zinc Phenomenology 6

2.1.1 Dissolution and Electrochemistry of Zinc 7

2.1.1.1 Oxidation of Zinc in an Aqueous Environment 8

2.1.1.2 Oxidation of Zinc through the Galvanic Protection of Iron 10

2.1.1.3 Summary of Dissolution and Electrochemical Phenomenology 11

2.1.2 Precipitation and Thermodynamic Equilibrium Simulations 12

2.1.2.1 Thermodynamic Modelling Software Inputs 12

2.1.2.2 Simulations for Zinc Precipitation in Unbuffered Coolant 14

2.1.2.3 Simulations for Zinc Precipitation in Unbuffered Coolant 17

2.1.2.4 Simulation Conclusions and Limitations of the Simulations 19

2.2 Historical Work and Literature Review 21

2.2.1 Integrated Chemical Effects Tests and Chemical Head Loss Experiment 21

2.2.2 Other GSI-191 Efforts 27

2.2.3 Non-GSI-191 Efforts 29

2.2.3.1 Dissolution 29

2.2.3.2 Complexation 32

2.2.3.3 Phosphating 33

CHAPTER 3: MATERIALS AND METHODOLOGY 37

3.1 Experimental Design 37

3.1.1 Testing Solution 38

3.1.2 Zinc Sources 39

3.1.3 Physical Testing Environment 40

3.1.4 Post-Testing Analyses 41

3.1.5 Complete Testing Matrix 42

3.1.5.1 Theme 1 Tests: Prompt Release 42

3.1.5.2 Theme 2 Tests: Zinc Phosphate Solubility and Precipitation 43

3.1.5.3 Theme 3 Tests: Zinc Phosphate Formation with TSP Addition after Prompt Release Phase 45

3.1.5.4 Theme 4 Tests: Zinc and Aluminum Integrated Effects 46

3.1.5.5 Theme 5 Tests: Chemical Descaling Methods to Quantify Scale Layer 47

CHAPTER 4: EXPERIMENTAL RESULTS AND ANALYSIS 49

4.1 Theme 1: Prompt Release 49

4.1.1 Theme 1 Zinc Release Analysis 49

4.1.2 Theme 1 Turbidity Analysis 57

4.1.3 Theme 1 pH Analysis 59

4.1.4 Theme 1 Surface Composition Analysis 60

4.1.5 Theme 1 Qualitative Imaging Analysis 63

4.2 Theme 2: Zinc Phosphate Solubility and Precipitation 67

4.2.1 Theme 2 Zinc Release Analysis 68

4.2.2 Theme 2 Turbidity Analysis 75

4.2.3 Theme 2 pH Analysis 78

4.2.4 Theme 2 Surface Composition Analysis 79

4.2.5 Theme 2 Qualitative Imaging Analysis 83

4.3 Theme 3: Zinc Phosphate Formation with TSP Addition after Prompt Release Phase 85

4.3.1 Theme 3 Zinc Release Analysis 87

4.3.2 Theme 3 Turbidity Analysis 96

4.3.3 Theme 3 pH Analysis 98

4.3.4 Theme 3 surface Composition Analysis.....99

4.3.5 Theme 3 Qualitative Imaging Analysis 104

4.4 Theme 4: Zinc and Aluminum Integrated Effects.....108

4.4.1 Theme 4 Zinc and Aluminum Release Analysis 109

4.4.2 Theme 4 pH Analysis 111

4.5 Theme 5: Chemical Descaling Methods to Quantify Scale Layer 112

4.5.1 Series 5.1 (Ammonium Persulfate) Analysis.....114

4.5.2 Series 5.2 (Ammonium Chloride) Analysis.....116

4.5.3 Series 5.3 (Ammonium Acetate) Analysis.....118

4.5.4 Series 5.4 (Hydrochloric Acid) Analysis.....120

CHAPTER 5: DISCUSSION AND CONCLUSIONS 122

5.1 Theme 1 Discussion 122

5.2 Theme 2 Discussion 123

5.3 Theme 3 Discussion 124

5.4 Theme 4 Discussion 125

5.5 Theme 5 Discussion 126

5.6 Conclusions **127**

5.7 Future Work **130**

REFERENCES 131

LIST OF FIGURES

FIGURE 1. ANIMATION OF LOCA, CONTAINMENT SUMPS, AND RWST [2] 2
FIGURE 2. PH RESPONSE TO TSP ADDITION IN 220 MM BORIC ACID SOLUTION 14
FIGURE 3. ZINC PRECIPITATION RESPONSE TO UNBUFFERED SOLUTION 15
FIGURE 4. SATURATION INDICES FOR UNBUFFERED 100 MG/L INITIAL ZINC 16
FIGURE 5. SATURATION INDICES FOR UNBUFFERED 1 MG/L INITIAL ZINC 16
FIGURE 6. ZINC PRECIPITATION IN BUFFERED COOLANT 18
FIGURE 7. ICET TANK [15] 22
FIGURE 8. METAL COUPON RACK FOR THE ICET EXPERIMENTS [16] 23
FIGURE 9. CHLE VERTICAL STRAINER HEAD LOSS COLUMNS [19] 25
FIGURE 10. CHLE T3 ZINC CONCENTRATION FILTERED AND UNFILTERED [14] 26
FIGURE 11. PARTICLE SIZE IN T3 (HAS ZINC) AND T4 (HAS NO ZINC) [14] 26
FIGURE 12. TURBIDITY AND HEAD LOSS RESPONSE IN T3 (HAS ZINC) AND T4 (HAS NO ZINC) [14] 27
FIGURE 13. HOT BATH WITH 1-LITER NALGENE BOTTLES 41
FIGURE 14. PROMPT RELEASE AT 85°C 50
FIGURE 15. PROMPT RELEASE AT 85°C, FIRST FOUR HOURS 51
FIGURE 16. SATURATION LIMIT RESPONSE TO TEMPERATURE WITH GALVANIZED STEEL 52
FIGURE 17. THEME 1 IRON RELEASE 56
FIGURE 18. SOLUTION TURBIDITY FOR SERIES 1.3, 1.4, 1.5, AND 1.6 57
FIGURE 19. THEME 1 TURBIDITY TO CONCENTRATION RATIO 58
FIGURE 20. THEME 1 TESTING SOLUTION FINAL PH 59
FIGURE 21. SERIES 1.1 SEM IMAGES, PART 1/2 64
FIGURE 22. SERIES 1.1 SEM IMAGES, PART 2/2 64
FIGURE 23. SERIES 1.6 SEM IMAGES, PART 1/3 65
FIGURE 24. SERIES 1.6 SEM IMAGES, PART 2/3 66

FIGURE 25. SERIES 1.6 SEM IMAGES, PART 3/3 66
FIGURE 26. SERIES 2.1 ZINC RELEASE 69
FIGURE 27. SERIES 2.2 ZINC RELEASE 70
FIGURE 28. SERIES 2.3 ZINC RELEASE 72
FIGURE 29. SERIES 2.4 AND 2.5 ZINC RELEASE 73
FIGURE 30. SERIES 2.6 AND 2.7 ZINC RELEASE 74
FIGURE 31. THEME 2 SERIES ZINC RELEASE 75
FIGURE 32. THEME 2 TURBIDITY 76
FIGURE 33. THEME 2 TURBIDITY TO CONCENTRATION RATIO 77
FIGURE 34. THEME 2 FINAL PH MEASUREMENTS 78
FIGURE 35. SERIES 2.1 (PURE ZINC) EDS SPECTRAL RESULTS 81
FIGURE 36. SERIES 2.3 (PURE ZINC) EDS SPECTRAL RESULTS 81
FIGURE 37. SERIES 2.6 (GALVANIZED STEEL) EDS SPECTRAL RESULTS 82
FIGURE 38. SERIES 2.1 SEM IMAGES 84
FIGURE 39. SERIES 2.3 SEM IMAGES 84
FIGURE 40. SERIES 3.1 ZINC RELEASE 87
FIGURE 41. SERIES 3.2 ZINC RELEASE 88
FIGURE 42. SERIES 3.3 AND 3.4 (85°C) ZINC CONCENTRATION 91
FIGURE 43. SERIES 3.5 AND 3.6 (65°C) ZINC CONCENTRATION 93
FIGURE 44. SERIES 3.7 AND 3.8 (45°C) ZINC CONCENTRATION 94
FIGURE 45. SERIES 3.9 AND 3.10 (25°C) ZINC CONCENTRATION 95
FIGURE 46. THEME 3 TURBIDITY MEASUREMENTS 97
FIGURE 47. SERIES 3.1 (PURE ZINC) EDS SPECTRAL RESULTS IN ATOMIC PERCENTAGE (%) WITH TESTING DURATION AND TSP CONCENTRATION IN MILLIMOLAR 99
FIGURE 48. SERIES 3.2 (PURE ZINC) EDS SPECTRAL RESULTS IN ATOMIC PERCENTAGE (%) WITH TESTING DURATION AND TSP CONCENTRATION IN MILLIMOLAR 100
FIGURE 49. SERIES 3.1 SEM IMAGES 104

FIGURE 50. SERIES 3.2 SEM IMAGES 105
FIGURE 51. SERIES 3.9 SEM IMAGES, PART 1/3 106
FIGURE 52. SERIES 3.9 SEM IMAGES, PART 2/3 107
FIGURE 53. SERIES 3.9 SEM IMAGES, PART 3/3 107
FIGURE 54. SERIES 4.1 ZINC RELEASE 109
FIGURE 55. SERIES 4.1 ALUMINUM RELEASE 110
FIGURE 56. THEME 4 FINAL PH 112
FIGURE 57. THEME 5 BASELINE SEM IMAGES 114
FIGURE 58. SERIES 5.1 SEM IMAGE AFTER DESCALING WITH AMMONIUM PERSULFATE 115
FIGURE 59. SERIES 5.2 SEM IMAGE AFTER DESCALING WITH AMMONIUM CHLORIDE 117
FIGURE 60. SERIES 5.3 SEM IMAGE AFTER DESCALING WITH AMMONIUM ACETATE 119
FIGURE 61. SERIES 5.4 SEM IMAGE AFTER DESCALING WITH 1% HYDROCHLORIC ACID 121

LIST OF TABLES

TABLE 1.ZINC-BASED CHEMICAL PRECIPITATES CONSIDERED 13

TABLE 2. SUMMARY OF PRECIPITATION CONDITIONS IN UNBUFFERED SIMULATIONS 17

TABLE 3. SOLUBILITY PRODUCT REACTION CONSTANTS FOR ZINC COMPOUNDS 34

TABLE 4. THEME 1 TESTING MATRIX 49

TABLE 5. SERIES 1.3-1.6 SUMMARY OF DISSOLVED ZINC CONCENTRATION MEASUREMENTS 53

TABLE 6. SUMMARY OF TURBIDITY-TO-CONCENTRATION RATIO IN SERIES 1.3 THROUGH 1.6 59

TABLE 7. SERIES 1.3 (GALVANIZED STEEL) EDS SPECTRAL RESULTS IN ATOMIC PERCENTAGE (%) 61

TABLE 8. SERIES 1.4 (GALVANIZED STEEL) EDS SPECTRAL RESULTS IN ATOMIC PERCENTAGE (%) 61

TABLE 9. SERIES 1.5 (GALVANIZED STEEL) EDS SPECTRAL RESULTS IN ATOMIC PERCENTAGE (%) 62

TABLE 10. SERIES 1.6 (GALVANIZED STEEL) EDS SPECTRAL RESULTS IN ATOMIC PERCENTAGE (%) 62

TABLE 11. THEME 2 TESTING MATRIX 68

TABLE 12. SUMMARY OF TURBIDITY-TO-CONCENTRATION RATIO IN SERIES 2.1 AND 2.6 77

TABLE 13. AVAILABLE EDS SPECTRAL RESULTS FOR THEME 2 TESTING 80

TABLE 14. THEME 2 EDS SPECTRAL RESULTS IN ATOMIC PERCENTAGE (%) 80

TABLE 15. THEME 3 TESTING MATRIX 86

TABLE 16. TSP ADDITION TECHNIQUES FOR THEME 3 TESTS 86

TABLE 17. THEME 3 PH MEASUREMENTS AFTER TSP ADDITION 98

TABLE 18. SERIES 3.1 AND 3.2 (PURE ZINC) EDS SPECTRAL RESULTS IN ATOMIC PERCENTAGE (%) 101

TABLE 19. SERIES 3.3 (GALVANIZED STEEL) EDS SPECTRAL RESULTS IN ATOMIC PERCENTAGE (%) 102

TABLE 20. SERIES 3.5 (GALVANIZED STEEL) EDS SPECTRAL RESULTS IN ATOMIC PERCENTAGE (%) 102

TABLE 21. SERIES 3.7 (GALVANIZED STEEL) EDS SPECTRAL RESULTS IN ATOMIC PERCENTAGE (%) 103

TABLE 22. SERIES 3.9 (GALVANIZED STEEL) EDS SPECTRAL RESULTS IN ATOMIC PERCENTAGE (%) 103

TABLE 23. SERIES 4.1 ALUMINUM CONCENTRATION AND BASELINE COMPARISON 111

TABLE 24. THEME 5 TESTING MATRIX AND DESCALING CHEMICAL COMPOSITION 113

TABLE 25. SERIES 5.1 TOTAL MASS LOST THROUGH DESCALING AND ZINC LOST THROUGH DESCALING .114

TABLE 26. SERIES 5.1 (PURE ZINC) EDS SPECTRAL RESULTS IN ATOMIC PERCENTAGE (%).....115

TABLE 27. SERIES 5.2 TOTAL MASS LOST THROUGH DESCALING AND ZINC LOST THROUGH DESCALING .116

TABLE 28. SERIES 5.2 (PURE ZINC) EDS SPECTRAL RESULTS IN ATOMIC PERCENTAGE (%).....117

TABLE 29. SERIES 5.3 TOTAL MASS LOST THROUGH DESCALING AND ZINC LOST THROUGH DESCALING .118

TABLE 30. SERIES 5.3 (PURE ZINC) EDS SPECTRAL RESULTS IN ATOMIC PERCENTAGE (%).....119

TABLE 31. SERIES 5.4 (PURE ZINC) TOTAL MASS LOST THROUGH DESCALING AND ZINC LOST THROUGH DESCALING.....120

TABLE 32. SERIES 5.4 EDS SPECTRAL RESULTS IN ATOMIC PERCENTAGE (%) 121

CHAPTER 1: INTRODUCTION

Modern nuclear reactors are highly complex systems with numerous functions and components. As with any complex system, multiple points of failure are inherent to the infrastructure of the nuclear industry. Accidents at Chernobyl (1986) and more recently at Fukushima Daiichi (2011) have shown that, even with sophisticated monitoring and advanced engineering, not all points of failure may be identified before an accident-triggering effect causes a failure which threatens the safety of the surrounding environment and inhabitants. The United States Nuclear Regulatory Commission (NRC) was established in 1975; one function of the U.S. NRC is to ensure that nuclear facilities observe guidelines to maintain the safety and health of the public, operators, and environment during normal operations and in the event of an accident. A Loss-of Coolant Accident (LOCA) is one accident type that has received attention from the NRC.

A LOCA is an event in which primary coolant pipes or coolant storage units are compromised, releasing the coolant into containment. Coolant that is lost during a pipe break transports throughout containment, until arriving at the Emergency Core Cooling Systems (ECCS) sump pump, which recycles the coolant back through the reactor core to mitigate the effects of coolant loss and to prevent core damage. Until the ECCS sumps are activated and circulate the coolant back into the reactor, injection pumps supplied by the refueling water storage tank (RWST) are used to add supplementary coolant to prevent core damage [1].

Figure 1. Animation of LOCA, containment sumps, and RWST [2]

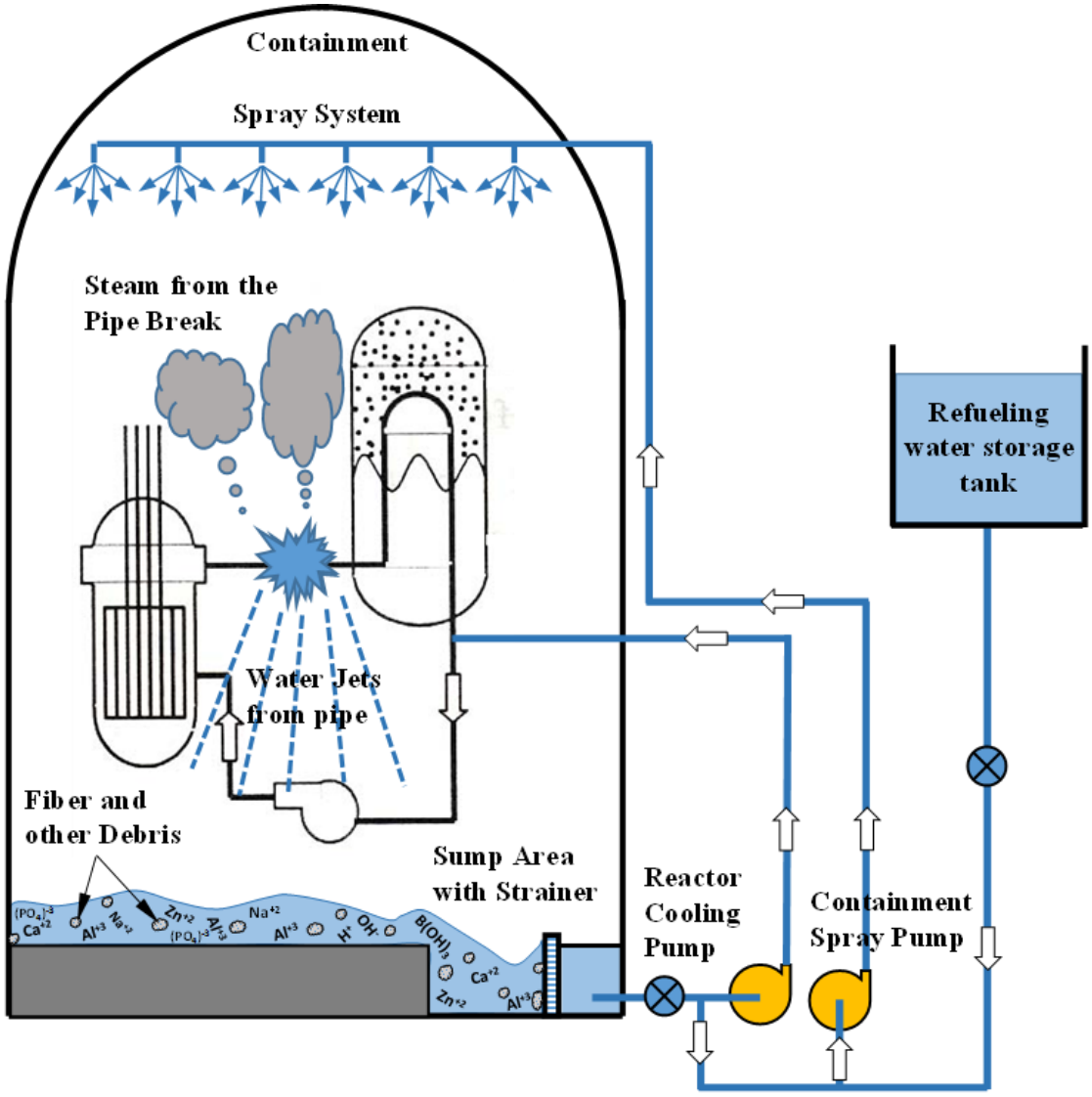

In 1979, the U.S. NRC developed Unresolved Safety Issue (USI) A-43 to address adequate coolant water availability following the events of a LOCA, and the ECCS sump functionality [3]. This study required that the recirculated water must be free of LOCA-generated debris and air ingestion to ensure that the recirculation capabilities are not degraded. USI A-43 was formally resolved in 1985 [4] [5]. A few events in the following

decade caused a re-evaluation of coolant availability and sump performance during a LOCA.

In 1992, the Swedish boiling water reactor (BWR) at Barsebäck Nuclear Power Plant Unit 2 experienced an event in which two of the containment vessel spray systems (CVSS) were plugged by mineral wool insulation from a pilot-operated relief valve only 70 minutes into the event [6]. In early 1993, the Perry Nuclear Power Plant experienced two events involving ECCS strainer clogging [7]. Debris in the suppression pools triggered both cases of strainer clogging; in the second event, corrosion products collected on accumulated glass fiber debris, and further hindered flow through the ECCS strainers. In 1995, Limerick Unit 1 experienced debris accumulation on suction strainers of the ECCS pumps [8]. In response to these events, the NRC issued Generic Safety Issue (GSI)-191: "Assessment of Debris Accumulation on PWR Sump Performance". It was found that the problem is mitigated by increasing the total exposed surface area of the sump strainers [9].

In the early 2000s, the NRC Office of Nuclear Regulatory Research Division of Fuel, Engineering and Radiological Research funded Los Alamos National Laboratory (LANL) to explore chemical effects and corrosion in a post-LOCA environment. In coordination with The University of New Mexico (UNM), LANL developed the Integrated Chemical Effects Test (ICET) project. A series of large-scale chemical tests with varying chemistry representative of several PWRs were conducted. These tests simulated the corrosive environment of a post-LOCA scenario with plant-specific chemicals, surfaces, and temperatures [10]. The research presented herein serves as additional confirmatory research for GSI-191.

This research has been developed to study the chemical effects of zinc-bearing materials and interpret their potential effects as they relate to the resolution of GSI-191. Batch tests with representative samples of zinc-bearing materials and Vogtle Electric Generating Plant (Vogtle)-specific LOCA chemical and physical conditions were performed. Zinc-bearing materials found in containment include galvanized steel gratings and untopcoated zinc-coated surfaces, such as inorganic zinc-coated steel (IOZ). Zinc-bearing materials tested include hot-dipped galvanized steel, IOZ, and pure zinc. Three phases of post-LOCA events have been considered: (1) early-stage LOCA, where no chemical buffering has been introduced to the coolant; (2) the transition-stage of the post-LOCA chemical environment, where zinc-bearing sources transition from exposure with coolant exclusively to when chemical buffering has been introduced to the coolant, thereby neutralizing its pH and reducing its corrosivity; and (3) middle- to late-stage post-LOCA, where chemical buffering is present, and the ECCS recirculation ensures well-mixed containment chemistry.

This research will demonstrate whether zinc-bearing materials found in containment warrant further consideration in sump performance concerns based on solubility, material release correlations, and precipitate formation. An accurate quantification of (1) release from zinc and (2) zinc corrosion product precipitation will conclusively determine whether zinc-bearing materials are capable of destructive interactions with ECCS operations. This will inform whether zinc-bearing materials in containment require additional attention in the resolution of GSI-191.

Several analytical and predictive techniques have been used to quantify the threat that zinc-based chemical products pose on ECCS sump performance. Techniques to

validate conclusions include equilibrium thermodynamic simulation, aqueous concentration measurement by inductively-coupled plasma optical emission spectroscopy (ICP-OES, or "ICP"), solution turbidity measurements for qualitative aqueous corrosion product suspension, surface analyses such as scanning electron microscopy (SEM) and Energy-Dispersive X-Ray Spectroscopy (EDS), and chemical responses such as pH shifts and electrochemical shielding. Limitations of this research primarily pertain to the experimental scale; all experiments are performed as 500mL aqueous batch tests using 1-inch square metallic surrogates.

CHAPTER 2: ZINC PHENOMENOLOGY AND BACKGROUND

2.1 Zinc Phenomenology

An aqueous chemical environment consisting of nuclear reactor coolant is a complex system. Several chemicals are present in varying amounts and concentrations, and decoupling chemical effects and attributing observations to specific chemicals or conditions is a challenge. It is necessary to establish a sound understanding of phenomenology of the chemical effects to aid in the attribution of specific effects to individual chemicals.

The primary goal of this research is to establish the credibility of the threat that zinc sources contribute to ECCS operation. Three primary phenomenologies will be examined, and will be applied to the body of research presented herein to assess the contributions of zinc to safe operations in a post-LOCA environment.

These phenomenologies include: (1) dissolution, or how readily zinc is introduced to the aqueous environment following a LOCA; (2) electrochemistry, or the interaction of zinc with other chemical species, including dissolved gasses, the base material onto which zinc or zinc-based coatings are applied (such as iron), and aqueous chemical species with electrochemical potentials which favor redox reactions with zinc; (3) the precipitation of zinc species, and how they may contribute to debris accumulation on the ECCS sump strainer's debris bed for head loss; and in addition to these phenomenologies, (4) thermodynamic equilibrium software, which will predict the favored chemical conditions

of the system and to aid in the resolution of competing factors such as dissolution and precipitation.

It is necessary to establish fundamental terminology to describe the state in which zinc is found. There are three classifications that are used, each with a unique and distinct meaning. These classifications include: (1) **metallic** zinc, or zinc which is in its original electronic configuration as a galvanic surface or in a corrosion resistant primer; (2) **dissolved** zinc, which describes zinc that has experienced oxidation to the divalent state, and is present as a solute in and aqueous solution, either as divalent zinc alone, or in aqueous chemical products; and (3) zinc **precipitate**, which is a chemical product of zinc and either one or multiple other chemicals and compounds, and which is not dissolved in solution, and has formed a solid compound that may contribute to ECCS sump blockage.

2.1.1 Dissolution and Electrochemistry of Zinc

The process of zinc dissolution is inherently an electrochemical phenomenon. Zinc-coatings, whether as a galvanic coating on steel or a zinc-based primer painted onto a wall, contain zinc in metallic form. Zinc is found neither oxidized nor reduced from a neutral electronic configuration.

There are two mechanisms of zinc dissolution and electrochemistry which are necessary for analysis of this body of research: (1) oxidation of zinc in aqueous environment, requiring the reduction of aqueous or dissolved species; and (2) the galvanic protection of iron.

2.1.1.1 Oxidation of Zinc in an Aqueous Environment

There are two considered mechanisms for zinc oxidation in the aqueous system of reactor coolant: the reduction of dissolved molecular oxygen and the consumption of excess hydronium to form molecular hydrogen.

Dissolved oxygen is present in any aqueous environment which is exposed to a source of oxygen, such as the atmosphere. Nuclear reactor containment buildings are kept sealed, but an inventory of oxygen is still present to supply technicians with breathable air.

The primary reaction that involves the reduction of dissolved oxygen and the oxidation of metallic zinc is shown in Equation 1.

Equation 1. Zinc oxidation with dissolved molecular oxygen

$$2Zn(s) + O_2(aq) \rightarrow 2ZnO(s) \qquad E^\circ > 0 \text{ [11]}$$

The quantity E° is the standard cell potential [11]. This quantity is related to the Gibbs free energy of the chemical reaction, as shown in Equation 2.

Equation 2. Relation of Gibbs free energy and electrochemical cell potential

$$nFE^\circ = -\Delta G^\circ$$
$$where\ n = number\ of\ electrons\ transfered\ in\ the\ electrochemical\ reaction$$
$$and\ F = Faraday's\ constant$$

The Gibbs free energy of the reaction indicates the thermodynamic favorability of a product over the starting reactants. A negative value designates a thermodynamically favorable reaction. Therefore, a positive electrochemical cell potential designates the direction of a thermodynamically favorable reaction.

In Equation 1, the electrochemical cell potential is positive. This shows that the reduction of dissolved molecular oxygen and the oxidation of metallic zinc is favorable. This mechanism is therefore one possible method by which zinc is transformed into divalent zinc from a metallic zinc source.

The second primary reaction for zinc oxidation in an aqueous environment involved the reduction of hydronium to molecular hydrogen. Hydronium content in a solution is typically quantified with the physical property pH, which is a logarithmic representation of hydronium content. A solution is said to have a numerical pH value of less than seven if the hydronium content dominates the hydroxide content; this solution is referred to as acidic.

Nuclear reactor coolant is primarily comprised of dissolved boron in the form of hydrogen borate, or boric acid. Boron is a neutron poison and serves as a chemical shim. In a boric acid aqueous environment, hydronium is readily available, and the solution is acidic. Other chemicals—such as lithium hydroxide—are also present, but are in trace amounts, and are insufficient to reduce the solution's hydronium content adequately to reduce the acidity of the reactor coolant. Lithium is added to alkalize the coolant solution, and is typically present in about 2 mg/L.

The reaction that involves the reduction of hydronium into molecular hydrogen and the oxidation of zinc is shown in Equation 3.

Equation 3. Zinc dissolution in acidic media

$$Zn(s) + 2H^{+}(aq) \rightarrow Zn^{2+}(aq) + H_2(g) \qquad E^{\circ} > 0 \text{ [11]}$$

In Equation 3, the electrochemical cell potential is again positive. This shows that the reduction of hydronium and the oxidation of metallic zinc is favorable. This mechanism is therefore one possible method by which zinc is transformed into divalent zinc from a metallic zinc source.

2.1.1.2 Oxidation of Zinc through the Galvanic Protection of Iron

Zinc is found in containment primary as a coating on steel structural materials as a sacrificial corrosion metal. The dissolution of iron in an acidic environment, such as reactor coolant, is considered in Equation 4.

Equation 4. Iron dissolution in acidic media

$$Fe(s) + 2H^{+}(aq) \rightarrow Fe^{2+}(aq) + H_2(g) \qquad E^{\circ} > 0 \text{ [11]}$$

The electrochemical cell potential of this reaction shows that in an environment with sufficient hydronium content, such as reactor coolant, iron will favorably oxidize to the divalent state.

For zinc to effectively protect steel from oxidation—and ultimately structural failure—the cell potential of metallic zinc with divalent dissolved iron must have a positive cell potential. If Equation 4 is subtracted from Equation 3, the resulting chemical reaction is shown in Equation 5.

Equation 5. Zinc galvanic protection of divalent iron

$$Zn(s) + Fe^{2+}(aq) \rightarrow Fe(s) + Zn^{2+}(aq) \qquad E^{\circ} > 0 \text{ [11]}$$

Equation 5 has shown that if iron begins to oxidize and dissolve, and if metallic zinc is in electrical contact—or able to transfer electrons—with the iron experiencing oxidation, the zinc will favorably oxidize before the iron, thereby galvanically protecting the iron-based steel.

If iron is found in the trivalent form, Equation 6shows that iron is still galvanically protected by metallic zinc.

Equation 6. Zinc galvanic protection of trivalent iron

$$3Zn(s) + 2Fe^{3+}(aq) \rightarrow 2Fe(s) + 3Zn^{2+}(aq) \qquad E^{\circ} > 0 \text{ [11]}$$

2.1.1.3 Summary of Dissolution and Electrochemical Phenomenology

The phenomenologies established in this section has shown that zinc may follow one of three mechanisms to experience oxidation from the metallic form to the divalent state. Dissolved molecular oxygen has a relatively high electrochemical cell potential when combined with metallic zinc, and will preferentially oxidize zinc. An acidic medium is also sufficient to oxidize both zinc and iron. The third mechanism for zinc oxidation is if iron is oxidized while in electrical contact with zinc, in which case iron will remain metallic and zinc will preferentially oxidize.

2.1.2 Precipitation and Thermodynamic Equilibrium Simulations

The previous sections introduced the mechanisms through which zinc may oxidize and dissolve into the aqueous environment in post-LOCA containment. This section will address how oxidized and dissolved zinc may contribute to ECCS sump strainer performance.

The thermodynamic equilibrium modelling package Visual MINTEQ™ [12] has been utilized for aqueous chemistry modelling, including such phenomenology as precipitation and solubility predictions.

2.1.2.1 Thermodynamic Modelling Software Inputs

There are three primary chemical constituents which are present post-LOCA and are considered in these simulations: dissolved zinc, trisodium phosphate (TSP) buffer, and soluble boron in the form of boric acid. TSP buffer was added to these simulations in quantities ranging from 5.58 millimolar to 10 millimolar, while other simulation contain no TSP, to match the experimental design established in Section 3: Materials and Methodology. Dissolved boron is present at 2400 ppm, which is equivalent to 220 millimolar boric acid. The dissolved zinc input is permitted to vary throughout simulations, depending on the expected values for the given initial conditions, which will be provided for each simulation.

With the chemicals listed above, there are seven chemical precipitates in the Visual MINTEQ database for the given aqueous system. These precipitates are detailed in Table 1.

Table 1.Zinc-based chemical precipitates considered

Precipitate	Chemical Composition
Zinc borate	$Zn(BO_2)_2$
Zinc hydroxide (am)	$Zn(OH)_2$
Zinc hydroxide (beta)	$Zn(OH)_2$
Zinc hydroxide (delta)	$Zn(OH)_2$
Zinc hydroxide (epsilon)	$Zn(OH)_2$
Zinc hydroxide (gamma)	$Zn(OH)_2$
Zinc Phosphate	$Zn_3(PO_4)_2{:}4H_2O$

All chemical solutions contain 220 millimolar boric acid. The baseline chemical pH of such as solution is roughly 4.5. Figure 2 shows how the solution pH reacts to the addition of TSP in amounts up to 10 millimolar.

Figure 2. pH response to TSP addition in 220 mM boric acid solution

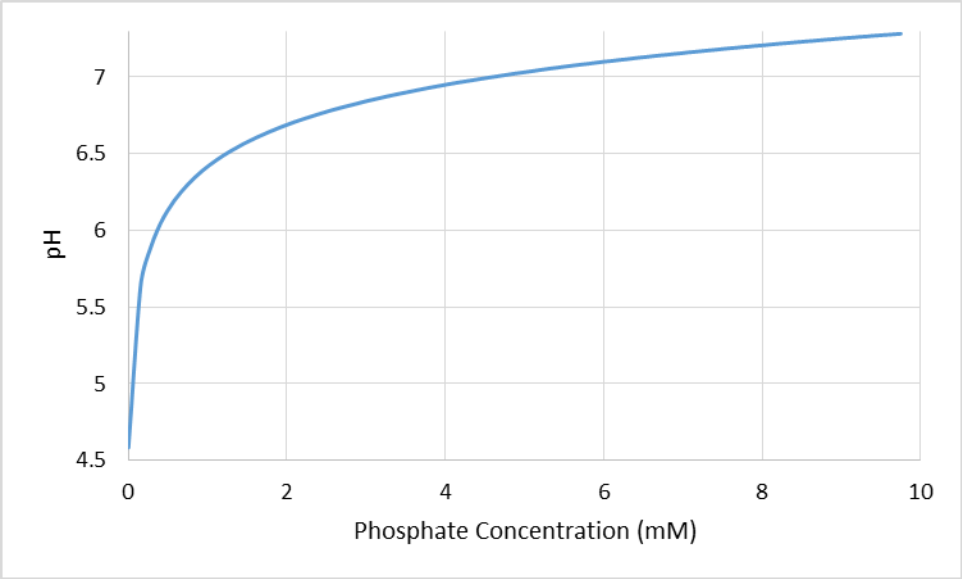

Figure 1 has shown that a solution of boric acid with no TSP added will settle at a pH of roughly 4.5-4.6. A solution containing 5.58 millimolar TSP will have a pH of 7.0-7.1. A solution with 10 millimolar TSP will settle at a pH of roughly 7.3. The addition of TSP has the greatest effect on the pH of the solution when there is little TSP already present.

2.1.2.2 Simulations for Zinc Precipitation in Unbuffered Coolant

Two simulations have been developed to show the solubility and precipitation activity of dissolved zinc in a chemical environment lacking TSP buffer. For these two simulations, arbitrary zinc concentrations have been selected: 100 mg/L and 1 mg/L dissolved zinc. These values are close to limits that have been established in historical efforts [13], [14]. Boric acid was present at 220 millimolar.

Simulations in which the pH was swept through a range of 0.1 to 14 pH units in 0.1 unit increments. The results of these simulations are shown in Figure 3.

Figure 3. Zinc precipitation response to unbuffered solution

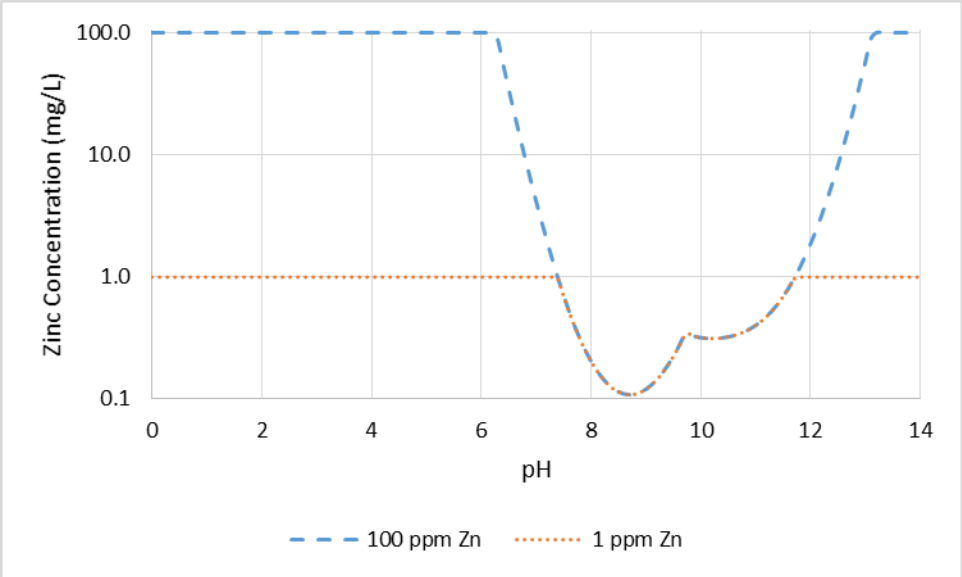

These simulations have shown that zinc precipitation is possible at sufficiently high pH. This plot has also revealed that zinc precipitation occurs in two forms, with the transition between precipitates occurring at a pH of roughly 9.7.

The identity of the chemical precipitates may be determined through saturation index analysis. When a saturation index is negative for a given chemical species, the species is aqueous, and not a precipitate. A saturation index value of zero corresponds to a pH region where precipitation occurs. The saturation index analysis for these two simulations is provided in Figure 4 and Figure 5.

Figure 4. Saturation indices for unbuffered 100 mg/L initial zinc

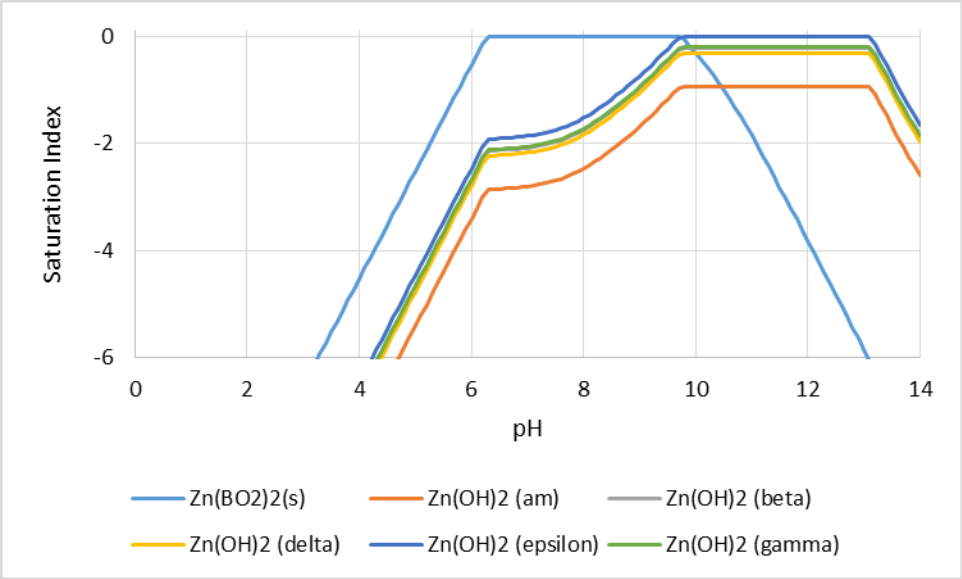

Figure 5. Saturation indices for unbuffered 1 mg/L initial zinc

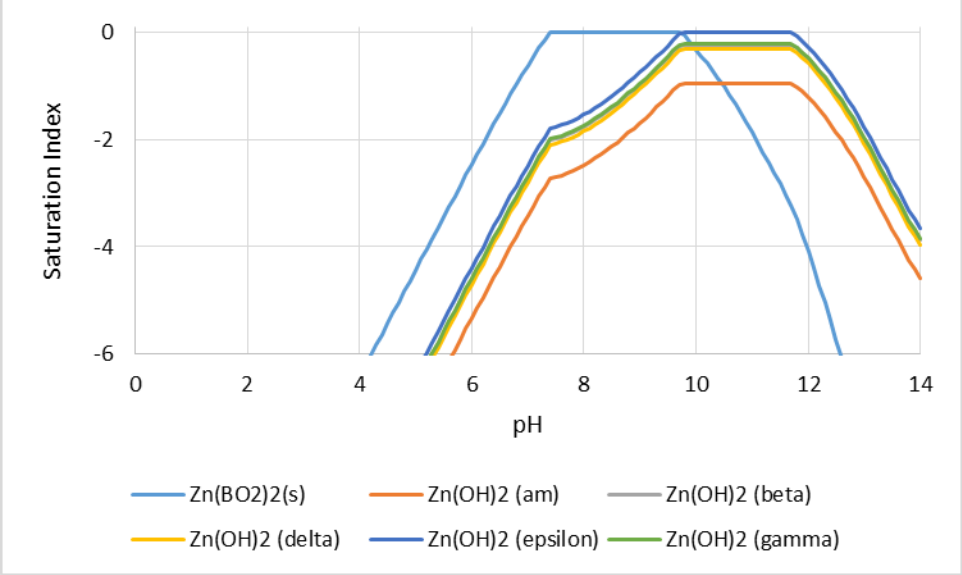

The saturation index analysis has shown that zinc will precipitate in one of two forms, zinc borate and zinc hydroxide.

The minimum necessary pH required for zinc borate precipitation from these simulations is detailed in Table 2. The maximum pH for precipitation is well beyond the range of expected pH values for a post-LOCA environment.

Table 2. Summary of precipitation conditions in unbuffered simulations

Initial Zinc Concentration	Minimum pH For Precipitation Of Zinc Borate	pH for Maximum Precipitation	Minimum Zinc Concentration
100 mg/L	6.3	8.7	0.108 mg/L
1 mg/L	7.4	8.7	0.108 mg/L

This analysis has shown that a pH increase of roughly 1.8 pH units from the initial borated solution is necessary to induce precipitation when 100 mg/L of zinc is available. An even greater pH increase is required to form zinc precipitates when the initial zinc concentration is below 100 mg/L.

There is no available mechanism that has been considered that would cause such a dramatic pH increase, without the addition of TSP buffer. Therefore, zinc precipitation in an unbuffered environment is not considered in this research.

2.1.2.3 Simulations for Zinc Precipitation in Unbuffered Coolant

The previous section has concluded that zinc precipitation in unbuffered systems is negligible. This section will discuss whether zinc precipitation in TSP-buffered systems should be considered.

Six simulations were developed to determine the conditions necessary to cause precipitation of dissolved zinc with TSP present. Three dissolved zinc concentrations and two TSP concentrations were used. Zinc content included 1 mg/L, 20 mg/L, and 100 mg/L; TSP content was either 5.58 millimolar or 10 millimolar. Boric acid was present at 220 millimolar.

For these six simulations, a bulk solution of boric acid and one concentration of zinc was developed. A titrant was created with the same composition, but with TSP also included. The titrant was mixed to the bulk solution in 100 equal additions to simulate the dissolution of TSP in containment. Dissolved zinc and saturation index quantities were calculated with each titrant addition. The dissolved zinc calculations are shown in Figure 6.

Figure 6. Zinc precipitation in buffered coolant

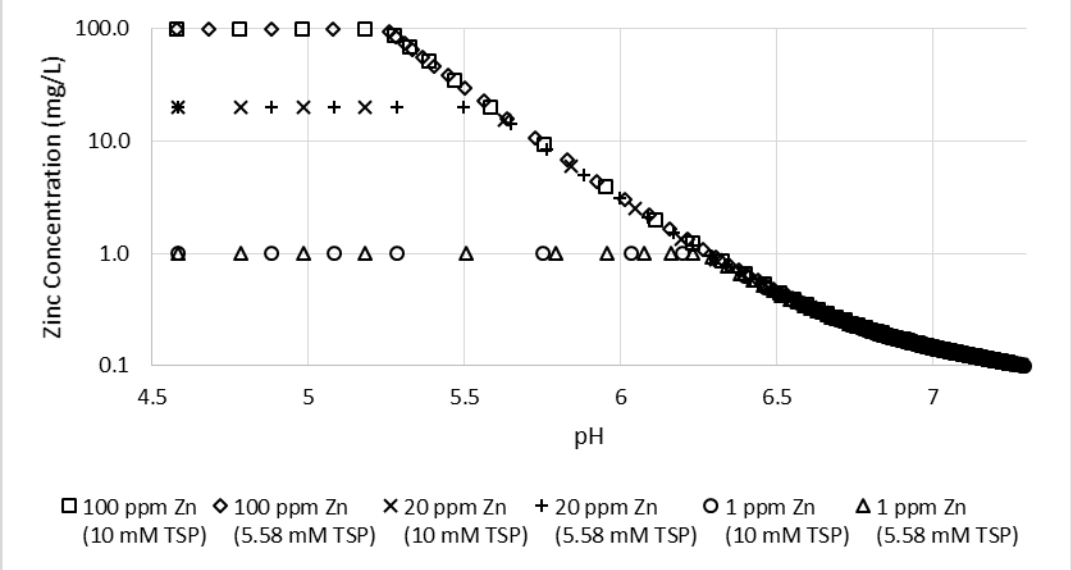

These simulations have shown that zinc precipitation will occur when TSP is added in sufficient amount. A value which is of note through these simulations is the predicted dissolved zinc concentration when all of the TSP inventory has been added. Dissolved zinc is limited to 0.10 mg/L when 10 millimolar TSP is present, and 0.13 mg/L when 5.58 millimolar TSP is present.

An interesting finding with these simulations is that precipitation consistently occurs along a common pH-zinc concentration curve, independent of the TSP or initial zinc concentration.

The identity of the chemical precipitates has been determined through saturation index analysis to be zinc phosphate only; no other precipitates formed within the pH range studied.

2.1.2.4 Simulation Conclusions and Limitations of the Simulations

There are two primary conclusions to be drawn from these simulations. First, zinc precipitation is more favorable in conditions where zinc is present in a greater concentration. This is true whether TSP buffer was present or not. The solubility product constant, K_{sp}, states that the concentration of dissolved zinc required to induce precipitation goes as a function of the zinc concentration to a positive integer power, which varies depending on the dissolved zinc species considered. As an example, the solubility product constant for zinc phosphate formation is shown in Equation 7.

Equation 7. Qualitative zinc phosphate solubility product constant relation

$$K_{sp,zinc\ phosphate} \propto [Zn]^3[PO_4]^2$$

Therefore, the discovery that zinc precipitation is more favorable at greater zinc concentrations is confirmed.

The second conclusion to be inferred from these simulations is that zinc phosphate is the only zinc-based chemical precipitate that is expected to form in a post-LOCA scenario. For simulations lacking TSP buffer, zinc borate was predicted to precipitate, but only at a pH that exceeds what is expected to occur in a post-LOCA environment. For simulations with TSP buffer, zinc phosphate precipitation dominated all other chemical precipitate formation.

However, there are limitations to Visual MINTEQ software and the assumptions in the simulations performed. All of these simulations were limited to room-temperature which may not be representative due to the temperature dependence of solubility and precipitation. The databases for Visual MINTEQ do not include accurate enthalpic information beyond standard temperature and pressure (STP).

Additionally, there may be several other chemicals present in a post-LOCA environment which were not considered for these simulations, such as calcium, silicates, aluminum, and lithium. This is not considered a significant hindrance, though, because the chemical expected to cause significant precipitation (phosphate) is typically present in great excess, and other chemical reactions would not parasitically remove the entire inventory of phosphate.

2.2 Historical Work and Literature Review

2.2.1 Integrated Chemical Effects Tests and Chemical Head Loss Experiment

In the early 2000s, LANL and UNM collaborated to perform the ICET series [10]. The ICET series was designed to examine the chemical effects of common containment materials in the event of a LOCA. Each of the five tests conducted was distinguished by a different combination of buffering agents and insulation materials. The buffering agents included TSP, sodium tetraborate, and the strong base sodium hydroxide (NaOH). Metallic surfaces—including aluminum, copper, carbon-steel, galvanized steel, and IOZ—were added to the testing environment to simulate the response these materials would have to the chemical environment of a LOCA. Galvanized steel and IOZ represent the sources of zinc in these experiments. The ICET series tests operated continuously for thirty days at 60°C, with a total aqueous inventory of 250 gallons.

Figure 7. ICET tank [15]

There were a few common trends across all ICET experiments which relate to the zinc effects. Galvanized steel coupons tend to gain the most net mass when exposed to TSP buffering. This observation suggests that a chemical product must be precipitating on the galvanized steel coupons which is not present in tests with the other chemical buffers. Phosphate is the only chemical present in TSP-buffered tests which does not also appear in the other tests, so therefore the logical supposition is that zinc phosphate has formed and precipitated on the galvanized steel surfaces.

Figure 8. Metal coupon rack for the ICET experiments [16]

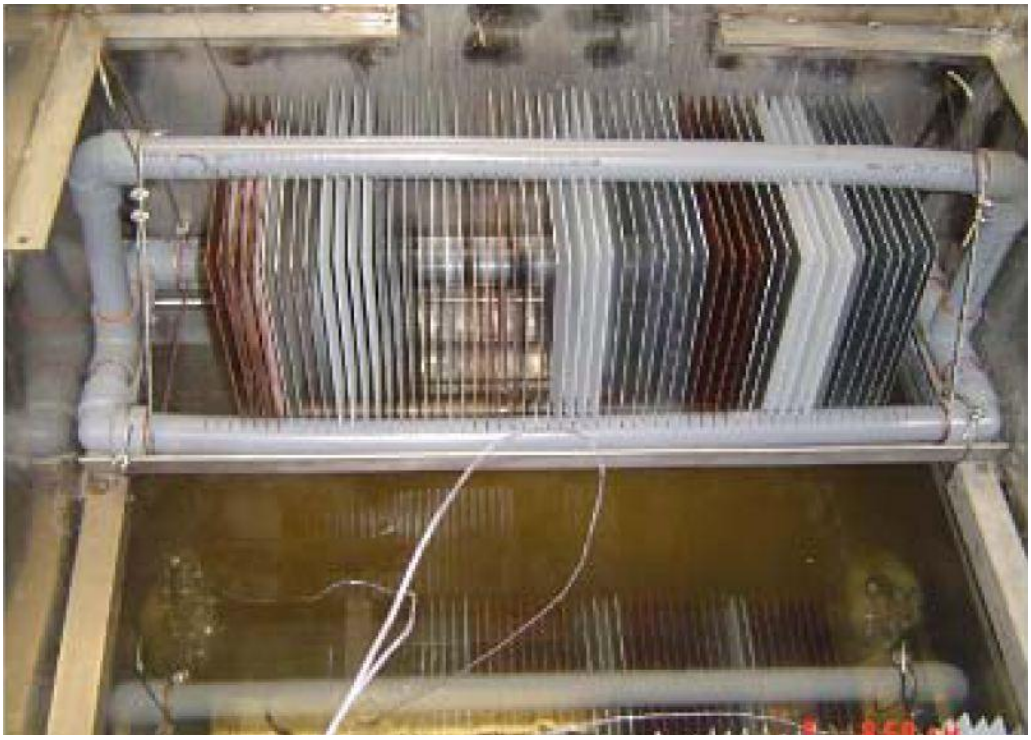

In the ICET series, the IOZ coating did not detach from the steel surfaces onto which they were applied. This confirmed that zinc is not released in particulate form, which would more destructively interfere with ECCS sump operations than smaller chemical precipitates.

In the ICET series, zinc tended to concentrate in solution early during the test, but the zinc in solution fell to below 1 mg/L within the first twenty-four hours for four tests; the fifth test required four days to fall below 1 mg/L total dissolved zinc.

The second of the ICET experiments, or "ICET 2" [16], had a chemical environment most similar to the body of research presented in Chapter 4. Therefore, special attention is paid to the findings of this test. ICET 2 coupon surfaces were found to be much more reactive to local chemistry; this effect is attributed to the presence of

phosphate. Also attributed to the presence of phosphate was the reduction of the quantity of chemical precipitates.

In ICET 2, the major contributor to both turbidity (a qualitative measurement of water clarity) and total suspended solids (TSS) was released zinc. The concentration and release behaviors of other chemicals did not correspond to changes in turbidity or TSS. This finding suggests that zinc has the potential to destructively interact with ECCS operations by producing chemical products that may become stuck in the ECCS strainers, preventing coolant flow through the sump.

At the conclusions of the ICET series, the testing facility was repurposed by UNM. The Chemical Head Loss Experiment (CHLE) program was design with the existing infrastructure. The capabilities of ICET were expanded to allow the aqueous inventory of experiments to pass through a vertical strainer which measured the head loss of recirculation pumps. Four of the CHLE tank tests will be discussed due to the similarities with this body of research; the included experiments are CHLE Tank Test #2 (T2) [17], T3, T4 [14], and T5 [18]. The CHLE tank testing series is ongoing at the time of this document's writing.

Figure 9. CHLE vertical strainer head loss columns [19]

In all four tests considered, it was determined that zinc was a primary source of solution turbidity. This suggests that as zinc undergoes electrochemical oxidation and dissolves into solution, it forms complexes which are either large or numerous or both (turbidity cannot resolve the difference), which become available to contribute to head loss. In fact, some of the head loss activity measured in the columns also corresponded with zinc concentration and turbidity, further reinforcing the contributions that zinc will have on ECCS operations. Elemental spectral data, through EDS and x-ray diffraction analysis (XRD), found that zinc phosphate scale transported throughout the system, becoming deposited in the tank floor, on the surfaces of coupons, and the fiberglass detector bed in the head loss columns.

Data for zinc concentration, particle size, head loss, and turbidity are included in Figure 10, Figure 11, and Figure 12.

Figure 10. CHLE T3 zinc concentration filtered and unfiltered [14]

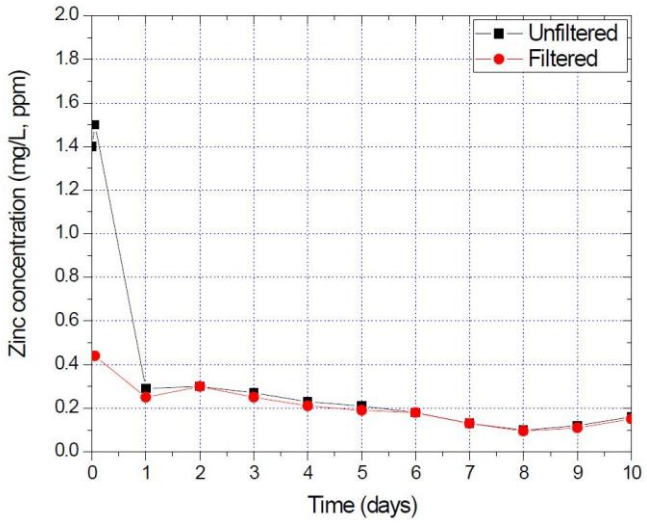

Figure 11. Particle size in T3 (has zinc) and T4 (has no zinc) [14]

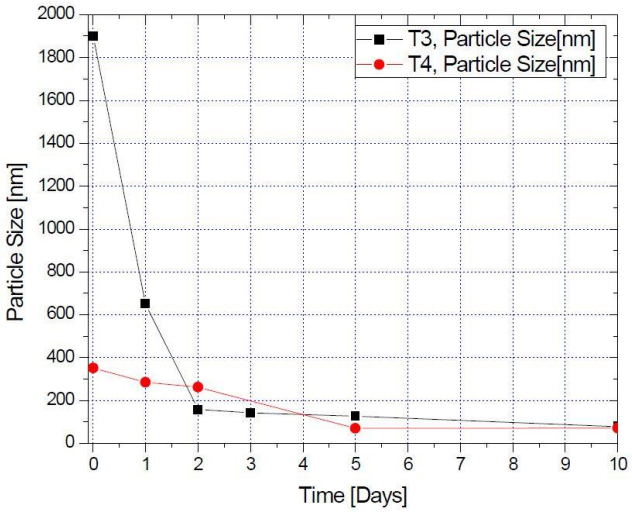

Figure 12. Turbidity and head loss response in T3 (has zinc) and T4 (has no zinc) [14]

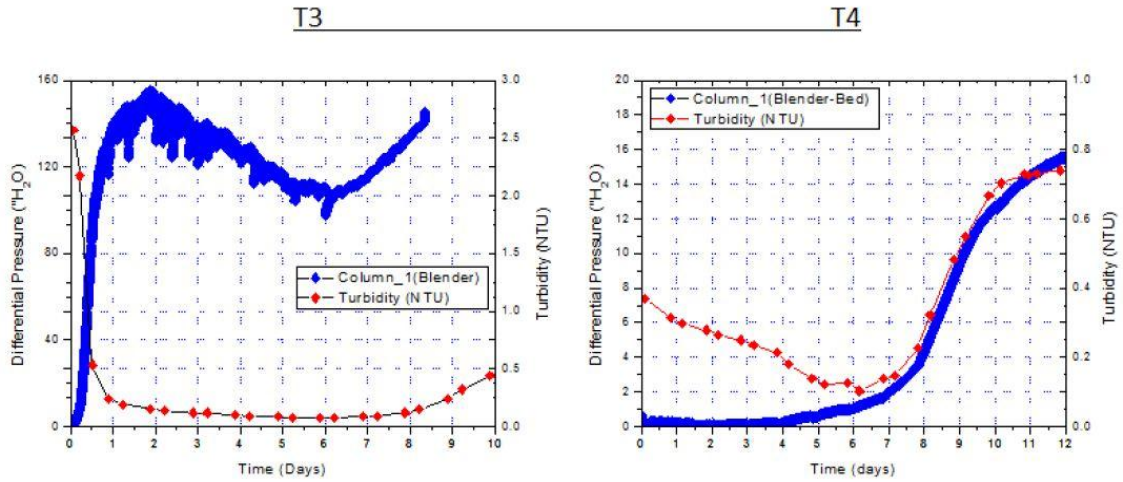

2.2.2 Other GSI-191 Efforts

Zinc corrosion experiments [20] performed by LANL and UNM were conducted to quantify the effect that zinc would have on sump head loss. This effort was divided into two groups of tests: bench-top corrosion experiments and dissolved metal salts tests. Zinc granules, zinc coupons, and crumbled IOZ were tested at the benchtop scale, and zinc nitrate salt was introduced into the vertical loop head loss column.

In the benchtop corrosion studies, it was found that zinc release is more favorable early-on in experiments, and scale formation is more favorable after one week. As a control, similar experiments were performed in pure water, which lack the LOCA chemistry; zinc ceased corrosion after four days, which suggests that zinc corrosion is dependent on LOCA chemistry.

In the dissolved metal salts testing, chemical head loss was not observed until zinc in solution reached a threshold concentration of 6.5 mg/L. This concentration of dissolved

zinc was only achieved on the benchtop tests in room-temperature solutions; the higher temperature solutions had a lower zinc concentration, which reinforces the concept of retrograde solubility with dissolved zinc.

Additional zinc corrosion tests were performed at the Finnish Centre for Radiation and Nuclear Safety [21]. These experiments revealed two key behaviors of zinc in a post-LOCA environment. The first was that the presence of borate was shown to significantly increase the solubility of dissolved zinc. The second observation was that, at a lower pH, zinc surfaces tend to interact more destructively with the testing solution. These two concepts work together, because in a post-LOCA environment, the borated coolant is at a low pH—two factors which are shown to increase zinc release and corrosion.

Head loss testing was executed at the KorrVA Testing Facility [13] to examine the influence of corrosion on ECCS sump head loss. Galvanized steel sources were introduced into a chemical and physical environment resembling a post-LOCA environment, and included boric acid, insulation, and recirculating capabilities through a head loss detector bed imitating the function of an ECCS sump strainer.

These experiments showed behavior with zinc and zinc-based corrosion products that was similar to the observations from other experiments. Dissolved zinc again showed the retrograde behavior of solubility through the experimental temperature spectrum, with zinc concentrations reaching as high as 90 mg/L at a temperature of 45°C. Lithium hydroxide, which is a common additive to reactor coolant, restricted the solubility of dissolved zinc, through the most probable mechanism of neutralizing the pH, which has been shown to limit the release and solubility of zinc.

The corrosion and removal of the protective coating on galvanized steel was found to be a precondition for an increase of head loss. The measured head loss only increased after this protective coating was compromised, which suggests that the underlying steel participated in corrosion and dissolution, with rust and other iron-based corrosion products transporting to the insulation detector bed. Head loss was found to be higher in more acidic conditions, because zinc- or iron-based chemical corrosion products are more likely under a more acidic condition, and transport to the debris bed on the insulation detector bed.

2.2.3 Non-GSI-191 Efforts

This section will introduce several bodies of research from peer-reviewed literature to establish the context behind various zinc corrosion phenomenology. The topics will include (1) oxidation and dissolution of zinc, (2) aqueous complexation of zinc and zinc compounds in similar and other fields, and (3) the phosphating of dissolved zinc, and the precipitation of zinc phosphate.

2.2.3.1 Dissolution

The dissolution of zinc into an aqueous environment requires as specific set of conditions. In metallic form, zinc exists as a neutral, non-ionic element. As a dissolved and oxidized element, zinc exists as a divalent cation. The divalent positive charge that is found with oxidized zinc is a result of the rejection of the 4s orbital electrons to an oxidant.

A method for measuring the dissolution and corrosion of galvanized steel has been presented [22]. In this article, the chemical response to alkaline solutions is presented with an electrochemical method for measuring the response to an applied current.

In the case of a pure zinc anode with no significant cathodic reactions, the rate of zinc dissolution may be measured through a potentiostat measurement, where a partial elementary current corresponds to the dissolution rate of zinc. A positive film growth rate suggests that the oxidation reaction dominates the dissolution reaction, and a film of zinc oxide/hydroxide has grown. Conversely, a negative film growth rate implies that the oxide/hydroxide film is dissociating and releasing into the solution.

The experimental scope included a stepwise increase in the ionic strength and alkalinity of the electrochemical solution by addition of sodium hydroxide resulting in 0.1 M to 1.0 M sodium. Through each addition of sodium hydroxide, a new electropotential was measured, and a calibration developed for a reaction rate of surface zinc to soluble speciation.

The main findings of the publication include a validation of the technique for measuring zinc dissolution. Three individual types of oxides have been distinguished based off of their respective potentials, which have been shown to induce different phases of oxides.

The main contribution this publication has to this body of research is that product formation kinetics are dependent on the saturation of zinc ions in the solution. If there is insufficient zinc in solution, a source will corrode and dissolve to achieve the saturation limit. Conversely, if a solution is oversaturated, zinc-based chemical products will be formed as a mechanism to reduce the concentration of dissolved zinc.

The dissolution and deposition mechanism for zinc in an acidic sulfate medium has been studied [23]. Electrochemical Impedance Spectroscopy (EIS) and Electrochemical Quartz Crystal Microbalance (EQCM) analytical techniques have been applied to monitor the dissolution and deposition. EIS is a technique applied due to its ability to interpret the electrochemical mechanisms of dissolution and passivation quantitatively. EQCM is used in conjunction with EIS because it has the capability to obtain information on the mass that is dissolved and deposited during electrochemical processes.

It was reported that between a potential of -1.05 and -1.35 V that zinc is reduced and deposited on a gold electrode. Through this electrochemical potential range, hydronium is also reduced, liberating hydrogen gas. In the range of potential between -1.05 and -0.70 V, it was reported that zinc dissolves and leaves the gold anode.

When electrochemical experiments with the dissolution potential and deposition potential run cyclically, hypothetically, there should be a balance that is established, where the dissolution and deposition are run to completion. This hypothesis was not observed, but rather, a non-compensated increase of zinc deposition was observed. This increase of mass through several cycles is attributed to the passivation of zinc and the adsorption of solution ions. There was a hysteresis of potential and deposition because the application time of the dissolution potential required would be steadily increasing between consecutive cycles to remove the disproportionately high deposited zinc.

These electrochemical experiments were run again, but with argon gas bubbled through the solution to remove dissolved oxygen. This resulted in the mass discrepancy being greatly reduced. In the absence of oxygen, the dissolution and deposition was far more reversible.

This set of experiments suggest that, with all else being equal, dissolved zinc favors precipitation over dissolution. Corrosion products that form are unlikely to re-dissolve into solution, meaning that their contribution to ECCS operations persists.

2.2.3.2 Complexation

Following the dissolution from its base metal, zinc will form aqueous complexes. Dissolved zinc exists in aqueous solutions as a hydrate complex in which the oxygen atoms from six water compounds are electrostatically attracted to the positively-charged zinc core, forming a geometrically octahedral complex. As the dissolved zinc freely transports through the aqueous medium, complexed anions including hydroxide, carbonate, or phosphate may be present.

The study of a method for removal of zinc from industrial waste water is presented [24]. Zinc is essential for human consumption, but sufficiently a sufficiently high zinc concentration in water supplies (100 mg/L) is toxic. There is a desire to treat zinc-rich industrial wastewater before disposal into natural water supplies. If a similar treatment system may be applied to a post-LOCA environment, the effects of zinc may be greatly minimized.

There are several methods by which zinc may be removed from a water supply. These methods include chemical separation, ion exchange, nanofiltration, ultrafiltration, reverse osmosis, and electrodialysis. The principle disadvantages of these methods include inadequate selectivity, periodical batch processes, and high residual metal concentrations, among others. This article presents bounding agent complexants that have the ability to be

split from the zinc and regenerated for future use. The reference pH for these tests was >8, or an alkaline solution.

Three complexation agents, including poly(ethylenimine) of various polymer lengths and poly(acrylic-acid) were applied to a zinc chloride solution before passing the complexes through several membrane filters. The optimal complexant was found to poly(acrylic acid) with the complexation occurring at the carboxylic acid sites of multiple polymer subunits for each zinc ion removed.

This complexation experiment has shown that a reusable polymer may be an effective method for zinc removal; however, its viability in a post-LOCA environment may be quite low. Polymerized compounds may present more of a strain to ECCS operations than zinc corrosion products.

2.2.3.3 Phosphating

A hydrated zinc complex will remain suspended in solution until a thermodynamically favorable reaction with an anion become possible. If the zinc and anion complexes electrostatically interact, they may precipitate to form new chemical compounds, such as zinc hydroxide, zinc oxide, zinc phosphate, or others. The reaction of zinc with these anions may also create a nucleation site which may catalyze the continued precipitation of similar aqueous species. A nucleation site may also be present on the surface of the original metallic zinc source.

A major controlling factor in the precipitation and solubility of metals in solution is the reaction constant of solubility, of K_{sp}. The K_{sp} values for relevant zinc compounds

are included in Table 3. Zinc phosphate is the product that will most dominantly control the solubility of zinc.

Table 3. Solubility product reaction constants for zinc compounds

Compound	K_{sp}
zinc carbonate	1.4×10^{-11}
zinc borate	10^{-12}
zinc hydroxide	1.2×10^{-17}
zinc phosphate	9.0×10^{-33}

Corrosion inhibition properties of several commercial inhibitor paints have been studied [25]. Among these pigments are zinc phosphate, zinc-aluminum phosphate, zinc-iron phosphate and zinc phosphomolybdate.

For the research detailed in this article, extracts of the pigments were prepared under varying pH conditions. Pigment extracts, once concentrated, were used as an electrolyte for studying carbon steel corrosion. The pH values employed include 4.5, 7.0 and 10.5. The concentrations of zinc and phosphorus were measured as a means to qualitatively rank the inhibition powers of the extract. By a significant margin, the most acidic condition (pH 4.5) resulted in the highest concentration of zinc, usually by an order of magnitude or more. This is an intuitive result. ICP-AES analysis of the solutions also show an inversely proportional relation between pH and solubility of zinc (i.e. low pH corresponds to high zinc concentration).

After qualitative assessment of the inhibition power from concentration measurements were conducted, a series of tests were performed to validate the results. A sample of carbon steel was exposed to a solution in which the pigment extracts served as

an electrolyte, and linear polarization measurements were made. These polarization measurements, along with a reference measurement with sodium chloride, provided a percent inhibition power.

The primary contribution of this publication is the finding that the solutions in which zinc- and phosphate-based extracts were applied to the carbon steel in an acidic solution resulted in the greatest relative corrosion inhibition power.

Phosphating studies have been performed on zinc [26], where a surface of zinc was dipped into a commercial zinc phosphate epoxy. The zinc was then suspended in a solution of zinc phosphate and sodium chloride, and tested with an electrical potential. The results are similar to the previous article in that the inhibition efficiency of the zinc phosphate corrosion layer was very high.

A precondition for corrosion layer inhibition was that the leaching of base metal must achieve an adequately high concentration in solution. This means that the zinc surface will not become passivated by zinc phosphate until sufficient zinc has released from the base metal, but also that the resulting passivation is a product of the zinc that had released in the first place. This suggests that zinc phosphate is an excellent corrosion inhibitor because it does not require other elements or compounds to be present beyond zinc and phosphate.

Self-healing protective films on a zinc surface have been studied [27]. A comparison between the respective corrosion resistance and self-healing capabilities of sodium phosphate is analyzed. A zinc electrode was washed with a zinc phosphate solution to allow pre-test phosphating of the surface. The zinc surfaces were then scratched with a

knife-edge to expose the pure zinc base metal to corrosion agents. These surfaces were then exposed to sodium chloride solution to test the corrosion protection properties.

The results from this experiment have a strong implication on the corrosion passivating nature of zinc phosphate films. The protective efficiency of the film was determined through electrochemical analysis, and was shown to increase as the zinc's exposure time to sodium phosphate increased. A significant observation from this research was that phosphates from the protective film migrated into the scratched surface, which was verified through electron microprobe. This suggests that the zinc phosphate film that developed through the pre-test phosphating dissolved from the film, and that it was thermodynamically favorable to reattach to the pure zinc base metal, with the result of passivating further zinc corrosion. In control tests where cerium nitrate was applied in place of sodium phosphate, there was no observed migration of the cerium phosphate to the scratched surface.

These findings have shown that zinc phosphate will preferentially nucleate and grow on pure zinc surfaces, which will help passivate further zinc release. In a post-LOCA scenario, this is a useful way to remove zinc from solution passively—without the need for operators to interfere. Intuitively, increasing the surface area of zinc would create more nucleation sites for zinc phosphate precipitation; however, a greater surface area will also have the capability to supply more zinc to the system, which may outweigh the benefits. No discussion has been presented regarding the shear strength of the resulting zinc phosphate scale depositions, so the transportability of the zinc corrosion products is not assessed.

CHAPTER 3: MATERIALS AND METHODOLOGY

The research performed is primarily focused to determine whether the sources of zinc in containment will destructively contribute to post-LOCA operations. Destructive contributions are defined as *any* impact that zinc-based products have on LOCA mitigation efforts which are detrimental to designed and anticipated operations of the ECCS and any damage to structural or operational containment components.

Sources of zinc include the materials onto which zinc is applied, such as galvanized steel and inorganic zinc primer-coated surfaces. The mechanism considered for destructive contribution to post-LOCA operations is the obstruction of flow through ECCS recirculation pumps through the release of, or generation of, zinc-based chemical products. These chemical products include any chemical precipitate that bears zinc (e.g. zinc phosphate, zinc borate, zinc hydroxide), any secondary chemical products which contribute to the loss of safety and operations protocol (e.g. hydrogen gas generation from zinc oxidation), and any electrochemical degradation of the surfaces that zinc interacts with (e.g. iron become rust).

3.1 Experimental Design

Experimentation was performed as bench-top batch tests ([28], [29], [30], [31], [32], [33], [34], [35], [36], [37]). Bench-top batch tests in several testing series were conducted in chemically inert 1-liter Nalgene bottles. Each of the testing bottles included 500 milliliters of testing solution and one source of zinc in the form of a solid coupon.

3.1.1 Testing Solution

All batch tests had a similar composition of the two primary components: demineralized water and boric acid. Each series was identified by a chemical addition that differed slightly from series to series. Unique chemical additions included quantities of sodium hydroxide, hydrochloric acid, and/or trisodium phosphate.

The baseline chemical solution for batch tests was designed to be representative of the reactor coolant. Demineralized water was supplied through two separate sources: reverse osmosis membranes or successive steps of filtration and deionization. The boric acid addition was calculated so that the total boron content was consistently held between 2380 and 2390 ppm boron; this is equivalent to a 220 millimolar solution of boric acid.

The strong base sodium hydroxide and the strong acid hydrochloric acid were included in select series to make adjustments to a baseline pH. Sodium hydroxide was selected because it shares a common ion with the buffering chemical trisodium phosphate. Hydrochloric acid was selected because the generated ion, the chloride ion, may be found in containment as a radiolysis-generated chemical upon the degradation of electrical network and systems. A base and an acid which were classified as "strong" were chosen to minimize the additional chemistry added to the solution. A "weak" acid or base would require an addition of a greater inventory of the reagent to cause the same change in pH when compared with a "strong" acid or base.

The containment buffering agent TSP was included in some tests. For tests which included TSP, it was added in one of three different methods: (1) TSP was added before testing in the baseline chemical solution at a constant concentration throughout testing, (2) coupons were exposed to un-buffered testing solution for a while, followed by TSP

addition that brought the buffer concentration up to the final limit in a single addition of TSP, and (3) testing solution was gradually brought up to the final limit of phosphate concentration through gradual additions of TSP doses during testing. In the third method discussed above, trisodium phosphate was absent at the beginning of the test, and added incrementally to the testing solution to simulate buffer dissolution following the scenario after coolant breaches the walls of the bioshield and has come in contact with the buffer basket.

3.1.2 Zinc Sources

Zinc surfaces that were tested include coupons of one of three compositions: 99.6% pure zinc, carbon steel with inorganic zinc primer coating, or hot-dipped galvanized steel. Each coupon was prepared by shearing a 1-inch square piece from a bulk metal sheet. Coupon thicknesses ranged from 2/32 to 3/32-inches. These dimensions result in a total surface area ranging from 14 to 15 square centimeters. A 1/8-inch circular hole was drilled near the top edge of each coupon which was used to suspend the coupon in the testing bottle with nylon thread and maintain at a constant elevation in the testing solution.

Pure zinc surfaces are not found in containment. They have been included in this research in order to study the isolated chemical effects of zinc. The other zinc sources—galvanized steel and IOZ—also contain steel and other metals and chemicals. The galvanized steel coupons are cut from a large sheet of galvanized steel, and the edges of the one-inch coupons have the underlying steel exposed. While the contribution of this

exposed steel is expected to be low, it still represents roughly 15% of the total coupon surface area. Therefore, some tests used pure zinc coupons to avoid additional chemistry.

One series of tests tracked the integrated effects of zinc and aluminum. Aluminum alloy 1100 coupons were prepared using the same methods and standards for zinc sources.

3.1.3 Physical Testing Environment

Batch tests were conducted in 1-liter Nalgene bottles, which served as the testing vessels. Each testing vessel kept the testing solution and sample in an air-tight and water-tight environment. Testing vessels were maintained at a specific temperature using a hot-water bath. The hot water bath temperature was maintained using a thermoregulator and coolant coils which were in conductive contact with the hot water bath. The thermoregulator operates on a simple premise: an electrical current is applied to a coil which is in contact with the primary coolant; the heated coolant is pumped through pipes in the hot water bath, depositing thermal energy in the bath.

Figure 13. Hot bath with 1-liter Nalgene bottles

The hot water bath is placed on an agitation table. The agitation table was set to rotate at 75 revolutions per minute. The agitation table was deemed necessary to promote mixing in the testing vessel, and to prevent concentration gradients from developing which may cause unrepresentative corrosion.

3.1.4 Post-Testing Analyses

Select coupons were examined by SEM and EDS. Untested coupon samples were examined prior to exposure to the testing solution to serve as representative initial-condition surfaces for comparison with samples following the completion of testing.

Measuring the concentration of zinc or other chemicals in solution is an analytical practice which, through careful inference, reveals phenomena including release rate, passivation, and precipitation. Chemical concentration was measured by a third-party analytical laboratory using ICP. The zinc content in all samples was measured, and other chemical were measured in select samples, such as iron in tests where galvanized steel was used as the source of zinc, and aluminum in the tests that included aluminum alloy 1100.

3.1.5 Complete Testing Matrix

Batch tests were organized by five distinct themes. The themes of interest are as follows: (1) the release of zinc in borated acidic environment with no phosphate, which is termed "prompt release", (2) release and corrosion with exposure to the containment buffer trisodium phosphate, (3) release and corrosion of zinc in a chemical environment simulating phosphate dissolution, (4) integrated release and corrosion characteristics of zinc and aluminum, and (5) descaling techniques for quantifying phosphate deposition by removing scale deposits.

3.1.5.1 Theme 1 Tests: Prompt Release

The first theme for testing was designed to replicate the early-stages of a developing LOCA. For these tests, no trisodium phosphate buffer was introduced to the tests, in order to study the *prompt zinc release* effect [38]. Tests were planned with all three sources of

zinc at four temperatures and with durations up to 24 hours. Six testing series were performed to study Theme 1.

The first testing series was designed using pure zinc coupons as a zinc source (Series 1.1). These tests were performed at 85°C, with durations spanning from 5 minutes to 24 hours.

The second testing series was designed using IOZ as a zinc source (Series 1.2). These tests were also performed at 85°C, with durations spanning from 30 minutes to 2.5 hours. The scope of testing durations was reduced because of anticipated similarities between zinc source materials.

The final four additional testing series were designed using galvanized steel as the source of zinc. Each series employed a different operating temperature; these temperatures included 85°C (Series 1.3), 65°C (1.4), 45°C (1.5), and 25°C (1.6). These four temperatures were selected with the expectation that a release correlation as a function of both time and temperature could be developed. Durations spanned from 5 minutes to 24 hours.

3.1.5.2 Theme 2 Tests: Zinc Phosphate Solubility and Precipitation

The second of the batch test themes was designed to simulate the long-term (beyond the first 24 hours) effects of zinc sources when exposed to phosphate-buffered coolant. Tests were designed with pure zinc coupons and a baseline testing solution containing 0.22 molar boric acid and 10 millimolar trisodium phosphate, and were operated at 85°C; the resulting pH of this baseline solution was 7.3. Seven testing series were performed that studied the

effects of altering one of the following testing conditions: zinc source, trisodium phosphate concentration, temperature, and pH. The first testing series (Series 2.1) served as the baseline series, and was operated with each of the conditions listed above for durations spanning from 30 minutes to 10 days.

In the second testing series (Series 2.2), the operating temperature was decreased to 60°C. This adjustment was made to study the effect that cooling may have on the solubility and precipitation of zinc during the first few hours of a LOCA under buffered conditions. Testing durations spanned 30 minutes to 2.5 hours.

The concentration of trisodium phosphate was adjusted from 10 to 5.58 millimolar for the third testing series (Series 2.3). As a result of the decrease of trisodium phosphate, the baseline pH dropped to 7.0. The sponsoring utility for this research anticipates a minimum trisodium phosphate concentration of 5.58 millimolar. Testing durations spanned 1 day to 5 days.

Two additional series were designed to observe the effect of slight pH variations while holding the phosphate concentration constant at 10 millimolar. The pH was decreased in one series by 0.5 pH units (down to pH 6.8) by adding hydrochloric acid (Series 2.4). The pH was increased in the other series by 0.5 pH units (up to pH 7.8) by adding sodium hydroxide (Series 2.5). Hydrochloric acid and sodium hydroxide are discussed in greater detail in Section 3.2.1. Testing durations spanned from 30 minutes to 10 days.

The final two series of tests were designed to test alternate sources of zinc, including hot-dipped galvanized steel (Series 2.6), and IOZ (Series 2.7). These tests were designed to study the similarities and differences between release rate, steady-state zinc

concentration, and changes in solution properties between the three zinc sources. The testing duration spanned from 30 minutes to 10 days.

3.1.5.3 Theme 3 Tests: Zinc Phosphate Formation with TSP Addition after Prompt Release Phase

The third theme of interest for this research is simulating the dissolution of trisodium phosphate as it would occur during a LOCA. The first theme studied the zinc release when no phosphate is added, and the second theme assumed a constant phosphate concentration from the start of testing. This third theme connects the first two themes into experiments which are more representative of the events during a LOCA: (1) a period of time where zinc is exposed to un-buffered coolant and (2) followed by the dissolution and incorporation of phosphate into the coolant. Fourteen series of tests were designed to explore this approach.

The first two testing series that contribute to this testing theme simulated gradual dissolution and containment mixing of trisodium phosphate. Trisodium phosphate was added to the testing vessel starting 20 minutes after the test began, and was added in three equal doses every 20 minutes for 60 minutes. The total amount of trisodium phosphate added over the 60 minute window of time included 5.58 millimolar (Series 3.1) and 10 millimolar (Series 3.2); one of these concentrations was used for each testing series. These tests were held at a constant temperature of 85°C, and continued for a total of 24 hours. Pure zinc was the zinc source.

The final eight series of tests (3.3-3.10) differed from the first two series in that the total inventory of trisodium phosphate was introduced in one large dose, and the source of zinc was galvanized steel. These tests are organized by two factors: (1) temperature and (2) whether the zinc source is present or absent following the addition of trisodium phosphate, which was added to a final concentration of 5.83 millimolar. These were designed to see how zinc precipitation differs when the zinc source is proximal or absent.

Hot-dipped galvanized steel coupons were exposed to un-buffered conditions to promote the prompt release of zinc, at four distinct temperatures: 85°C, 65°C, 45°C, and 25°C, and for times spanning 5 minutes to 24 hours. Two series were run at each temperature. These two series differed from each other by how the zinc source was treated following the addition of trisodium phosphate. In one series, the galvanized steel coupon was removed from the testing vessel, while in the other series, the galvanized steel coupon remained in solution for the remainder of the test. Following the addition of trisodium phosphate, the tests continued to a total of 48 hours.

3.1.5.4 Theme 4 Tests: Zinc and Aluminum Integrated Effects

The fourth theme for zinc experimentation includes the integrated effects that zinc sources may have with sources of aluminum in containment. Aluminum is primarily found in containment in the following forms: structural members, coatings, small components such as valves, and foil coatings on insulation [39]. The source of zinc in these tests was pure zinc.

One series of tests (Series 4.1) was designed to quantify the integrated release, corrosion, and precipitation effects of zinc and aluminum on each other. In each test in the series, a coupon of aluminum alloy 1100 and a pure zinc coupon were suspended in the testing solution. These coupons were suspended such that neither was in direct physical contact with the other; this precaution was necessary to eliminate galvanic reactions between the two metals.

The testing solution was maintained at conditions similar to the baseline conditions from the first series of prompt release tests. The testing solution temperature was held at 85°C. The concentrations of trisodium phosphate and boric acid were designed to be 10 millimolar and 0.22 molar, respectively, resulting in a pH of 7.3. Testing durations spanned from 5 hours to 5 days.

The results of this testing series were compared with the results of previous experiments in which zinc and aluminum were tested in isolation. Because of the identical physical and chemical conditions, the results from the first series of tests from Theme 2 experiments were used as the baseline results for comparison with this series. Previous experiments conducted under identical chemical and physical conditions will serve as a baseline for comparison for the response of aluminum when zinc is present, and those results will be provided with the discussion in Chapter 4.

3.1.5.5 Theme 5 Tests: Chemical Descaling Methods to Quantify Scale Layer

The final theme for testing explored several descaling methods for zinc surfaces. These were designed to improve the analytical methods that were employed to quantify the

corrosion of- and release from- zinc sources, and the precipitation of chemical products back onto to coupon surface. Four descaling solutions were applied to two zinc sources. The descaling solutions were found in [40] and [20], and include prescribed concentrations of ammonium persulfate (Series 5.1), ammonium chloride, ammonium acetate, and hydrochloric acid. Select coupons from Series 2.1 (pure zinc) were repurposed following the conclusion of testing under Theme 2 conditions.

The first decaling method [40] required 5 minutes of exposure to a solution of 100 g/L of ammonium persulfate at 22°C. The second decaling method [40] required 5 minutes of exposure to a solution of 100 g/L of ammonium chloride at 70°C. The third decaling method [40] required 5 minutes of exposure to a solution of 100 g/L of ammonium acetate at 70°C. The fourth decaling method [20] required 10 seconds of exposure to a solution of 1% hydrochloric acid at 22°C. The descaling solutions were analyzed for total zinc content.

CHAPTER 4: EXPERIMENTAL RESULTS AND ANALYSIS

4.1 Theme 1: Prompt Release

The first testing theme studied the prompt release effects of zinc sources. Table 4 shows a summary of the testing matrix. Additional details for these tests are provided in Section 3.1.5.1.

Table 4. Theme 1 testing matrix

Series	Zinc Source	Operating Temperature	Testing Duration
1.1	Pure Zinc	85°C	5 min. – 24 hrs.
1.2	IOZ	85°C	30 min. – 2.5 hrs.
1.3	Galvanized Steel	85°C	5 min. – 24 hrs.
1.4	Galvanized Steel	65°C	5 min. – 24 hrs.
1.5	Galvanized Steel	45°C	5 min. – 24 hrs.
1.6	Galvanized Steel	25°C	5 min. – 24 hrs.

4.1.1 Theme 1 Zinc Release Analysis

Zinc release was measured through ICP by a third-party analytical laboratory, Hall Environmental Analytical Laboratory (HEAL). Figure 14 shows the zinc release results for all tests from Series 1.1 1.2, and 1.3, which were all conducted at 85°C.

Figure 14. Prompt release at 85°C

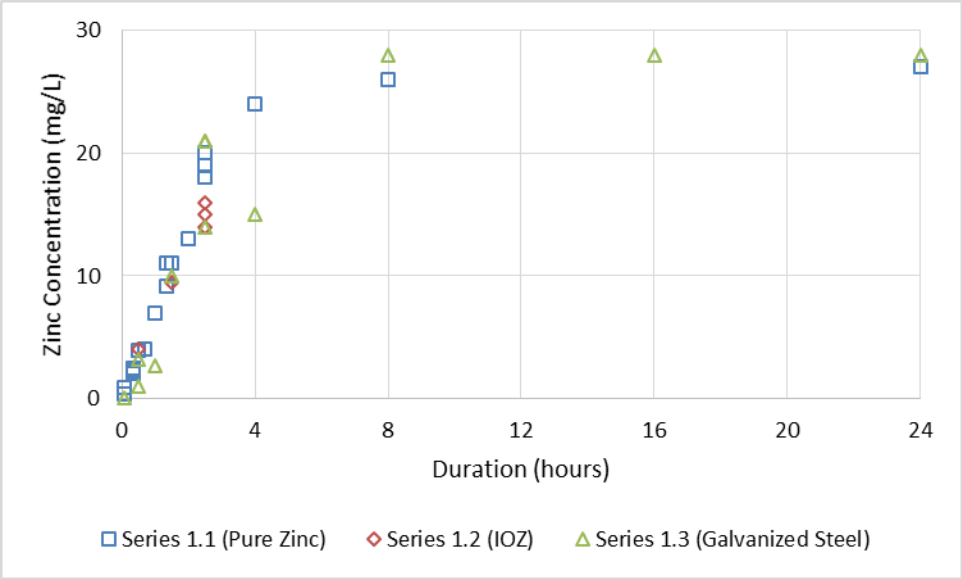

The prompt release from Series 1.1-1.3 displayed in Figure 14 show that, even across the three sources of zinc, the release is consistent. The widest experimental variability exists at 4 hours, with a range of 9 mg/L.

A notable observation from this series is the apparent saturation limit that is achieved by the eighth hour of testing by both galvanized steel and pure zinc sources. This saturation limit is 27 mg/L for pure zinc and 28 mg/L for galvanized steel; this difference is within the observed experimental variability during the earlier sampling times. The solubility is likely controlled by zinc borate species (Figure 3). The prompt release period in these tests, through the fourth hour, is shown in Figure 15.

Figure 15. Prompt release at 85°C, first four hours

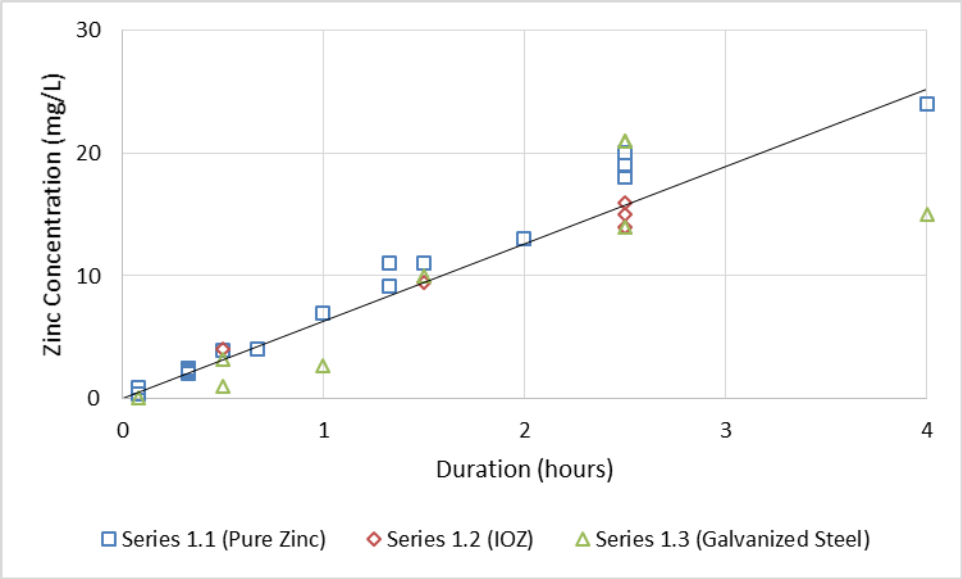

A linear trend for zinc release from all three sources is overlaid with the data from the first four hours of Series 1.1-1.3 in Figure 15. An average release rate of 6.3 mg/L per hour is observed, with a coefficient of determination of 0.86. This confirms that zinc continues to release from the zinc-bearing source at a consistent and predictable rate. This release rate is an average of all three zinc sources. It will be shown later during the analysis of the galvanized steel tests that the release is dependent on the zinc source and temperature.

The prompt release model shown above is useful for environments which are maintained at 85°C. Many LOCA environments will not remain at 85°C, so it is therefore useful to see how the saturation limit of released responds to different temperatures. The saturation limit is a useful quantity to establish how much dissolved zinc is available for chemical and physical reactions, such as precipitation, which is discussed in greater detail with the discussion of Theme 2 testing results where phosphate has been added.

Zinc release and the concentrations from Series 1.3, 1.4, 1.5, and 1.6 demonstrate the response that the dissolved zinc saturation limit has when the testing solution temperature is adjusted. These results are shown in Figure 16.

Figure 16. Saturation limit response to temperature with galvanized steel

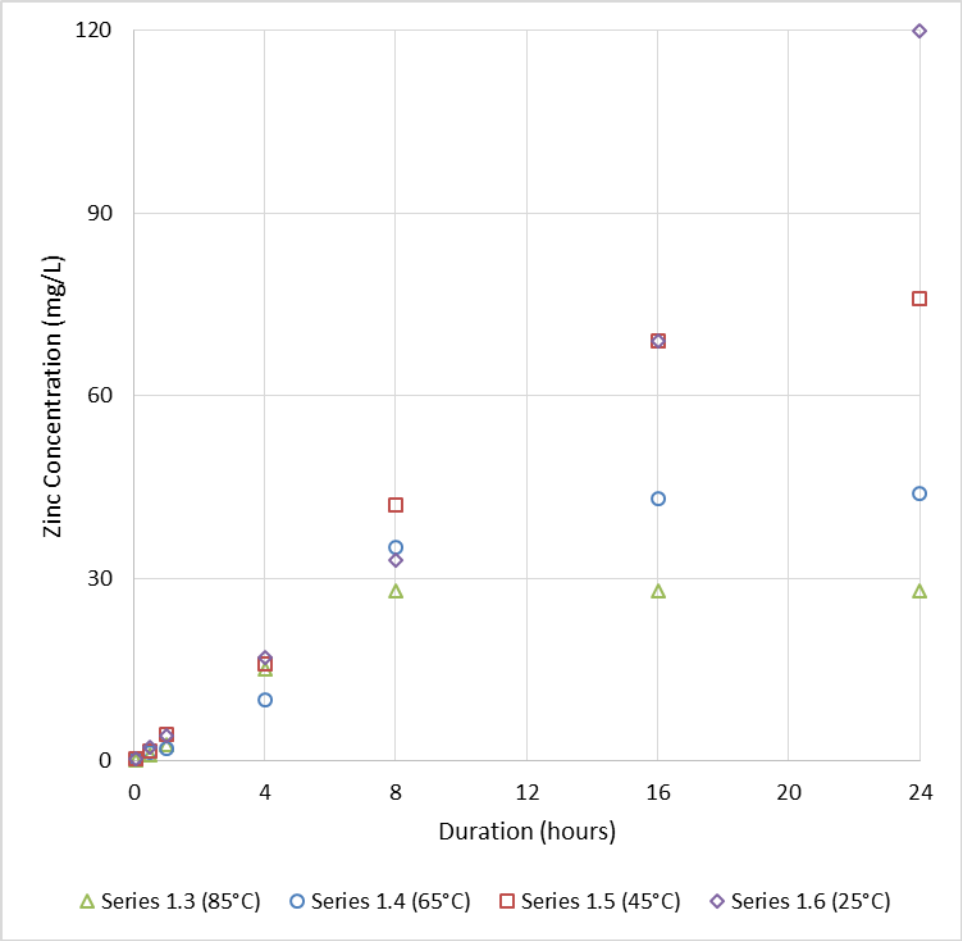

The concentration results from Series 1.3, 1.4, 1.5, and 1.6 show that the saturation limit of zinc does respond to temperature. Most chemicals respond to increasing temperatures with an increase in solubility. Dissolved zinc is displaying retrograde solubility, where an increase of temperature results in a decrease in solubility. Table 5

shows the release rate, observed saturation time boundaries, saturation limit, and the calculated saturation time. The surface-area normalized release rate is included, assuming a zinc surface area of 2 square inches (12.9 square centimeters)

Table 5. Series 1.3-1.6 summary of dissolved zinc concentration measurements

Testing Series and Temperature (°C)	Release Rate (mg/L per hr.)	Surface-Normalized Release Rate (mg/L*hr*cm^2)	Observed Saturation Time (hrs.)	Saturation Limit (mg/L)	Saturation Time from the Release Rate (hours)
1.3 (85°C)	3.5	0.27	4 < t < 8	28	8
1.4 (65°C)	4.0	0.31	8 < t < 16	44	11
1.5 (45°C)	4.5	0.35	16 < t < 24	76	17
1.6 (25°C)	4.7	0.36	≥ 24	≥ 120	N/A

The estimated saturation times and the saturation limits for Series 1.3, 1.4, and 1.5 follow a predictable trend as a function of absolute temperature, as shown in Equation 8 and Equation 9. These equations are second-order polynomial fits of the data from Table 5 for Series 1.3, 1.4, and 1.5.

Equation 8. Time to saturation for prompt release as a function of absolute temperature

$$Time\ to\ Saturation\ (hrs) = 0.02T(K)^2 - 14.72T(K) + 2734.48$$

Equation 9. Saturation limit for prompt release as a function of absolute temperature

$$Saturation\ Limit\ (mg/L) = 0.00375T(K)^2 - 2.76T(K) + 515.465$$

These equations for Series 1.3 through 1.5 may be extrapolated to the temperature of Series 1.6 to estimate the true saturation time and saturation limit. By applying Equation

8 and Equation 9 to the temperature of Series 1.6, the saturation time is estimated to be 26 hours, and the saturation limit is 124 mg/L. Both of these calculated values are within the range permitted, as shown in Table 5.

Equation 8 and Equation 9 are only physically meaningful in temperatures ranging from 273 K to 373 K (0°C to 100°C). Beyond this range, the solution experiences a phase away from a liquid state, which makes aqueous expressions such as concentration meaningless.

The arrival to the saturation limit in these series corresponds with a surface oxide-scale layer development, which is discussed in greater detail in Section 4.1.4.

The hot-dipped galvanized steel surfaces have from 10 to 50 micrometers of zinc coating on the surface. An important question to ask is whether the highest saturation limit (124 mg/L) may correspond with complete removal of the galvanized layer. If the underlying steel is exposed, additional iron-based corrosion products may contribute to ECCS operations.

To calculate whether 124 mg/L represents the whole inventory of zinc on the surface, some conversions are first necessary. A concentration of 124 mg/L is equivalent to 124 milligrams per liter. Each testing vessel had one-half liter of testing solution, and each galvanized steel coupon had two square inches of zinc coating. The calculation for how much mass was lost per unit area is shown in Equation 10.

Equation 10. Mass of zinc lost per unit area on galvanized steel

$$124\ ppm = 124\frac{milligrams}{L} \times \frac{0.5\ L}{experiment} \times \frac{experiment}{2\ in^2\ zinc} = 31\frac{milligrams}{in^2\ zinc}$$

Equation 10 has shown the maximum amount of zinc that will be lost from one square inch of a galvanized steel surface is 31 milligrams. This equation is converted to a surface depth in Equation 11 by applying the density of metallic zinc.

Equation 11. Calculation for maximum thickness of zinc layer lost during prompt release

$$31\frac{mg\ zinc}{in^2\ zinc} \times \frac{cm^3\ zinc}{7140\ mg\ zinc} \times \frac{1\ in^2}{6.452\ cm^2} = 0.0006729\ cm \approx 6.7\ micrometers$$

These calculations have shown that under the conditions that promote the greatest release of zinc from the galvanized steel surface, a substantial amount of zinc will remain as a coating on the galvanized steel. By assuming the thinnest expected zinc layer coating (10 micrometers) and the highest zinc concentration (124 mg/L), there is still more than three micrometers of zinc remaining on the surface.

Series 1.3, 1.4, 1.5 and 1.6 were conducted with galvanized steel coupons, so analysis on dissolved iron concentration may be useful to determine the effectiveness of the galvanic shielding that zinc provides. Released iron measurements are included in Figure 17.

Figure 17. Theme 1 iron release

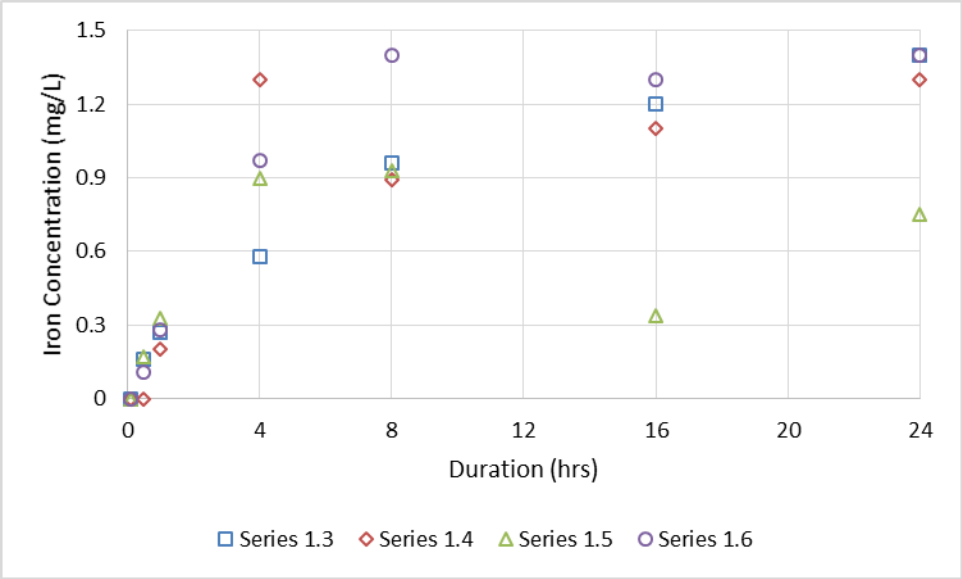

Figure 17 shows that iron is released from the galvanized steel coupon at a reasonably predictable rate. Initially, iron is released in a linear rate. The dissolved iron concentration also seems to approach a saturation limit of 1.4 mg/L by the twenty-fourth hour of testing. ICP analysis does not resolve between divalent or trivalent iron species. This observed passivation of iron release may be attributed to the galvanic protection that zinc provides.

In the first four hours of testing, iron is released at a linear rate of 0.24 mg/L per hour, with a coefficient of determination of 0.88. If this iron release rate is extrapolated to the twenty-fourth hour, the expected dissolved iron concentration is over 5.7 mg/L. However, the maximum iron concentration measured in the first twenty four hours is only 1.4 mg/L, which confirms that some passivation mechanism is in effect. The ratio of expected iron release and the observed iron release is roughly 4. The suspected mechanism for iron passivation is zinc's cathodic protection.

4.1.2 Theme 1 Turbidity Analysis

Turbidity is a useful analytical technique to qualitatively assess solution clarity. A Hach™ 2100P Turbidimeter was used to measure solution turbidity with the standard unit of Nephelometric Turbidity Units (NTU). Turbidity measurements from Series 1.3-1.6 is shown in Figure 18.

Figure 18. Solution turbidity for Series 1.3, 1.4, 1.5, and 1.6

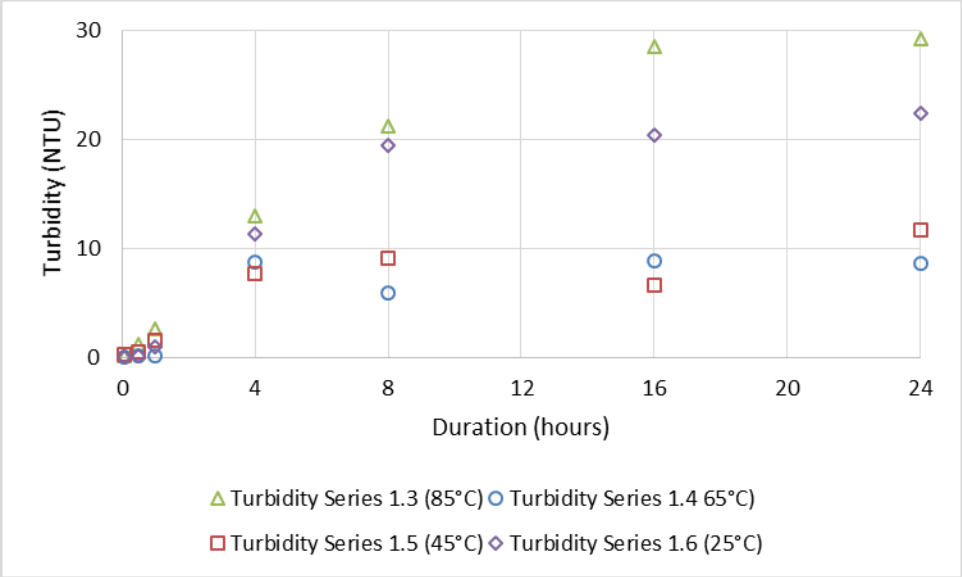

These turbidity results display interesting behavior. For the series operated at the highest temperature (Series 1.3, 85°C), the turbidity is highest, and approaches a value of 28 NTU by the twenty-fourth hour of testing. The next highest turbidity values correspond to the series operate at the *lowest* temperature (Series 1.6, 25°C), and remains at a stable value around 20-21 NTU. The remaining two series have turbidity values which are roughly equivalent, within a range of 7-11 NTU.

Solution turbidity is a good indicator of dissolved zinc at 85°C, but a poor indicator of dissolved zinc at lower temperatures (Figure 19). A ratio between turbidity (in NTU) and concentration (in mg/L) is graphically expressed. For a concentration to be accurately represented by a measured turbidity, the ratio must remain consistent. This analysis may prove to be a useful technique for estimating zinc concentration in an economical and rapid manner.

Figure 19. Theme 1 turbidity to concentration ratio

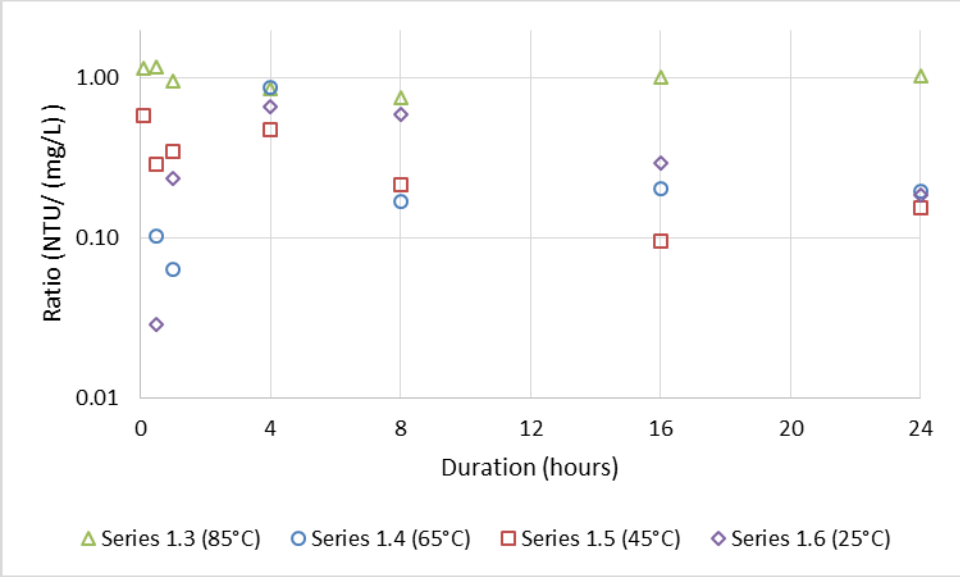

This analysis has shown that the turbidity to concentration ratio is only useful for the tests that were operated at 85°C. For Series 1.3, the percent deviation from the average turbidity is only 15%, but the other series have average with higher standard deviations. These values are shown in Table 6.

Table 6. Summary of turbidity-to-concentration ratio in Series 1.3 through 1.6

Series	Temperature (°C)	Average Turbidity to Concentration Ratio	Percent Standard Deviation
1.3	85	1.0	15%
1.4	65	0.23	126%
1.5	45	0.31	58%
1.6	25	0.29	93%

4.1.3 Theme 1 pH Analysis

Knowing the pH of a solution is a useful way of determining the relative corrosivity or causticity of a solution. All series in Theme 1 have initial chemistry that includes 220 millimolar boric acid, which naturally achieves a pH value of 4.5. The trends in pH through the course of testing is shown in Figure 20 for all tests exposed to 85°C testing solution.

Figure 20. Theme 1 testing solution final pH

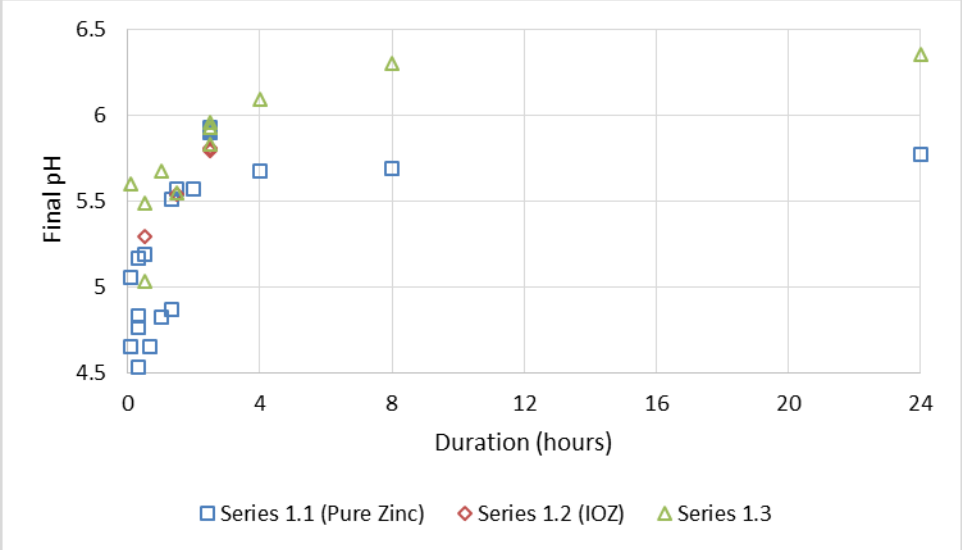

Three trends in pH have emerged from this analysis. The first of these trends may be seen during the initial period through the fourth hour of testing, where the pH is steadily and consistently increasing. The second trend is the gradual approach to a final pH value from the fourth hour to the twenty-fourth hour. The third trend is that the pH of the galvanized steel solutions is consistently higher than the pH of pure zinc tests; there is not enough data to conclude this for the IOZ solutions. This steady-state pH limit value is unique between the two sources for which this data exists, with pure zinc tests approaching pH 5.8 and galvanized steel tests approaching pH 6.3.

The general increase in pH is attributed to the consumption of hydronium by zinc as it dissolves (Equation 3). The difference between pH values for galvanized steel and pure zinc may be attributed to the presence of iron (Figure 17). As iron corrodes in acidic media, hydronium is consumed (Equation 4) in the same manner as it is for zinc, which increases the pH.

4.1.4 Theme 1 Surface Composition Analysis

EDS is a powerful tool to identify surface chemical composition. Spectral data is available for Series 1.3, 1.4, 1.5, and 1.6, and is shown in Table 7, Table 8, Table 9, and Table 10. These testing series contained galvanized steel zinc source in borated solution.

Table 7. Series 1.3 (galvanized steel) EDS spectral results in atomic percentage (%)

Testing Duration	Zinc	Oxygen	Aluminum	Iron
5 min.	100			
30 min.	100			
1 hr.	100			
4 hrs.	79.11	20.89		
8 hrs.	73.28	26.72		
16 hrs.	77.62	22.38		
24 hrs.	25.25	57.92	2.22	14.6

Table 8. Series 1.4 (galvanized steel) EDS spectral results in atomic percentage (%)

Testing Duration	Zinc	Oxygen
5 min.	100	
30 min.	100	
1 hr.	100	
4 hrs.	100	
8 hrs.	71.24	28.76
16 hrs.	75.2	24.8
24 hrs.	73.01	26.99

Table 9. Series 1.5 (galvanized steel) EDS spectral results in atomic percentage (%)

Testing Duration	Zinc	Oxygen	Aluminum
5 min.	100		
30 min.	100		
1 hr.	100		
4 hrs.	100		
8 hrs.	100		
16 hrs.	61.63	38.37	
24 hrs.	53.51	38.21	8.28

Table 10. Series 1.6 (galvanized steel) EDS spectral results in atomic percentage (%)

Testing Duration	Zinc	Oxygen	Aluminum
5 min.	100		
30 min.	100		
1 hr.	100		
4 hrs.	100		
8 hrs.	100		
16 hrs.	100		
24 hrs.	66.43	24.24	9.34

The galvanized steel coupons experience a dramatic change in elemental surface composition over the course of the testing duration. Through the first hour of testing, all of the galvanized steel surfaces maintain their pure zinc surface layer.

A zinc oxide layer develops on the surface as a function of temperature and time, starting at the fourth hour of testing in the testing series with the hottest solution. This oxide layer development corresponds with the saturation limit, discussed in Section 4.1.1.

The galvanized steel coupon surface becomes oxidized just before the solution reaches a saturation limit.

In Series. 1.3, solution saturation is achieved between the fourth and eighth hour (Table 5), and the surface composition includes high quantities of zinc and oxygen (presumably zinc oxide) by the fourth hour. In Series 1.4, a similar trend is observed: saturation is achieved between the eighth and sixteenth hour, and a surface oxide layer develops by the eighth hour. This trend is similarly observed for the other two series as well, where an oxide layer develops just before solution saturation.

The presence of aluminum and iron on the surface of the galvanized steel coupons has a simple explanation. Iron is a major component of galvanized steel, and aluminum may be a product of the underlying steel alloy corrosion. Iron is only present in the twenty-four hour sample in the hottest solution (Series 1.3), and absent from all other EDS spectrums; therefore, it is assumed that the galvanic protection on a sample of galvanized steel is compromised after twenty-four hours of exposure to 85°C borated coolant. Under such conditions, the iron-based corrosion products may also contribute to the local chemistry of the post-LOCA environment, adding to sump head loss and additional corrosion effects.

4.1.5 Theme 1 Qualitative Imaging Analysis

SEM imaging is often used to qualitatively assess surface structures and surface cleanliness. Surface imaging, taken at 1000 times magnification, is available for select tests from Series 1.1 (Figure 21 and Figure 22) and Series 1.6 (Figure 23, Figure 24, and

Figure 25). The scale on each image is 50 microns. A clean, untested coupon has been included for reference.

Figure 21. Series 1.1 SEM images, part 1/2

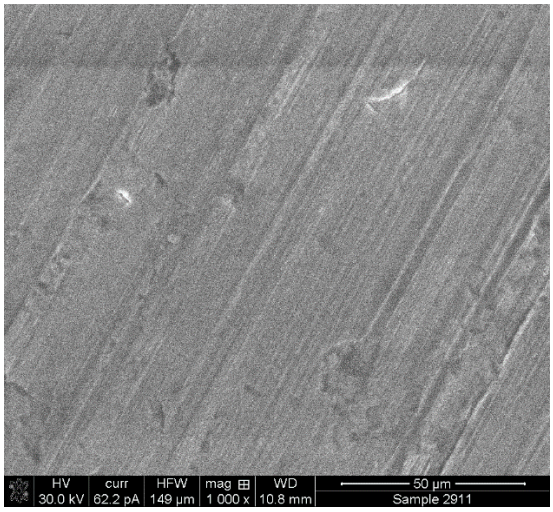

Untested surface

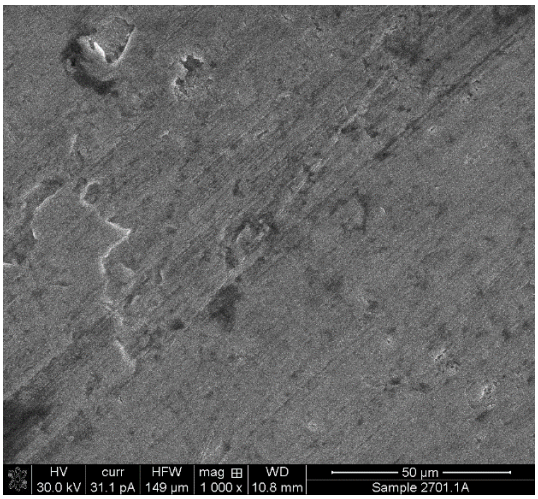

5 min. prompt testing

Figure 22. Series 1.1 SEM images, part 2/2

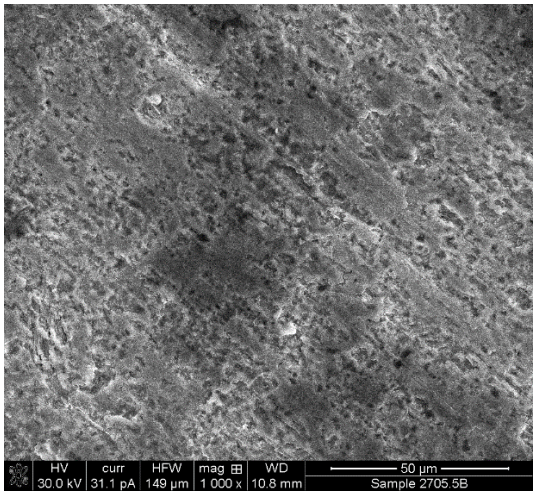

4 hrs. prompt testing

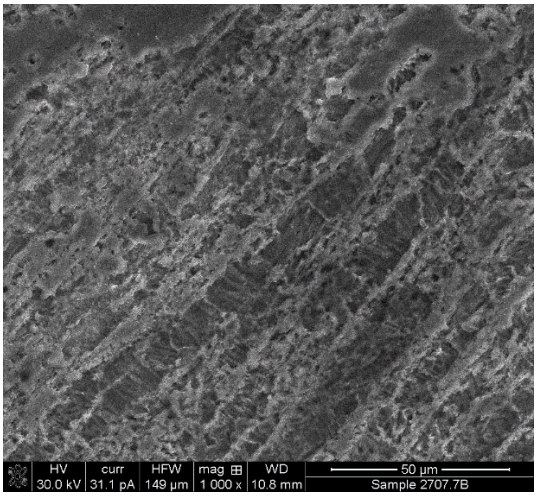

24 hrs. prompt testing

The SEM images from Series 1.1 reveals a surface texture change as a function of time. In the first five minutes of testing, the pure zinc coupon experiences slight pitting

and surface erosion, though these effects are not greatly pronounced. After four hours of exposure to boric acid, the zinc surface is exhibiting a much wider range of pitting and corrosion, with a majority of the surface experiencing some degree of destruction. By the twenty-fourth hour of exposure, the surface wear has become very pronounced, and the pitting and corrosion has started to penetrate to deeper surface levels than for shorter testing durations.

Figure 23. Series 1.6 SEM images, part 1/3

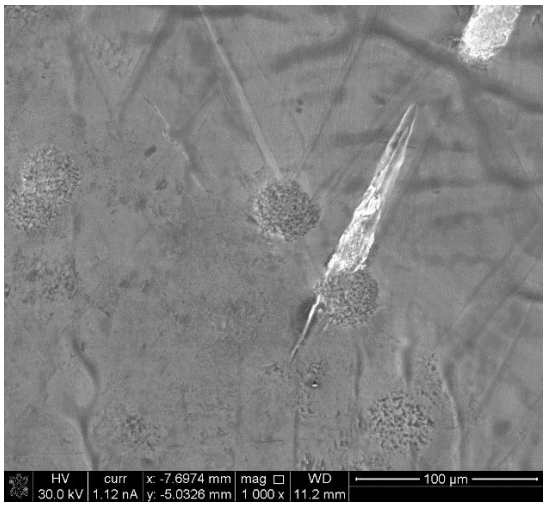

Galvanized steel, 5 min. prompt testing

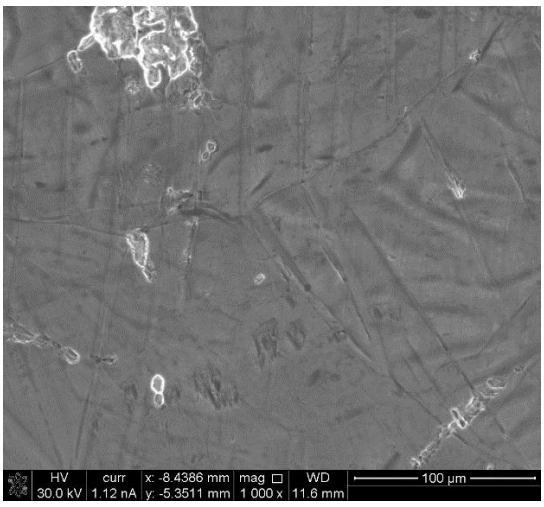

Galvanized steel, 1 hr. prompt testing

Figure 24. Series 1.6 SEM images, part 2/3

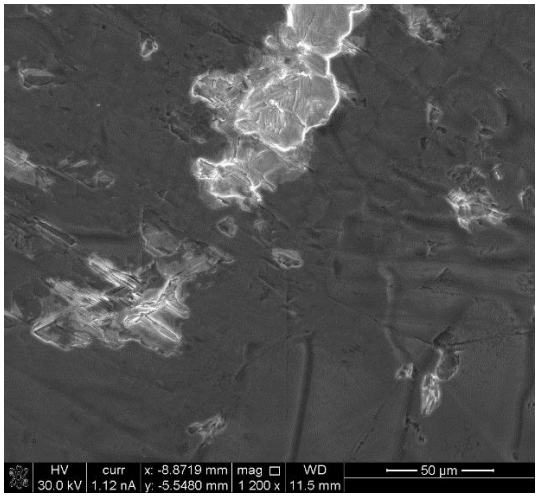

Galvanized steel, 4 hrs. prompt testing

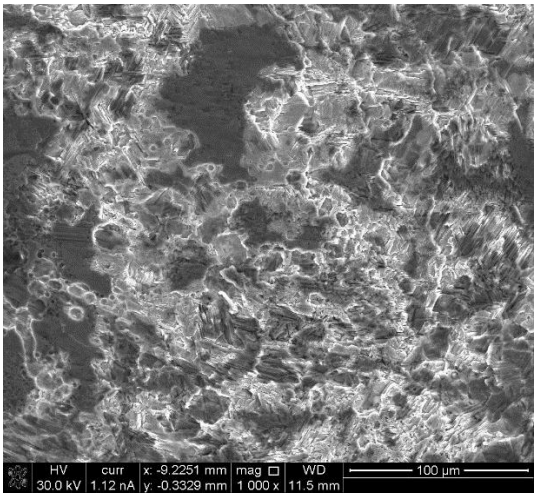

Galvanized steel, 8 hrs. prompt testing

Figure 25. Series 1.6 SEM images, part 3/3

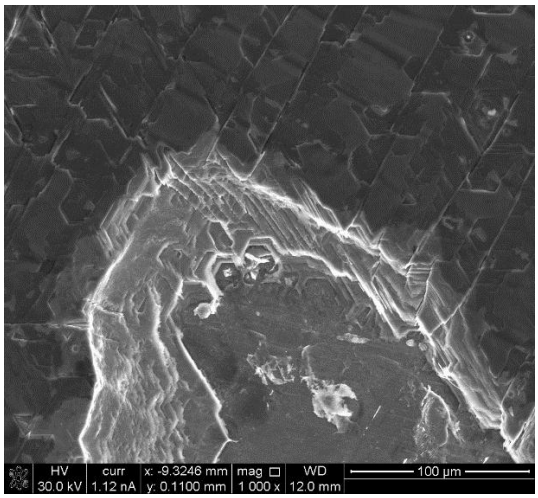

Galvanized steel, 16 hrs. prompt testing

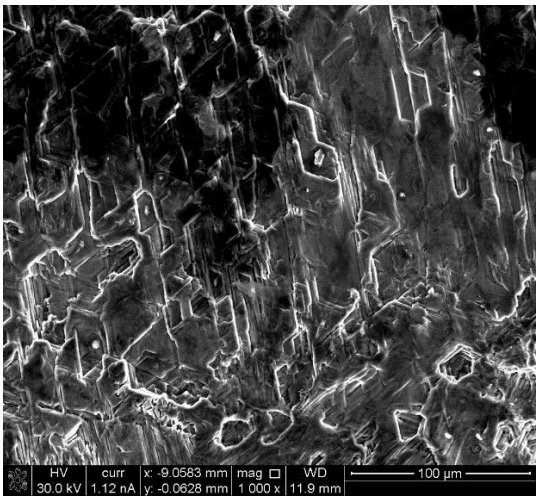

Galvanized steel, 24 hrs. prompt testing

The samples in Figure 23, Figure 24, and Figure 25 show the evolution of surface corrosion and dissolution on galvanized steel coupon exposed to boric acid at 25°C (Series 1.6). Similar to the Series 1.1 SEM imaging, Series 1.6 images show a progression of surface dissolution as a function of time. After five minutes of testing, the surface shows

clustered pitting. These pits are the source of zinc that was measured and discussed in Section 4.1.1. The pitting has grown by the thirtieth minute of testing to reveal larger swaths of dissolved zinc. This effect is progressively more pronounced through the remainder of testing durations.

An interesting transition occurs at the sixteenth hour of testing. Here, the large swaths of corroded surface layers have merged into an increasingly large pit. At the twenty-fourth hour, the surface begins to break down further, losing any real coherent structure. EDS analysis confirmed that the underlying steel layers were not detected for these tests.

A curious feature of the removal of surface layers is the revelation of hexagonal pitting formations. This is especially pronounced in the sixteen-hour test. This hexagonal pitting is attributed to the hexagonal close packed crystal structure of metallic zinc. However, these hexagonal pitting structures are only present in galvanized steel coupon samples; none were discovered in pure zinc coupons for tests in any Theme. It is therefore presumed that the hexagonal wear is either an artifact of the hot-dipping process for galvanized steel coupons, or obscured by trace metal additions in the pure zinc alloy, which is 99.6% pure.

4.2 Theme 2: Zinc Phosphate Solubility and Precipitation

The second testing theme studied the interaction of containment zinc sources with a coolant solution that is buffered by TSP, and how the release and corrosion are effected by the

presence of the buffer. Table 11 shows a summary of the testing matrix. Additional details for these tests are provided in Section 3.1.5.2.

Table 11. Theme 2 testing matrix

Series	Zinc Source	TSP	Operating Temperature	Baseline pH	Testing Duration
2.1	Pure Zinc	10 mM	85°C	7.3	30 min. – 10 days
2.2	Pure Zinc	10 mM	60°C	7.3	30 min. – 2.5 hrs.
2.3	Pure Zinc	5.58 mM	85°C	7.0	24 hrs. – 5 days
2.4	Pure Zinc	10 mM	85°C	6.8	30 min. – 10 days
2.5	Pure Zinc	10 mM	85°C	7.8	30 min. – 10 days
2.6	Galvanized Steel	10 mM	85°C	7.3	30 min. – 10 days
2.7	IOZ	10 mM	85°C	7.3	30 min. – 10 days

4.2.1 Theme 2 Zinc Release Analysis

Zinc release was measured through ICP by HEAL, as described in Section 4.1.1. Figure 26 shows the zinc release results for all tests from Series 2.1, which were conducted at 85°C and with 10 millimolar TSP concentration.

Figure 26. Series 2.1 zinc release

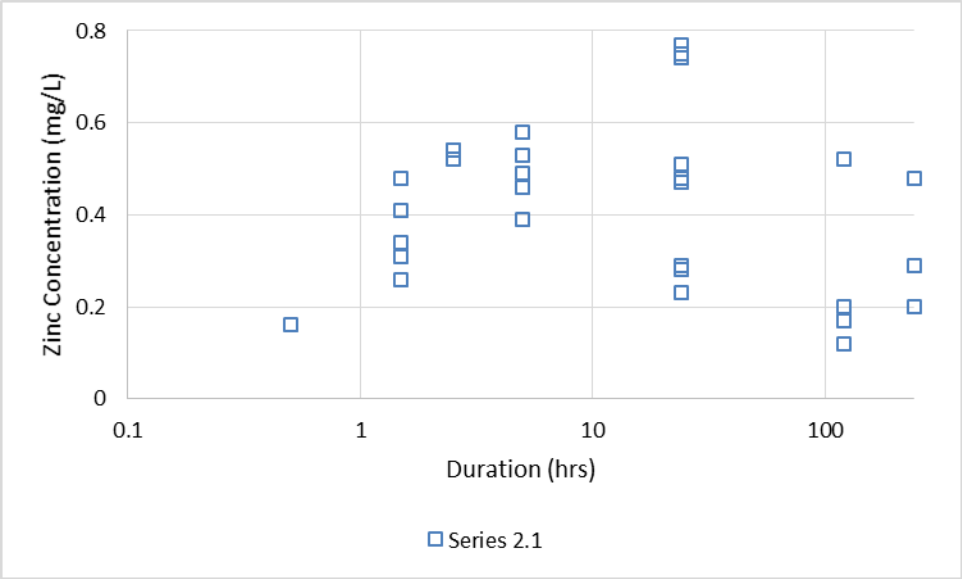

From this series of testing, a few general trends in zinc dissolution become evident. The first trend is that through the first 2.5 hours of testing, the dissolved zinc concentration is consistently increasing. The second trend begins at the fifth hour, and continues until the testing was completed at the tenth day. Here, the dissolved zinc concentration tended to vary greatly. At the twenty-fourth hour, the range of concentrations spanned from 0.23 mg/L to 0.77 mg/L, but are nevertheless bounded in the 0.2 to 0.8 mg/L range.

The final trend is the expression of competing mechanisms throughout the duration of testing. These mechanisms are the dissolution of zinc from the metallic coupon and the removal of zinc from solution via precipitation. In the first 2.5 hours of testing, release is the dominant mechanism for zinc activities; however, at later times, there is a release-precipitation equilibrium that has begun to be established.

Another trend of note is the magnitude of the zinc concentration in solution. For all durations, the concentration of zinc in solution is bounded by 0.1 mg/L and 0.8 mg/L,

which is markedly lower than the concentration of dissolved zinc as seen in the un-buffered tests from Theme 1. A concentration of 1 mg/L dissolved zinc was achieved—and surpassed—within the first thirty minutes of testing in all series from Theme 1 tests, and the concentration after twenty-four hours reached as high as 120 mg/L.

This stark difference in concentration may be attributed to several factors, including, but not limited to, the presence of trisodium phosphate buffer and the pH of the testing solution. The saturation limit of dissolved zinc under these conditions may be inferred from this data to be roughly 0.8 mg/L. This compares reasonably well with the solubility limit calculated in Chapter 2, which was approximately 0.1 mg/L.

Series 2.2 was designed to show how zinc dissolution responds to a temperature change, similar to the objectives of Theme 1 tests in Series 1.3, 1.4, 1.5, 1.6, but on a reduced scale. The concentration measurements from Series 2.2 are overlaid on the results of Series 2.1 in Figure 27, below.

Figure 27. Series 2.2 zinc release

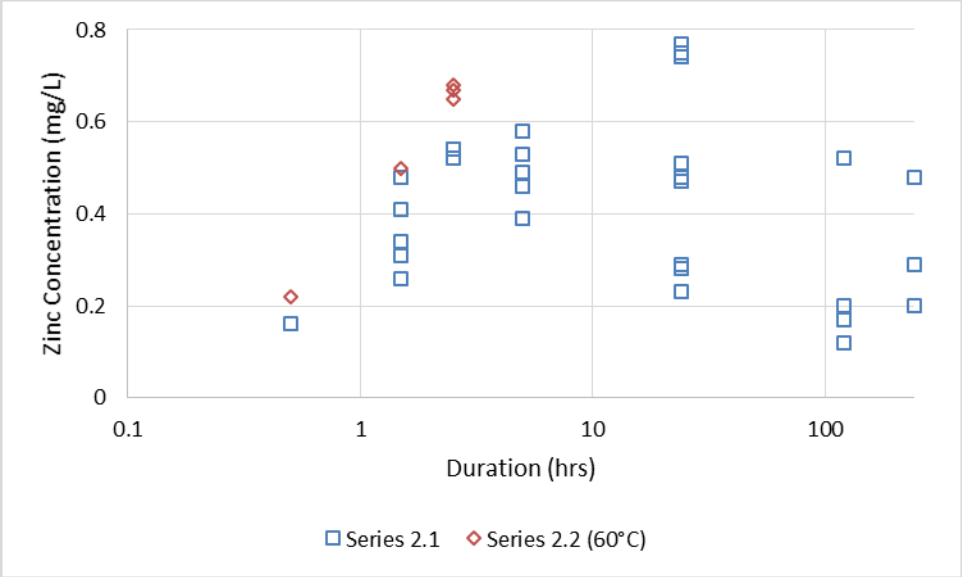

The measured zinc concentration results from Series 2.2 have shown that dissolved zinc concentration follows a pattern of retrograde solubility. This is a similar result to what was observed with Series 1.3 through 1.6 in Theme 1 testing (Section 4.1.1). With all available data at each available testing duration, the concentration of dissolved zinc in Series 2.2 is greater than the concentration measured in Series 2.1.

There is insufficient data to determine the saturation limit under these conditions. The retrograde solubility behavior of zinc would indicate that as the temperature decreases further, the solubility limit of dissolved zinc should continue to increase. This is observed in Series 2.1.

To test the effect that a different concentration of trisodium phosphate would have on zinc release and solubility, Series 2.3 was designed. The tests in Series 2.3 were conducted with 5.58 millimolar TSP. This change in TSP concentration resulted in a pH shift from 7.3 (10 mM TSP) to 7.0 (5.58 mM); this will be discussed in more detail in Section 4.2.3. The concentration measurements from Series 2.3 are overlaid on the results of Series 2.1 in Figure 28, below.

Figure 28. Series 2.3 zinc release

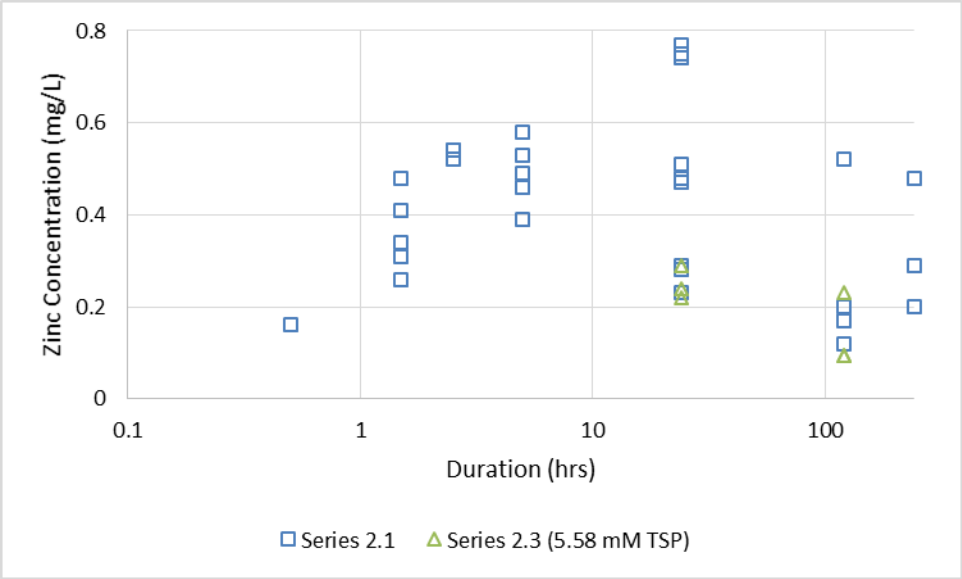

The measured zinc concentration for Series 2.3 testing shown that the results are not strongly influenced by either 10 or 5.58 millimolar TSP concentrations. This is a predictable conclusion, because trisodium phosphate is present in a great excess in either case. The phosphate concentrations of 5.58 and 10 millimolar are equivalent to 530 mg/L and 950 mg/L phosphate, respectively. The limiting reactant in zinc phosphate formation—the primary mechanism to remove zinc from solution using phosphate—is dissolved zinc.

An observation of note is that the concentration of dissolved zinc in Series 2.3 tends to be toward the lower limit of zinc concentration from Series 2.1. There is insufficient data to resolve this potential trend conclusively. One possible explanation may be that this observation is an artifact of the lower solution pH in Series 2.3.

Additional tests were performed in Series 2.4 and 2.5 to investigate the effect of changing the pH without altering the TSP concentration. Hydrochloric acid (HCl) and

sodium hydroxide were used to lower or raise the pH by 0.5 units in Series 2.4 and 2.5, respectively. These series are discussed in greater detail in Section 3.1.5.2. The concentration measurements from Series 2.4 and 2.5 are overlaid on the results of Series 2.1 in Figure 29, below.

Figure 29. Series 2.4 and 2.5 zinc release

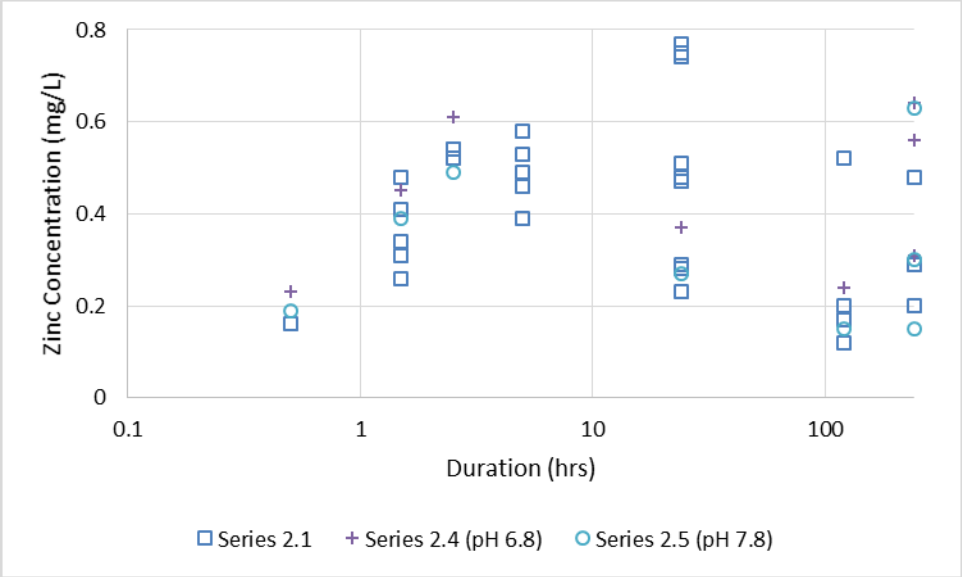

The measured zinc concentration for Series 2.4 and 2.5 testing show that the results are not strongly influenced by a pH shift of 0.5 units. For testing durations up to, and including, 5 days, the zinc concentration in Series 2.4 is greater than the dissolved zinc concentration in Series 2.5, through both also tend to be within the range established with Series 2.1 tests at pH 7.3. For tests with durations of ten days, there is a high degree of variability in the measured dissolved zinc concentrations. As discussed previously, this effect may be attributed to the competing mechanisms of dissolution and precipitation.

The final two series of Theme 1 testing were designed to see if the results found with pure zinc tests are comparable to the sources of zinc found in containment: IOZ and galvanized steel. The concentration measurements from Series 2.6 and 2.7 are overlaid on the results of Series 2.1 in Figure 30, below.

Figure 30. Series 2.6 and 2.7 zinc release

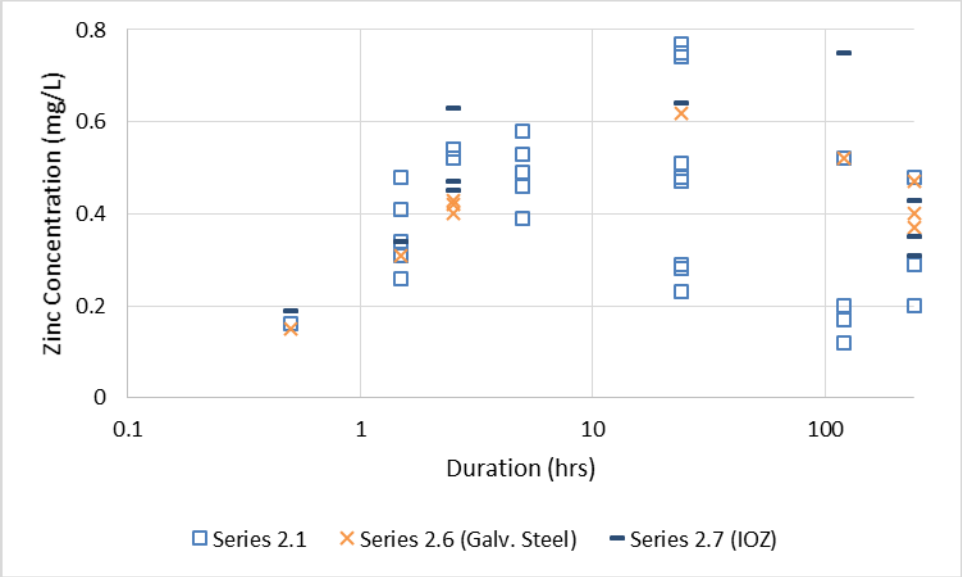

The measured zinc concentration for Series 2.6 and 2.7 testing show that the results are not strongly influenced by the source of zinc. For testing durations up to, and including, 5 days, the zinc concentration in Series 2.7 is greater than the dissolved zinc concentration in Series 2.6, through both also tend to be within the range established with Series 2.1 using pure zinc coupons. There are two testing durations for which the release from Series 2.7 exceeds the release from pure zinc coupons—at 2.5 hours and at 5 days—however, the measured dissolved zinc concentration is still bounded by the limits establish by Series 2.1: 0.1 mg/L and 0.8 mg/L.

The measured concentrations for all tests in Theme 1 series are included in Figure 31.

Figure 31. Theme 2 series zinc release

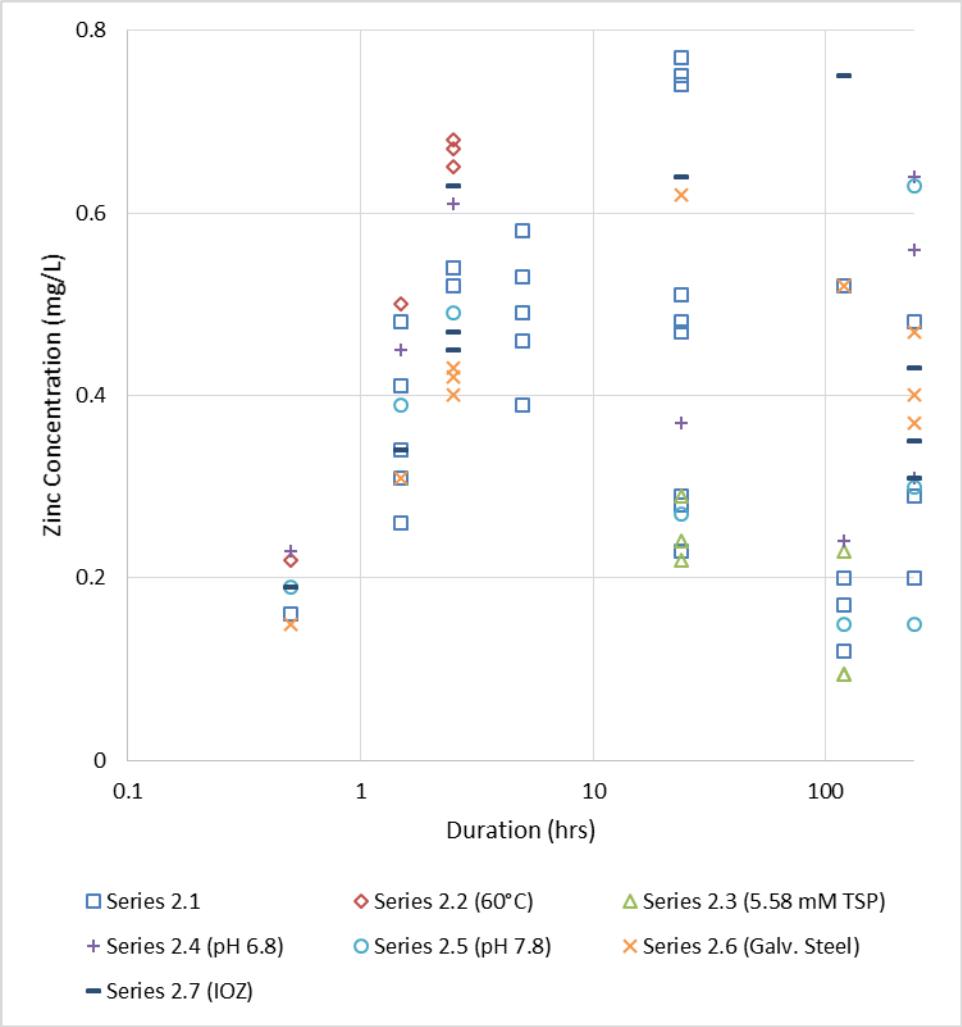

4.2.2 Theme 2 Turbidity Analysis

Turbidity data for Theme 2 tests is available from select tests in Series 2.1 and 2.6. These turbidity measurements are shown in Figure 32. An interesting trend that has

emerged from this analysis is that the turbidity measurements (in NTU) is bounded by the same limits that dissolved zinc concentration was bounded by (in mg/L). These bounds are 0.1 NTU and 0.8 NTU.

Figure 32. Theme 2 turbidity

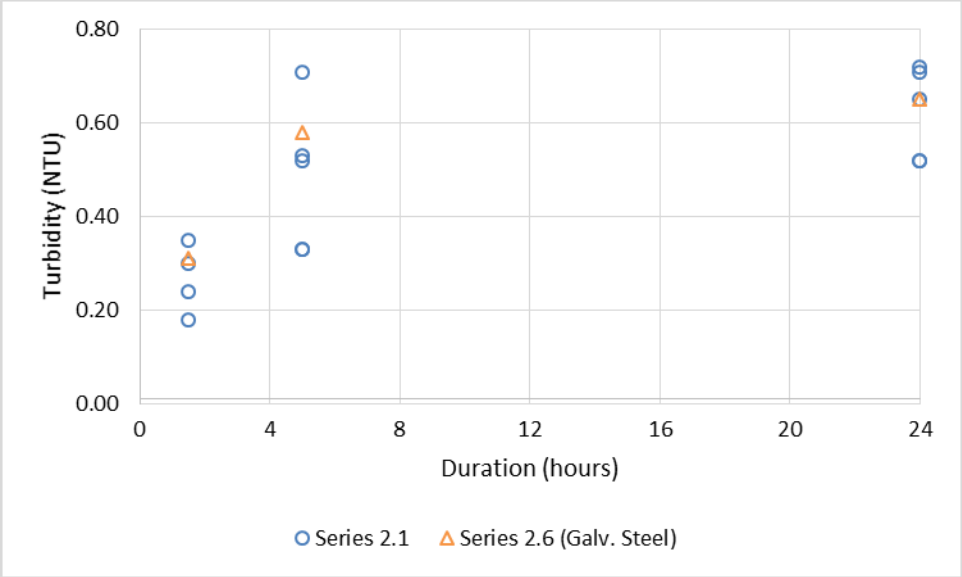

These results suggest that solution turbidity may be a good indicator for dissolved zinc, as was the case for Series 1.3 in Theme 1 testing. A ratio between turbidity (in NTU) and concentration (in mg/L) is graphically expressed in Figure 33, similar to what was done for Series 1.3-1.6 in Section 4.1.2.

Figure 33. Theme 2 turbidity to concentration ratio

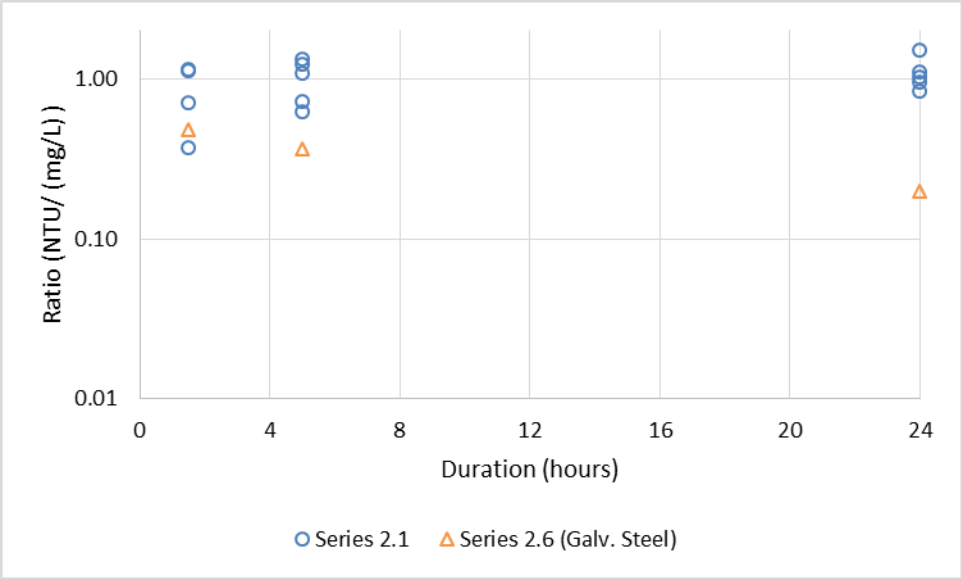

This analysis has shown that the turbidity to concentration ratio is only useful for the tests in Series 2.1, which had pure zinc as the zinc source. This analysis is most useful when the turbidity to concentration ratio tends toward 1. Additional analysis of this data may be found in Table 12.

Table 12. Summary of turbidity-to-concentration ratio in Series 2.1 and 2.6

Series	Zinc Source	Duration (hours)	Average Turbidity to Concentration Ratio	Percent Standard Deviation
2.1	Pure Zinc	All	0.98	31%
2.6	Galvanized Steel	All	0.35	45%

The analysis in Table 12 has shown that using a turbidity measurement to estimate dissolved zinc is more useful with a pure zinc source than for a galvanized steel source.

4.2.3 Theme 2 pH Analysis

All series in Theme 2 have initial chemistry which includes 220 millimolar boric acid and either 5.58 or 10 millimolar TSP, which naturally settles at a pH value of 7.0 to 7.3. Series 2.4 and 2.5 have pH adjusting chemicals (HCl or NaOH) which adjusts this natural pH value by 0.5 pH units. The trends in pH through the course of testing are shown in Figure 34 for all tests.

Figure 34. Theme 2 final pH measurements

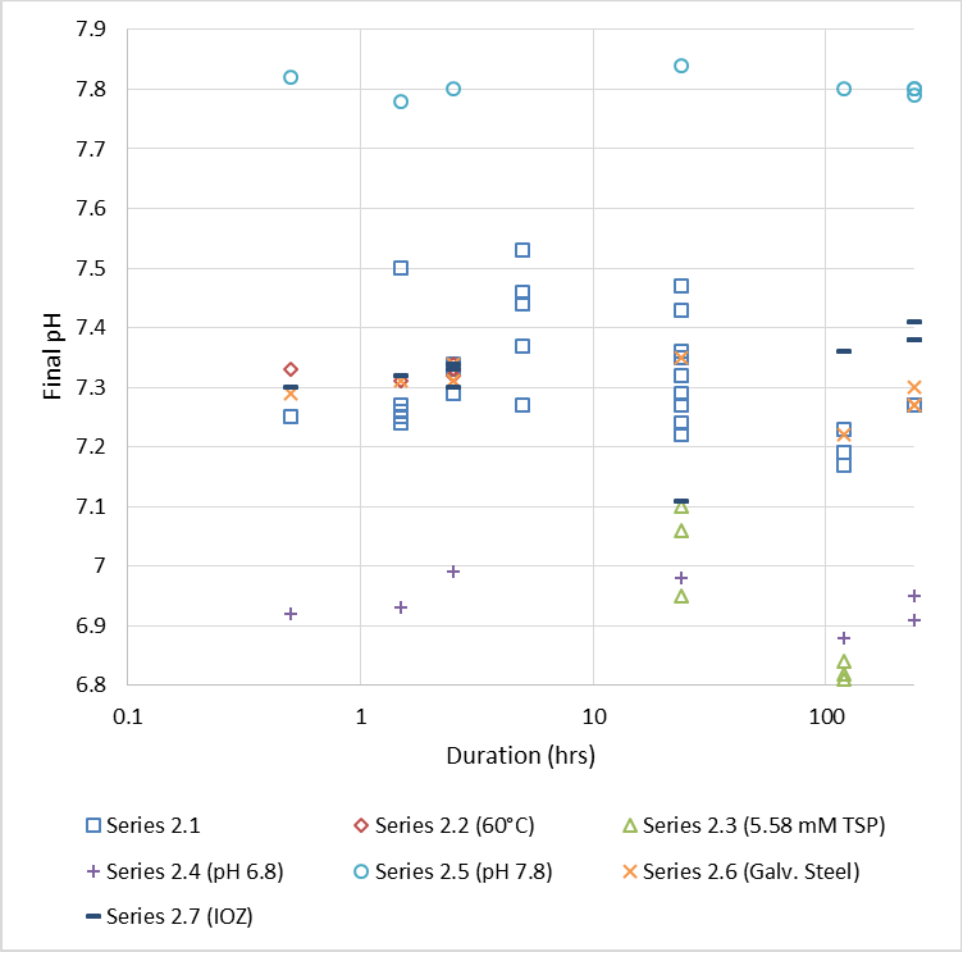

Tests with an initial pH of 7.3, which include Series 2.1, 2.2, 2.6 and 2.7, will be analyzed separate from the other series. The final pH of these tests remains within the pH bounds of 7.1 and 7.55 for all testing durations, with most of the tests remaining between 7.2 and 7.4. The observed fluctuations are within +/- 0.2 pH units of the initial pH, and may be attributed to the stochastic behavior of the chemical environment, or attributed to the measuring sensitivity of the pH meter used.

Series 2.3 tests had an initial pH of 7.0. When the pH was sampled after 24 hours of testing, the pH remained within 0.1 pH units of the initial pH. After 5 days of testing, however, a consistent drop in the pH to a range of 6.80 to 6.85 was observed. The drop in pH may be attributed to the reduced buffering capacity of phosphate upon its consumption while forming zinc phosphate precipitate.

Series 2.4 and 2.5 has initial solution pH values of 6.8 and 7.8, respectively. Series 2.4 (pH 6.8) saw an increase in pH by 0.1 to 0.2 pH units. Series 2.5 (pH 7.8) tended to remain very close to the initial pH, remaining within 0.05 pH units of the initial pH. In all series, the buffering capacity of phosphate is shown. Large changes in pH were observed in Theme 1 testing (Section 4.1.3), when no phosphate was present.

4.2.4 Theme 2 Surface Composition Analysis

Spectral data from EDS analysis is available for select tests in Series 2.1, 2.3, and 2.6. The matrix of available data is outlined in Table 13. The available EDS spectral data is shown in Table 14.

Table 13. Available EDS spectral results for Theme 2 testing

Series	Zinc Source	TSP	testing Temperature	Baseline pH	EDS Spectrum Available For Testing Durations
2.1	Pure Zinc	10mM	85°C	7.3	2.5 hours, 24 hours, 10 days
2.3	Pure Zinc	5.58mM	85°C	7.0	24 hours, 5 days
2.6	Galvanized Steel	10 mM	85°C	7.3	2.5 hours, 10 days

Table 14. Theme 2 EDS spectral results in atomic percentage (%)

Testing Series	Testing Duration	Zinc	Oxygen	Phosphorus	Aluminum
2.1	2.5 hours	72	24	3.4	
2.1	24 hours	40	52	8	
2.1	10 days	24	58	17	
2.3	24 hours	36	49	12	
2.3	5 days	34	53	12	
2.6	2.5 hours	70	25	1.8	1.4
2.6	10 days	19	58	8.5	2

To show the progression of surface scale development, the spectral results are shown in Figure 35, Figure 36, and Figure 37.

Figure 35. Series 2.1 (pure zinc) EDS spectral results

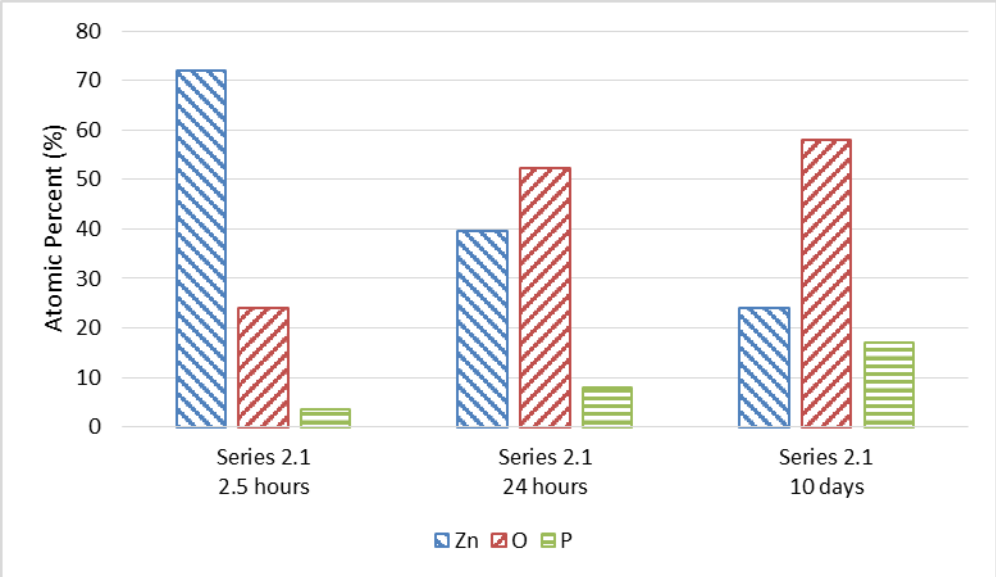

Figure 36. Series 2.3 (pure zinc) EDS spectral results

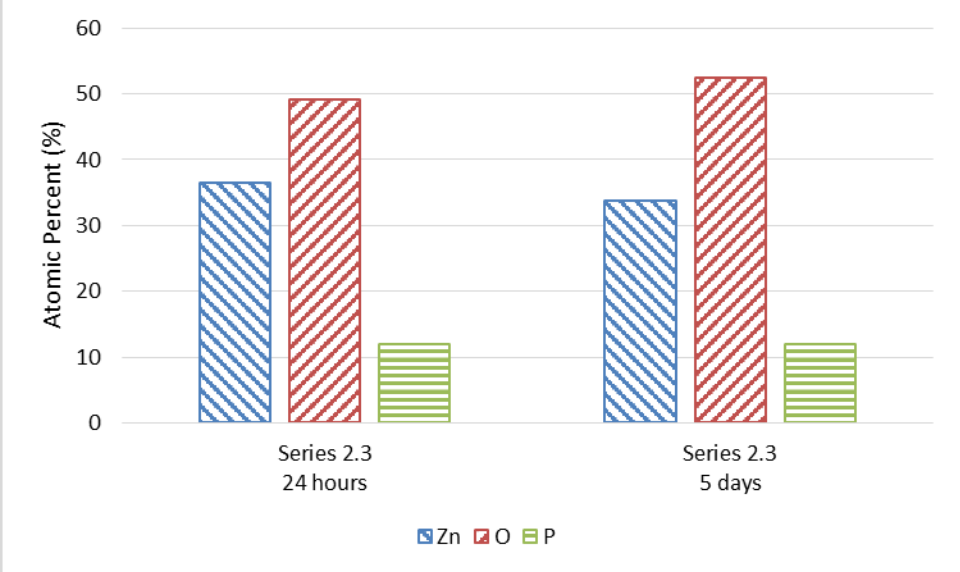

Figure 37. Series 2.6 (galvanized steel) EDS spectral results

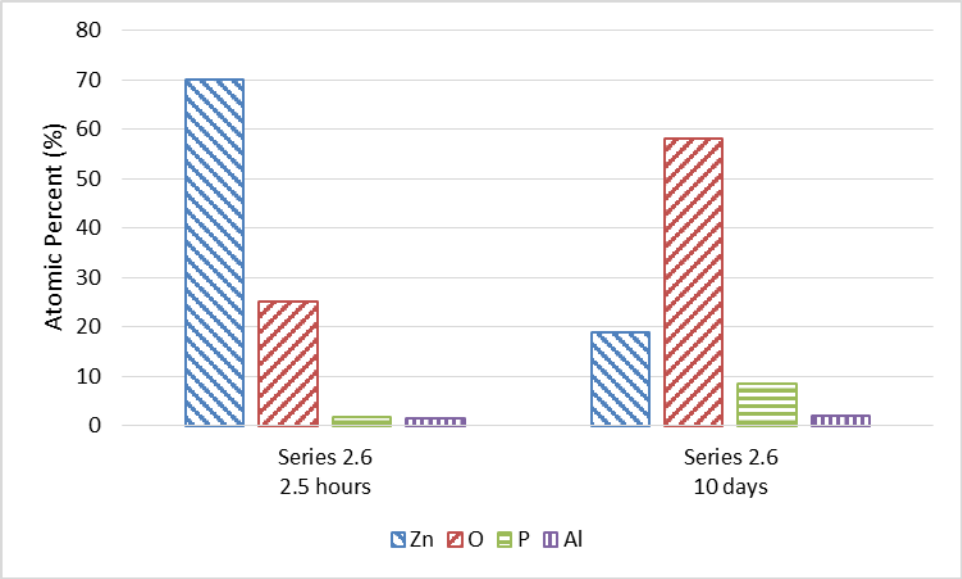

A few trends of note have emerged from the spectral analysis. In Series 2.1 (Figure 35), the decreasing surface composition of zinc corresponds with an increase in surface composition of both phosphorus and oxygen. This has shown that as exposure time to the solution increases, more zinc phosphate product precipitates onto the surface. This corresponds with the zinc concentration data in Section 4.2.1, which shows that the average dissolved zinc concentration decreases from the twenty-fourth hour to the tenth day of testing. The decrease in concentration is therefore attributed to zinc phosphate precipitation, and nucleation on the surface of the original zinc coupon.

In Series 2.3 (Figure 36), the surface composition between the twenty-fourth hour and fifth day of testing remains essentially constant. This leads to the conclusion that precipitation of phosphate-bearing chemical products onto the surface of the coupon ceases by the twenty-fourth hour of testing. The dissolved zinc concentration data was insufficient to conclusively determine a trend in zinc concentration; however, this EDS analysis

confirms that if additional zinc precipitation occurs beyond the twenty-fourth hour, the precipitation products remain in solution, either suspended or as a solid product.

In Series 2.6 (Figure 37), a trend similar to what was observed with Series 2.1 is seen. From the first 2.5 hours of testing through the tenth day of testing, the decreasing surface composition of zinc corresponds with an increase of both phosphorus and oxygen. This again suggests that zinc phosphate precipitation products are nucleating on the original galvanized steel coupon. The presence of trace aluminum has been discussed in Section 4.1.4—aluminum may be a product of the decomposition of the underlying steel in the galvanized steel coupons.

4.2.5 Theme 2 Qualitative Imaging Analysis

Surface imaging from SEM analysis is available for select tests in Series 2.1 and 2.3. All Theme 2 surface imaging was performed at 1000 times magnification, and is found in Figure 38 and Figure 39.

Figure 38. Series 2.1 SEM images

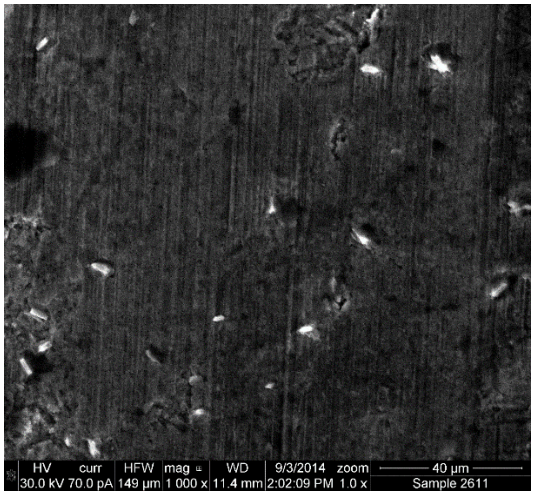

Pure zinc, 24 hrs. testing, 10 mM TSP

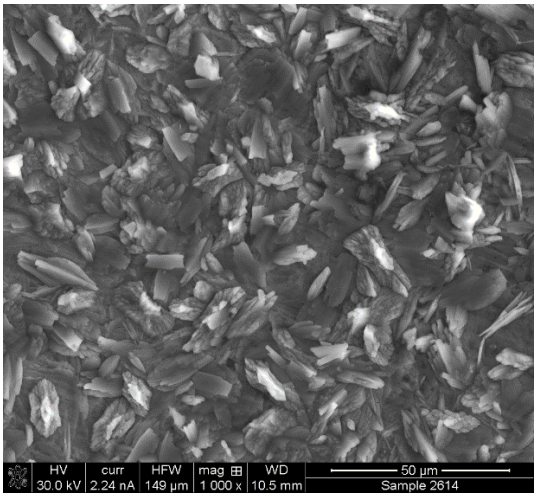

Pure zinc, 5 days testing, 10mM TSP

Figure 39. Series 2.3 SEM images

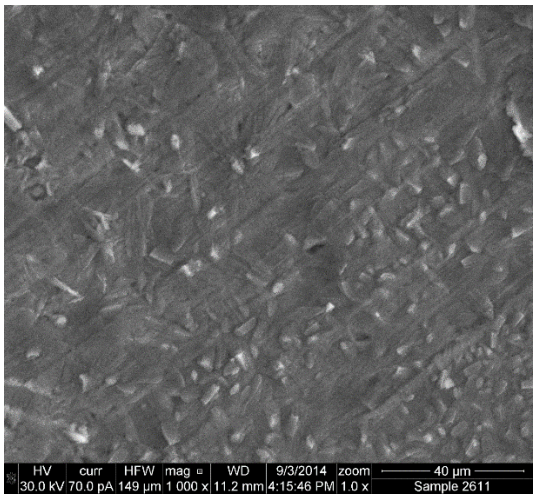

Pure zinc, 24 hrs. testing, 5.58 mM TSP

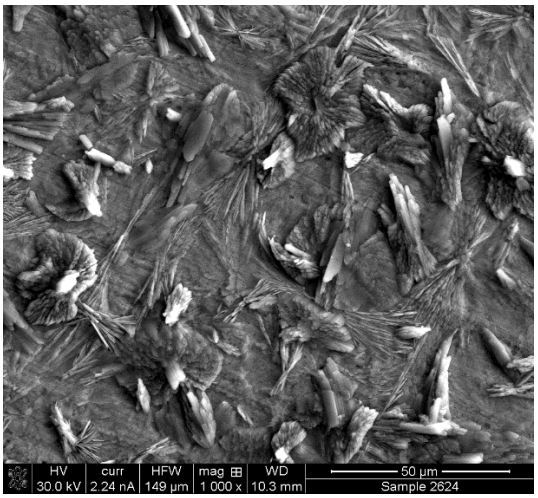

Pure zinc, 5 days testing, 5.58 mM TSP

Figure 38 and Figure 39 show that the scale layers on the zinc coupon samples continue to develop through the fifth day. In both series, which are defined by the concentration of TSP added to the testing solution, the samples begin with small, isolated scale deposits. By the fifth day of testing, the isolated scale deposits have merged and

grown into larger scale structures. EDS spectral results have shown the identity of these scale deposits to be primarily comprised of zinc, phosphorus, and oxygen, likely zinc phosphate.

4.3 Theme 3: Zinc Phosphate Formation with TSP Addition after Prompt Release Phase

For the tests in the third testing Theme, the concepts of the first two themes were combined. Sources of zinc were exposed initially to borated, unbuffered, testing solutions. After a prescribed duration, TSP buffer was added to the solution. Table 15 shows a summary of the testing matrix. Table 16 describes the three TSP addition techniques. Additional details for these tests is provided in Section 3.1.5.3.

Table 15. Theme 3 testing matrix

Series	Zinc Source	Final TSP	TSP Addition Technique	Operating Temperature	Testing Duration
3.1	Pure Zinc	10 mM	A	85°C	24 hours
3.2	Pure Zinc	5.58 mM	A	85°C	24 hours
3.3	Galvanized Steel	5.83 mM	B	85°C	2 days
3.4	Galvanized Steel	5.83 mM	C	85°C	2 days
3.5	Galvanized Steel	5.83 mM	B	65°C	2 days
3.6	Galvanized Steel	5.83 mM	C	65°C	2 days
3.7	Galvanized Steel	5.83 mM	B	45°C	2 days
3.8	Galvanized Steel	5.83 mM	C	45°C	2 days
3.9	Galvanized Steel	5.83 mM	B	25°C	2 days
3.10	Galvanized Steel	5.83 mM	C	25°C	2 days

Table 16. TSP addition techniques for Theme 3 tests

TSP Addition Technique	TSP Addition Time	TSP Addition Amount	Number of Additions	Other Notes
A	20, 40, and 60 min.	1/3 of final concentration	3	Coupon left in solution
B	5 or 30 min., or 1, 4, 8, 16, or 24 hrs.	All at once	1	Coupon left in solution
C	5 or 30 min., or 1, 4, 8, 16, or 24 hrs.	All at once	1	Coupon removed from solution prior to TSP addition

4.3.1 Theme 3 Zinc Release Analysis

Zinc release was measured through ICP by HEAL, as described in Section 4.1.1. Figure 40 and Figure 41 show the zinc release results for Series 3.1 and 3.2, along with the TSP concentration at the corresponding sampling times. These two series utilized TSP addition technique A, which involved a gradual increase in TSP concentration during the early stages of testing.

Figure 40. Series 3.1 zinc release

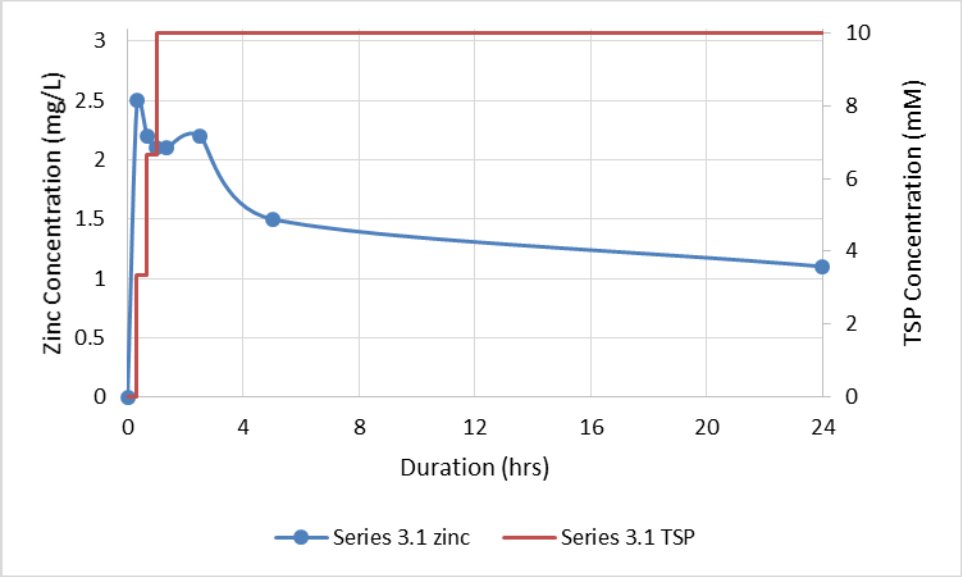

Figure 41. Series 3.2 zinc release

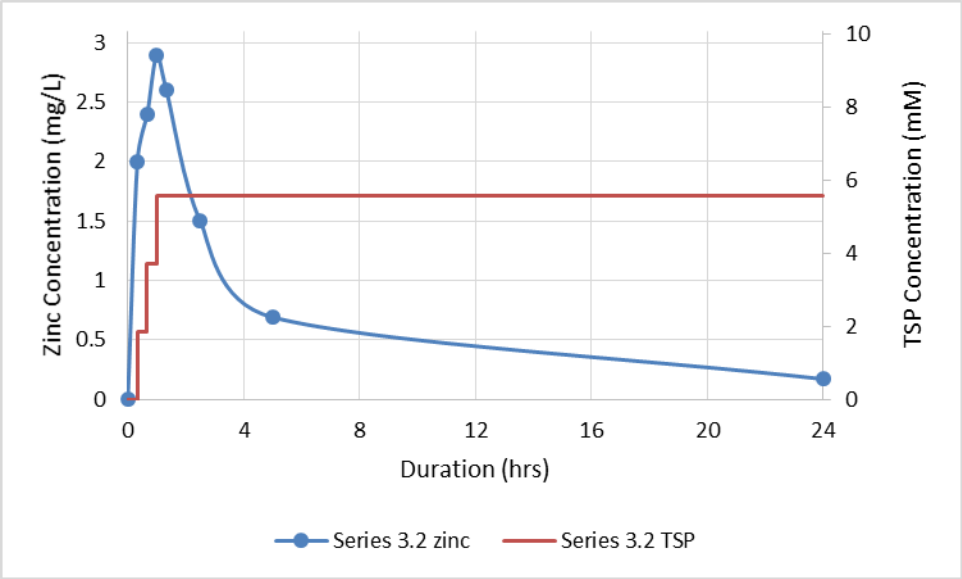

Striking similarities exist between both of these series. In each case, the concentration of dissolved zinc experienced a sharp increase while the tests were unbuffered, achieving a concentration of 2.5 mg/L and 2.0 mg/L in Series 3.1 and 3.2, respectively. This trend was expected from the results of Theme 1 testing. Another similarity between these tests is that the addition of TSP into the solution has an immediate impact on the release and precipitation of dissolved zinc, with consecutive additions of TSP resulting in a more dramatic response by the dissolved zinc; this is especially evident in Series 3.2. The last similarity between these two series is the final trend of dissolved zinc, which in both cases, falls to be approximately within range of the dissolved zinc concentrations from Theme 2 testing. But what make these tests unique is their differences.

In Series 3.1, the release of zinc into solution is the dominant mechanism only when there is no TSP present; once TSP is added (3.33 mM TSP), the concentration of dissolved zinc begins decreasing, indicating that the precipitation mechanism begins to dominate

release. These results contrast with Series 3.2, where zinc continues to release into solution after the first addition of TSP, albeit at a decreased rate. The maximum dissolved zinc concentration is not defined in Series 3.2 until the final dose of TSP is added, which reveals a local maximum in zinc concentration at 60 minutes. After the requisite quantity of TSP is added to the solution in all tests, the zinc concentration continues to trend lower.

The reaction to the TSP additions is unique between tests. From the time that the maximum dissolved zinc concentration is achieved until the fifth hour of testing, the differences between these series become evident. In Series 3.1, the zinc concentration reduces from 2.5 to 1.5 within the first five hours of testing, and finally to a value of 1.1 mg/L by the twenty-fourth hour. In Series 3.2, however, the higher maximum of 3.0 mg/L decreases to 0.69 mg/L by the fifth hour, and falls even more to 0.17 mg/L by the twenty-fourth hour.

This behavior may be a result of the high sensitivity of chemical precipitation to factors such as phosphate concentration, zinc availability, and precipitate nucleation site availability. The series with the greatest zinc concentration fell to a lower zinc concentration more rapidly, suggesting that the difference between the two maxima of the series represents a requite threshold of zinc concentration necessary to induce precipitation. Surface precipitation will be discussed in greater detail in Section 4.3.4.

Testing Series 3.3 through 3.10 depart from the testing conditions in Series 3.1 and 3.2. Galvanized steel is chosen as the source of zinc, four different temperatures are used, and buffer addition occurs all at once. With even-numbered series, beginning with 3.4, the source of zinc is removed prior to buffer addition to compare precipitation with and without a zinc source coupon present. Figure 42-Figure 45 show the measured dissolved zinc

concentration of Series 3.3 through 3.10. Also included in these figures is the corresponding prompt release data from Series 1.3 through 1.6. Each yellow or blue colored line represents a single test in a given series. The data for these lines exists at their origin on the red curve—the prompt release series which corresponds to the series included in the plot—and at the final shown then the duration has reached 48 hours. The lines are added as a visual guide between the two points on the prompt release curve and at 48 hours, but do not necessarily inform about the release profile.

Figure 42. Series 3.3 and 3.4 (85°C) zinc concentration

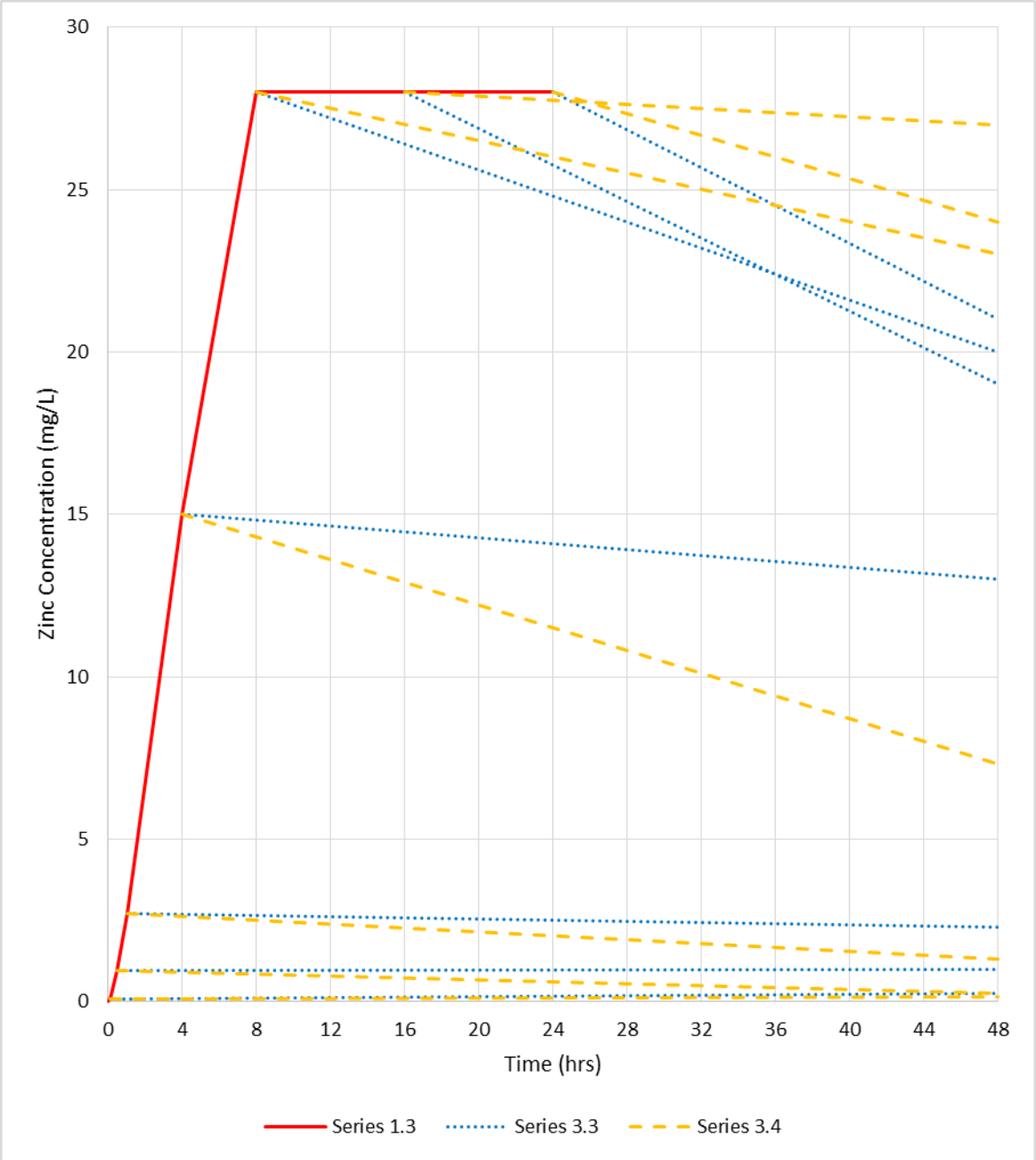

Dissolved zinc precipitation follows a few key trends in Series 3.3 and 3.4. In Series 3.3, zinc in solution decreased in solution for all tests that were exposed to boric-acid-only solution for greater than thirty minutes prior to TSP addition. This suggests that

zinc phosphate precipitation occurs, but surface analysis is required to determine if precipitation occurs in solution or on the coupon surface. Adding TSP after 30 minutes (or less) of prompt release testing is not sufficient to stop zinc release, which suggests that precipitation is dominated by release.

In Series 3.4, zinc concentration decreased in solution for all (see exception, below) tests following TSP addition. This suggests that zinc phosphate precipitates in solution, and may be available to interact the ECCS sump pump debris beds. The only exception to this observation occurs during the test where TSP was added after only five minutes of exposure. However, the difference between the prompt release point and the datum at forty-eight hours of testing is 0.05 mg/L, which is within the reportability limit of HEAL's ICP report.

When comparing Series 3.3 with 3.4, more trends in precipitation emerge. When TSP is added to the solution after eight hours or less of boric acid-only exposure, zinc removal by precipitation is greatest when no coupon is present. This suggests that surface precipitation may be competing with release when a coupon sample is present. However, beyond eight hours of boric acid-only testing, when TSP is added, precipitation is greatest when the coupon is present. This suggests that with a high enough zinc concentration under these testing conditions, a galvanized steel coupon promotes precipitation.

Figure 43. Series 3.5 and 3.6 (65°C) zinc concentration

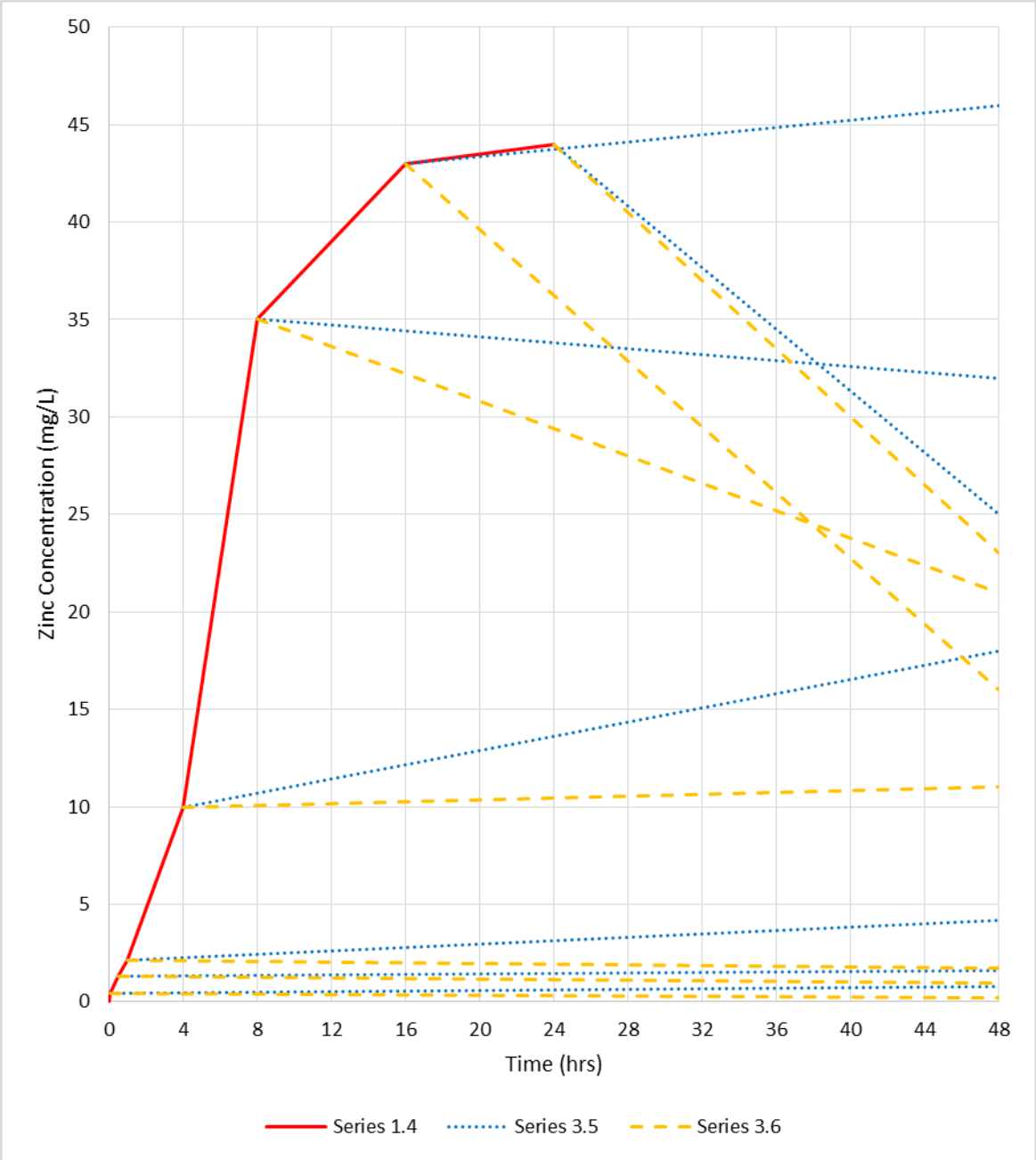

Zinc removal by precipitation appears to be less orderly in Series 3.5 and 3.6 when compared with Series 3.3 and 3.4. The precipitation of zinc in Series 3.5 appears stochastic, with release and precipitation serving as competing mechanisms for the duration of testing.

For Series 3.6, dissolved zinc is only removed from solution when the concentration of zinc exceeds 10 mg/L prior to TSP addition.

Figure 44. Series 3.7 and 3.8 (45°C) zinc concentration

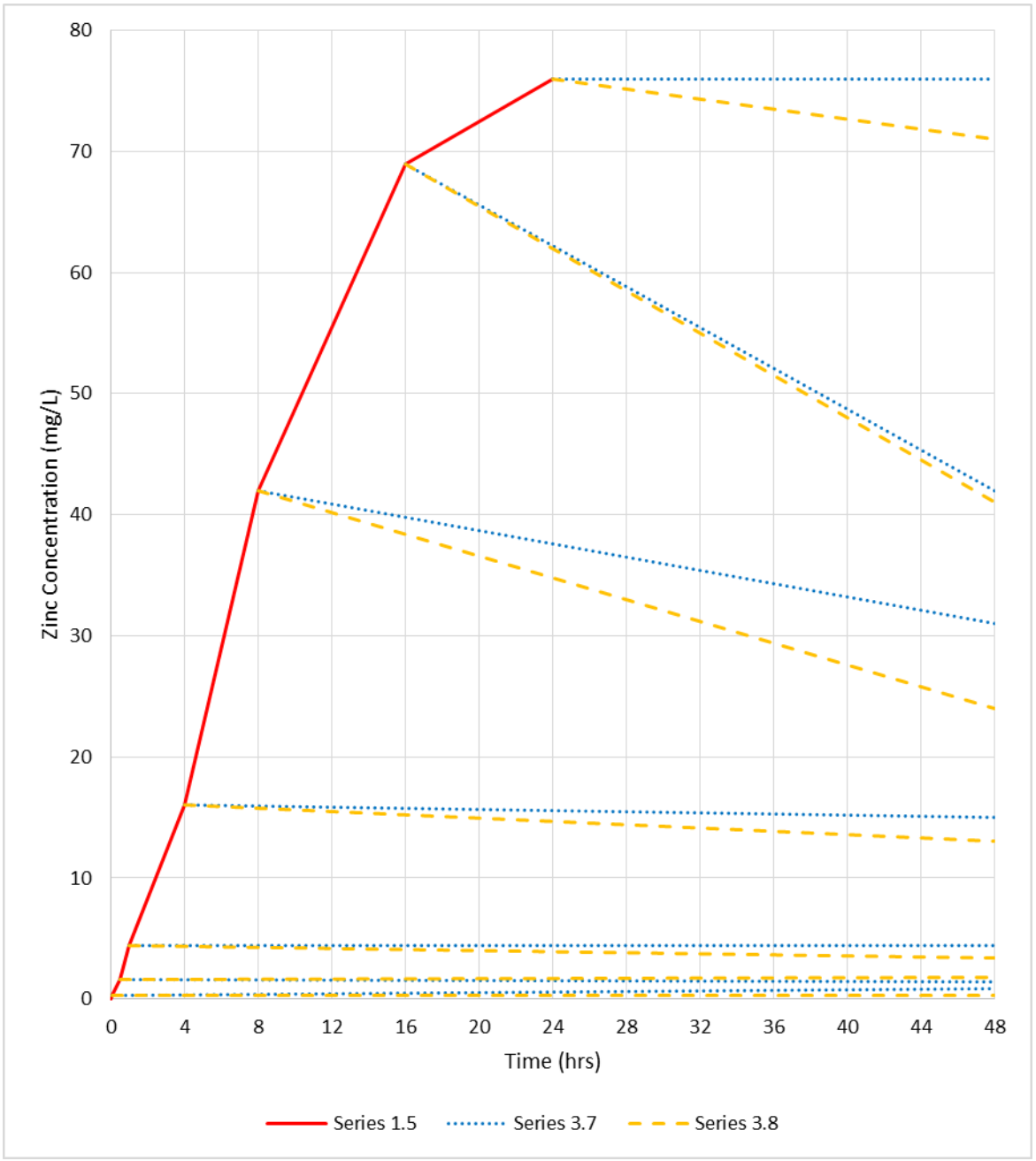

For the tests conducted at 45°C, the presence of the zinc source in solution did not strongly influence the removal of dissolved zinc from solution. For both Series 3.7 and 3.8, the rate of precipitation was greatest when the dissolved zinc concentration in solution was between 40 mg/L and 70 mg/L.

Figure 45. Series 3.9 and 3.10 (25°C) zinc concentration

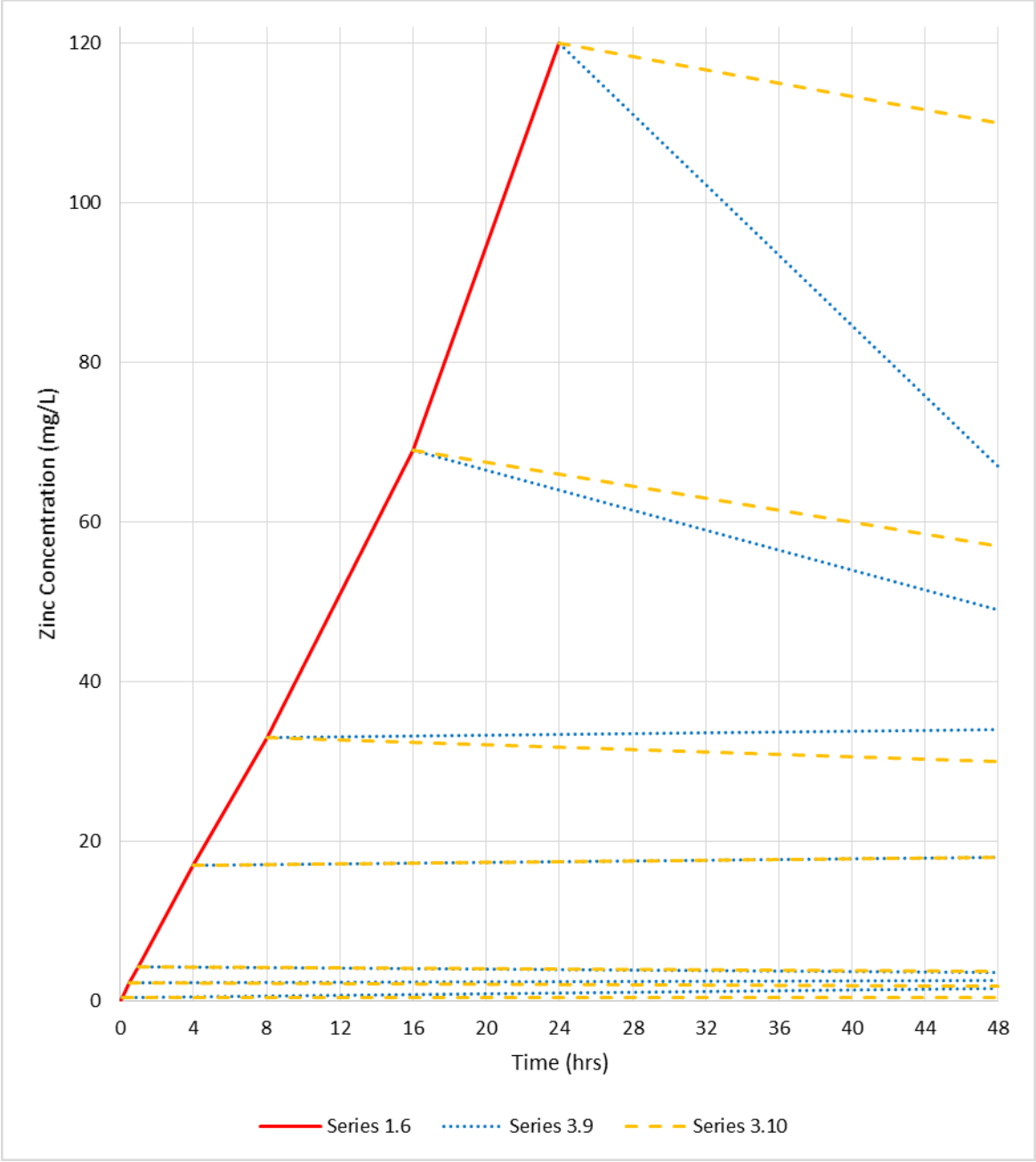

In Series 3.9 testing, the coupon played a significant role in the competing mechanisms of release by dissolution and precipitation. Zinc continued to release from galvanized steel after TSP was added for tests that were under prompt release conditions for eight hours or less. One exception to this was the test where TSP was added after one hour: the prompt release concentration was 4.2 mg/L at 1 hour of testing, and the zinc concentration at the forty-eighth hour was 3.5 mg/L. This 18% difference may not be significant.

In Series 3.10 tests, the removal of the coupon from the testing solution always resulted in a decrease in the dissolved zinc concentration. This suggests that zinc phosphate precipitates in solution, and may be available to interact the ECCS sump pump debris beds.

In comparing Series 3.9 with 3.10, another trend is observed. At sufficiently high zinc concentration—greater than 60 mg/L —the galvanized steel coupon (Series 3.9) promoted greater precipitation than when the coupon was not present (Series 3.10). This suggests that the inventory of zinc being removed by precipitation has been deposited on the coupon surface, and is less likely to interact with the ECCS sump pump. In contrast, at lower zinc concentrations—lower than 60 mg/L —precipitation was not consistently aided or hindered by the presence of the coupon.

4.3.2 Theme 3 Turbidity Analysis

Turbidity data for Theme 3 tests is available from tests in Series 3.3 through 3.10. The *changes in turbidity* from the prompt release period (Series 1.3-1.6) to the final turbidity measurements taken after forty-eight hours of testing are plotted Figure 46.

Figure 46. Theme 3 turbidity measurements

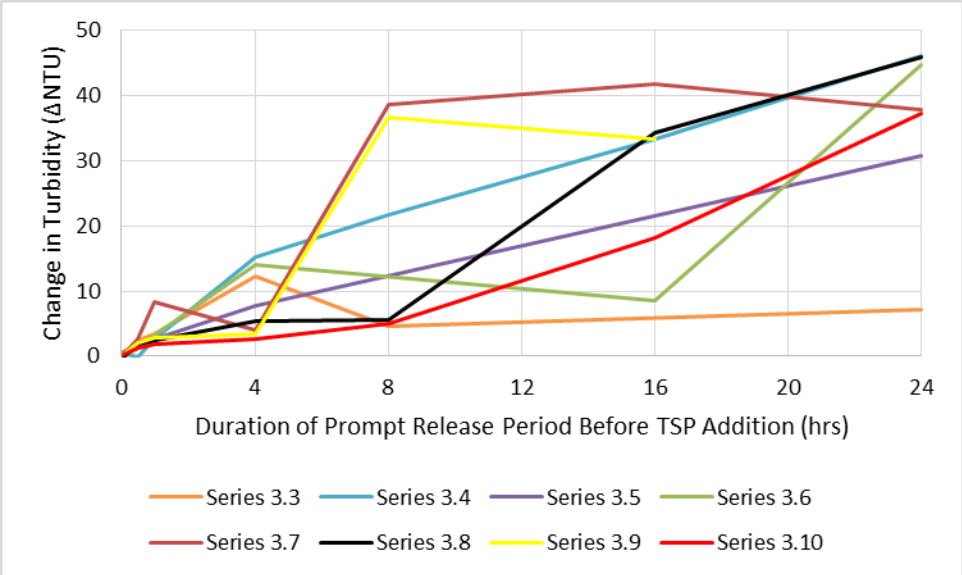

At first glance, this data (Figure 46) does not display a clear trend. But one key trend is observed with the change in turbidity following addition of TSP. There is an upward drift in the change in turbidity. This suggests that longer exposure times to the unbuffered coolant solution will increase the turbidity by increasing amounts.

In general, it was found that the concentration of zinc tended to increase during the prompt release period of the Series 1.3 through 1.6 tests (Section 4.1.1). This corresponds with a higher total change in turbidity (Figure 46) from the measured prompt turbidity (Section 4.1.2).

Recall that turbidity is a relative measurement of the clarity of water. A higher turbidity corresponds with a more particulate-rich aqueous environment. The trend observed in these series confirms that zinc released later during the prompt zinc release period is increasing more of a threat to develop particulates and precipitates which may interact with the ECCS sump strainer.

4.3.3 Theme 3 pH Analysis

All series in Theme 3 have initial chemistry identical to Theme 1 tests: 220 millimolar boric acid. Following the addition of TSP, the testing solution chemistry more resembles Theme 2 tests in that there is phosphate buffer present. Therefore, it is expected that the final pH of the testing solutions should be similar to Theme 2 tests. The pH measurement results are available for Series 3.3 through 3.10, and are shown in Table 17.

Table 17. Theme 3 pH measurements after TSP addition

Series	Operating Temperature	TSP Added	Average pH after TSP addition	Standard Deviation
3.3	85°C	5.83 mM	7.42	0.06
3.4	85°C	5.83 mM	7.41	0.05
3.5	65°C	5.83 mM	7.42	0.05
3.6	65°C	5.83 mM	7.44	0.06
3.7	45°C	5.83 mM	7.30	0.07
3.8	45°C	5.83 mM	7.29	0.03
3.9	25°C	5.83 mM	7.23	0.04
3.10	25°C	5.83 mM	7.20	0.10

The pH measurements from these tests show that the final pH of the testing solution is dependent on the temperature of the solution. Pure water follows a different trend, where a higher temperature corresponds to a lower pH. The pH measurements collected for these series then suggests that a non-ideal behavior is exhibited by the solution, perhaps due to the presence of either a retrograde soluble metal (zinc) or two competing buffers (phosphate and borate).

4.3.4 Theme 3 surface Composition Analysis

Spectral data from EDS analysis is available for all tests which contained a zinc source coupon—Series 3.1, 3.2, 3.3, 3.5, 3.7, and 3.9. The available EDS spectral data for Series 3.1 and 3.2 are shown in Figure 47 and Figure 48.

Figure 47. Series 3.1 (pure zinc) EDS spectral results in atomic percentage (%) with testing duration and TSP concentration in millimolar

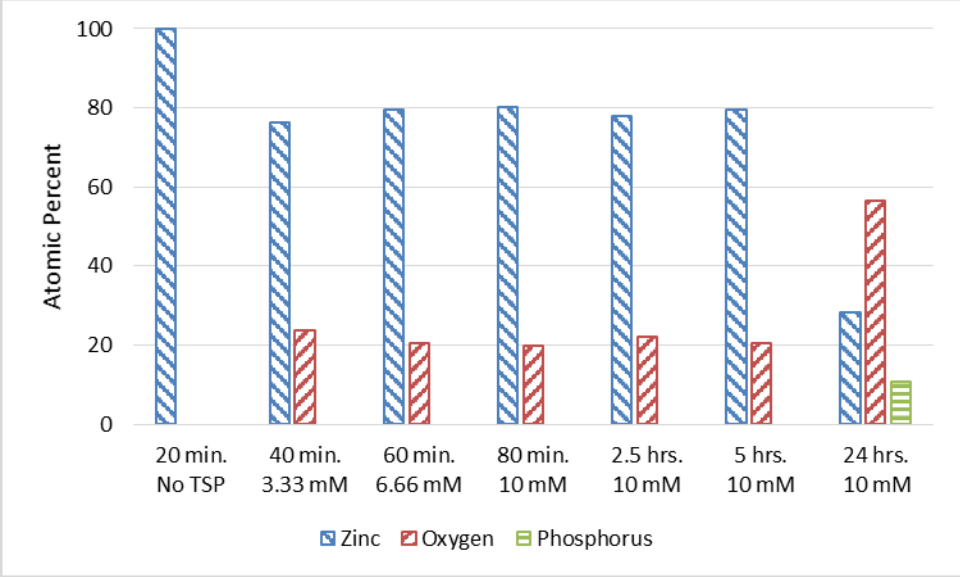

Figure 48. Series 3.2 (pure zinc) EDS spectral results in atomic percentage (%) with testing duration and TSP concentration in millimolar

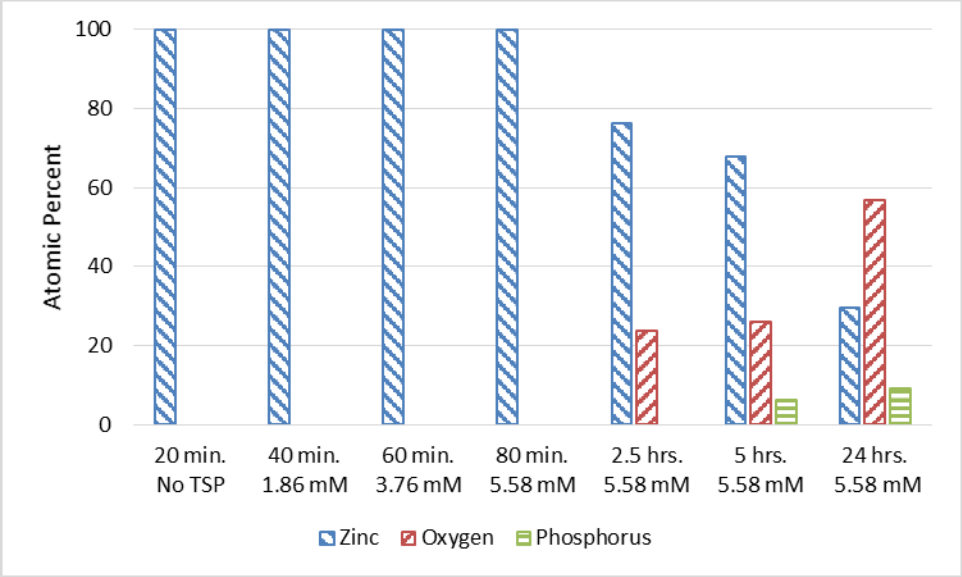

The data shows distinct behavior in the development of oxide scale and phosphate scale layers. Series 3.1 had a more rapid rate of TSP introduction, and is displaying an earlier development of zinc oxide scale layers. Series 3.2 had a slower rate of TSP introduction, and is displaying a later development of zinc oxide scale layers. Interestingly, though, is that phosphate scale layers develop in reverse order.

The earlier development of phosphate scale layers on the tests in Series 3.2 may be a response to the earlier chemical environment of these tests. The ICP measurements indicated that the dissolved zinc in solution concentration reached a higher maximum (3.0 mg/L) than Series 3.1 tests (Section 4.3.1), which may be an essential contributor to the earlier development of the zinc phosphate surface precipitation.

By the twenty-fourth hour of testing, there is approximately equal surface composition of zinc, oxygen, and phosphate for both series. These quantities are shown in Table 18.

Table 18. Series 3.1 and 3.2 (pure zinc) EDS spectral results in atomic percentage (%)

Series	Zinc	Oxygen	Phosphorus
3.1	28.3	56.6	10.8
3.2	29.6	56.9	9.3
Average	29.0	56.8	10.1

Zinc phosphate [$Zn_3(PO_4)_2$] has an atomic composition ratio of zinc: oxygen: phosphorus equal to 3:8:2. Assuming that phosphate is dominantly found in the form of zinc phosphate, the whole inventory of 10.1% phosphate may be attributed to zinc phosphate, which means that 40.4% oxygen and 15.2% zinc are also bound to zinc phosphate on the coupon surface. Subtracting these values from the total measured atomic percentages leaves 13.8% zinc and 16.4% oxygen. Zinc oxide has an elemental composition of equal parts zinc and oxygen (ZnO). The remaining amounts of zinc and oxygen roughly account for development of zinc oxide. Therefore, after twenty-four hours of testing, zinc is found in zinc phosphate and zinc oxide in roughly equivalent amounts: 52.4% of the available zinc is in phosphate form, and 47.6% is found in zinc oxide form.

The EDS spectral data from Series 3.3, 3.5, 3.7, and 3.9 is also available, and is shown in Table 19, Table 20, Table 21, and Table 22.

Table 19. Series 3.3 (galvanized steel) EDS spectral results in atomic percentage (%)

TSP added after…	Zinc	Oxygen	Phosphorus	Aluminum
5 min	83.14	16.86		
30 min	23.26	65.56	10.53	
1 hr	83.96	16.04		
4 hrs.	24.47	61.24	13.66	
8 hrs.	63.79	32.01	4.2	
16 hrs.	26.95	60.3	11.99	
24 hrs.	33.83	55.8	10.37	

Table 20. Series 3.5 (galvanized steel) EDS spectral results in atomic percentage (%)

TSP added after…	Zinc	Oxygen	Phosphorus	Aluminum
5 min	100			
30 min	100			
1 hr	100			
4 hrs.	100			
8 hrs.	50.73	41.92	7.35	
16 hrs.	37.95	50.34	11.71	
24 hrs.	32.38	54.44	12.07	

Table 21. Series 3.7 (galvanized steel) EDS spectral results in atomic percentage (%)

TSP added after…	Zinc	Oxygen	Phosphorus	Aluminum
5 min	100			
30 min	100			
1 hr	100			
4 hrs.	100			
8 hrs.	100			
16 hrs.	27.16	56.93	14	1.59
24 hrs.	41.2	48.58	10.23	

Table 22. Series 3.9 (galvanized steel) EDS spectral results in atomic percentage (%)

TSP added after…	Zinc	Oxygen	Phosphorus	Aluminum
5 min	100			
30 min	100			
1 hr	100			
4 hrs.	100			
8 hrs.	29.16	57.15	11.79	1.91
16 hrs.	65.3	30	4.7	
24 hrs.	58.09	41.91		

These EDS spectral results have shown that zinc phosphate will precipitate on the surface of coupons, but only if the prompt release testing conditions were maintained for a sufficiently duration. Interestingly, zinc phosphate did not precipitate at all on the sample exposed to prompt release conditions for twenty four hours in Series 3.9. This may suggest that a sufficiently dominant surface oxide layer developed, hindering zinc phosphate precipitation, as was seen in the five-hour test of Series 3.1 (Figure 47).

4.3.5 Theme 3 Qualitative Imaging Analysis

Surface imaging from SEM analysis is available for select tests in Series 3.1, 3.2, and 3.9. All Theme 2 surface imaging was performed at 1000 times magnification. Figure 49 and Figure 50 contain the images corresponding to the fifth and twenty-fourth hours of testing in Series 3.1 and 3.2. For these two series, TSP was slowly introduced to the testing solution with Series 3.1 receiving a larger total quantity of TSP.

Figure 49. Series 3.1 SEM images

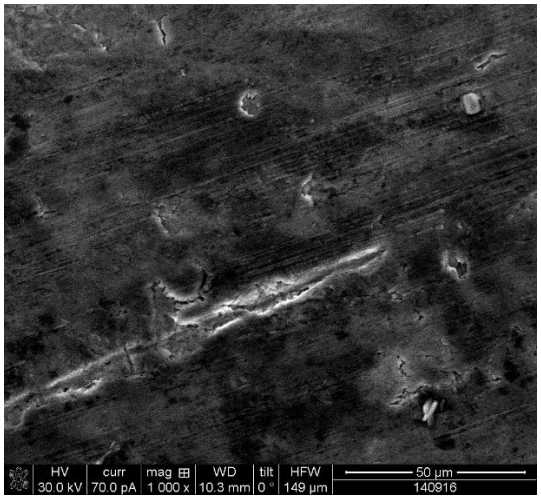

5 hrs. testing, 0-10 mM TSP

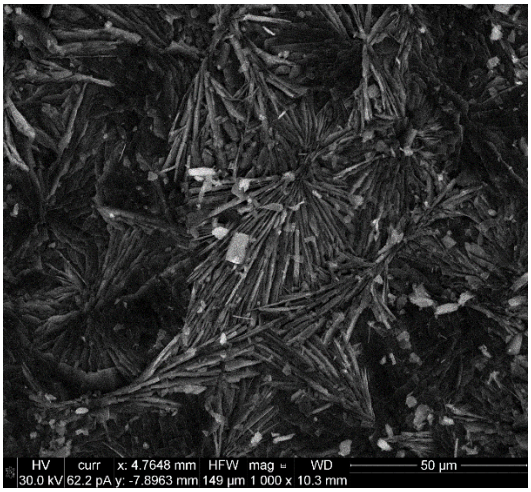

24 hrs. testing, 0-10 mM TSP

Figure 50. Series 3.2 SEM images

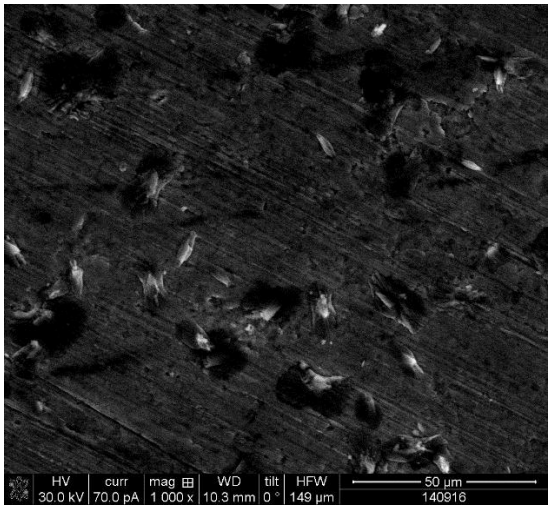

5 hrs. testing, 0-5.58 mM TSP

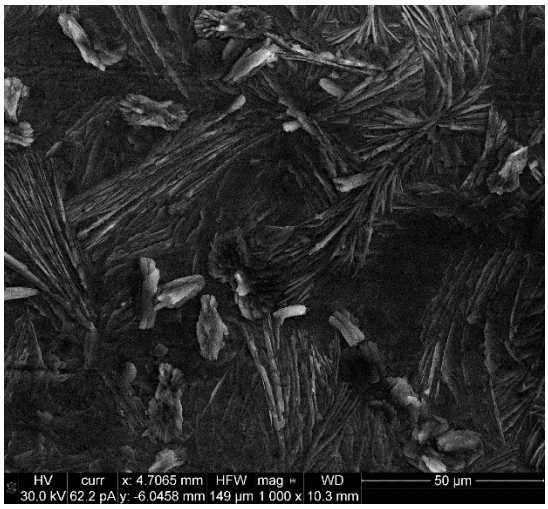

24 hrs. testing, 0-5.58 mM TSP

The SEM imaging from Series 3.1 and 3.2 has confirmed the findings presented with the EDS spectral results in Section 4.3.4. In both series, the twenty-four-hour tests had equivalent elemental surface composition comprising primarily of zinc, phosphorus, and oxygen. The SEM imaging reveals similar qualitative surface properties, specifically with the scale formation and qualitative surface roughness.

The crucial difference between the samples from the fifth hour of testing in these series was the confirmation of the presence of phosphorus on the surface on the Series 3.2 coupon sample. By examining the SEM images, this critical difference in surface composition may be observed—the Series 3.2 coupon visibly contains small precipitate deposits which resemble smaller versions of the scale deposits present on coupon samples tested for twenty-four hours. These small deposits may serve as nucleation points for further zinc phosphate precipitation. The discussion in Section 4.3.4, which explained that the surface composition is a product of the sensitive chemical environment during the TSP additions, is supported by these findings.

The SEM surface imaging results from Series 3.9 are shown in Figure 51, Figure 52, and Figure 53.

Figure 51. Series 3.9 SEM images, part 1/3

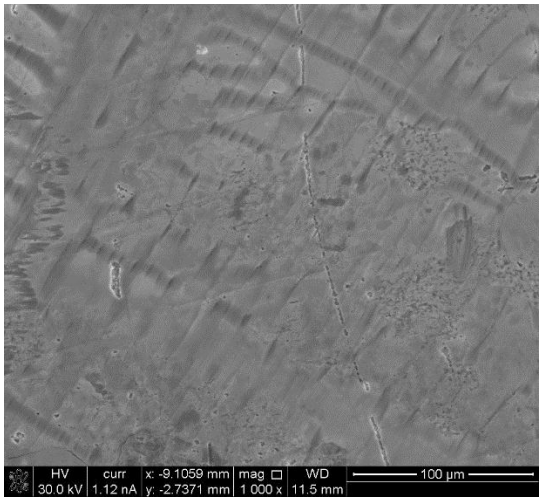

5 min. prompt testing, then
Exposed to 10 mM TSP 47 hrs. 55 min.

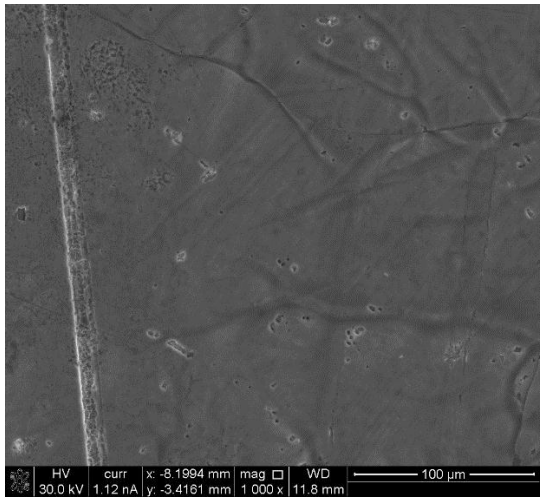

60 min. prompt testing, then
Exposed to 10 mM TSP 47 hrs.

Figure 52. Series 3.9 SEM images, part 2/3

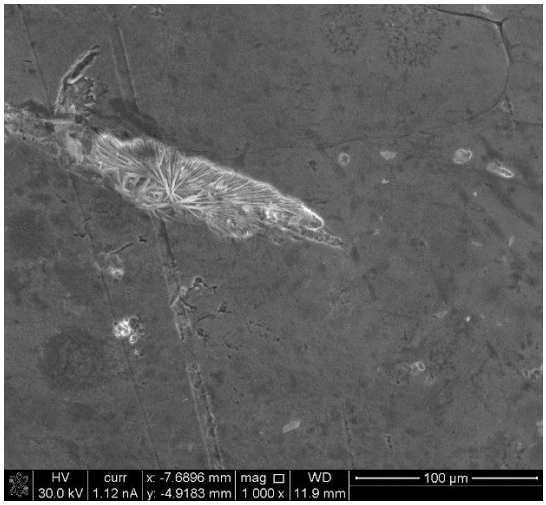

4 hrs. prompt testing, then
Exposed to 10 mM TSP 44 hrs.

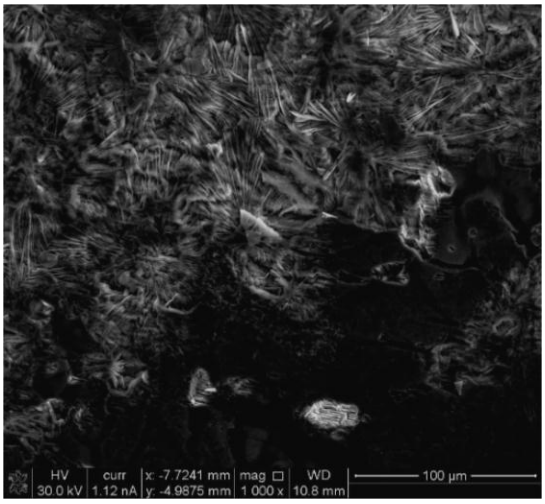

8 hrs. prompt testing, then
Exposed to 10 mM TSP 40 hrs.

Figure 53. Series 3.9 SEM images, part 3/3

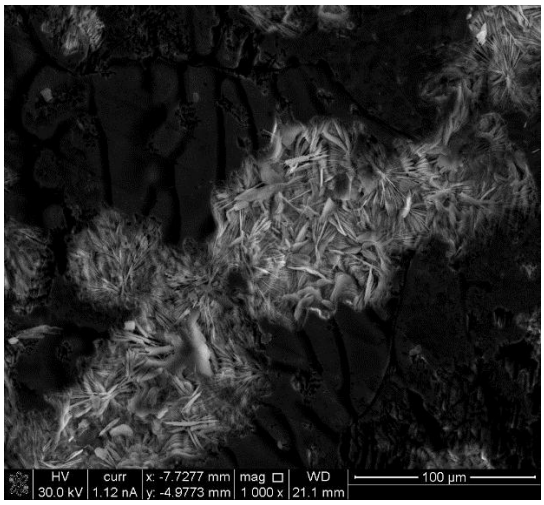

16 hrs. prompt testing, then
Exposed to 10 mM TSP 32 hrs.

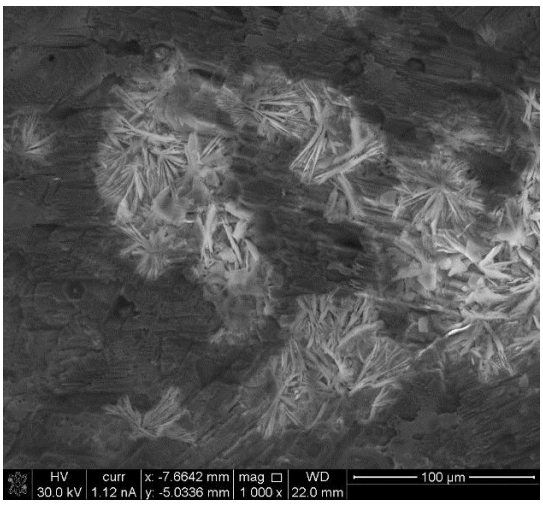

24 hrs. prompt testing, then
Exposed to 10 mM TSP 24 hrs.

The SEM imaging of Series 3.9 shares prominent similarities with both the Theme 1 and Theme 2 SEM images. The first two images in this series resemble the first two

images from Series 1.6—there is slight, but noticeable, destruction on the coupon surface. In these images, pitting, which is often in clusters, is the presumed mechanism for zinc release from the coupon.

The final four images of Series 3.9 look a lot like the final four images of Series 1.6 imaging, with one key difference: the pitting and voids that are on the coupon surface have been filled with zinc phosphate crystals, which resemble the scale crystals found in Theme 2 imaging. Remarkably, these zinc phosphate crystal structures appear to be restricted to the regions where small pitting clusters merged into large pits, suggesting that the zinc phosphate growth is promoted and is thermodynamically favorable in the texturally-rough pits rather than on the smoother surfaces of the non-dissolved and non-pitted areas.

Another notable finding in the final image is the presence of a hexagonal pit, similar to those found in Series 1.6 images (Section 4.1.5). This pit is located near the left-center of the image, and is noticeable with careful inspection. More hexagonal pitting may be present; if so, they are concealed by zinc phosphate crystal growth.

4.4 Theme 4: Zinc and Aluminum Integrated Effects

The fourth testing theme was developed to quantify the integrated chemical effects of zinc and aluminum when combined in a representative testing solution. There is only one testing series in this Theme: Series 4.1. Additional details for this series is provided in Section 3.1.5.4. Analyses for Series 4.1 is limited to dissolved metal concentrations and pH. Turbidity and surface data (EDS and SEM) are not available.

There are tests outside of Theme 4 testing which will serve as a baseline for comparison for Series 4.1. To determine the effects that aluminum has on the behavior of zinc, Series 2.1 will serve as the baseline tests. Series 2.1 tests were conducted under the same conditions as Series 4.1, except that in Series 4.1, aluminum has been added. The baseline tests for aluminum reference may be found in [41].

4.4.1 Theme 4 Zinc and Aluminum Release Analysis

Zinc and aluminum release was measured through ICP by HEAL, as described in Section 4.1.1. Figure 54 shows the Series 4.1 zinc release results compared with Series 2.1 zinc measurements. Figure 55 contains the Series 4.1 aluminum release results compared with the baseline aluminum tests (Section 4.4).

Figure 54. Series 4.1 zinc release

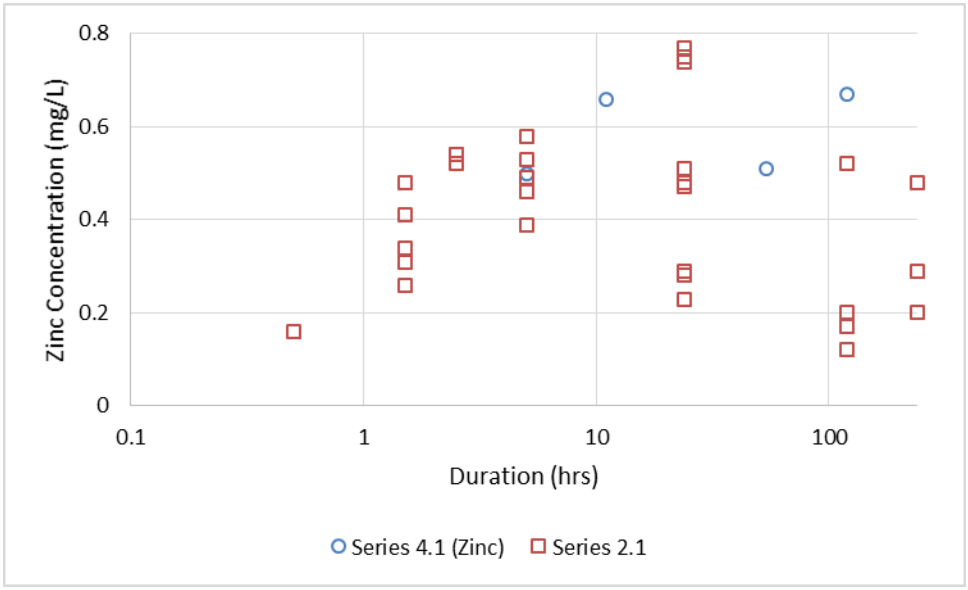

The ICP measurements for dissolved zinc concentration in Series 4.1 show that the results agree well with the measurements made in Series 2.1. Aluminum does not have an appreciable effect on the release of zinc.

Figure 55. Series 4.1 aluminum release

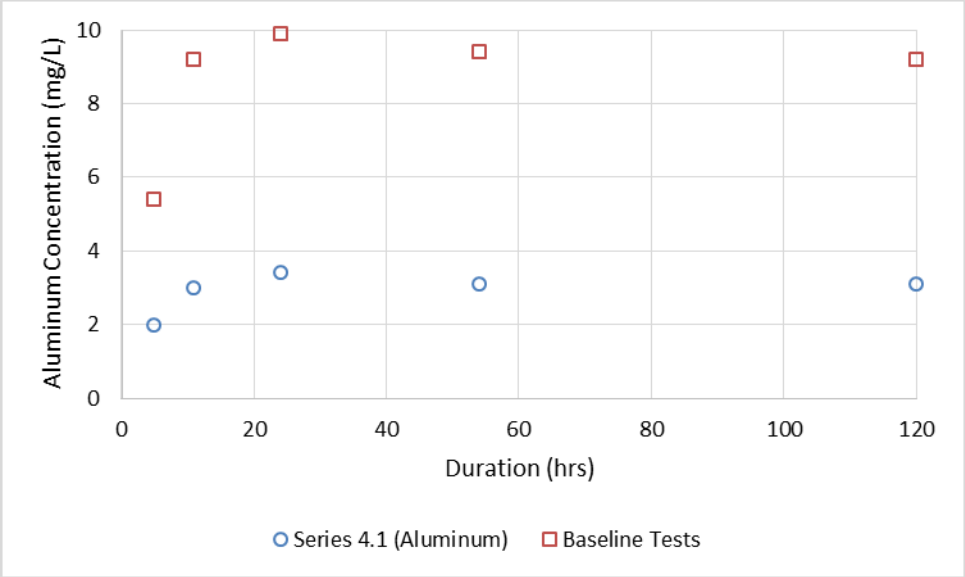

The ICP measurements for dissolved aluminum concentration in Series 4.1 show that there is a significant response to the presence of zinc. There is a dramatic reduction in the dissolved aluminum concentration when zinc has been added to the testing solution. The comparison between each available datum is shown in Table 23.

Table 23. Series 4.1 aluminum concentration and baseline comparison

Test Duration	Baseline Dissolved Aluminum Content	Series 4.1 Dissolved Aluminum Content	Ratio of Series 4.1 Aluminum Concentration to baseline
5 hrs.	5.4 mg/L	2.0 mg/L	0.37
11 hrs.	9.2 mg/L	3.0 mg/L	0.33
24 hrs.	9.9 mg/L	3.4 mg/L	0.34
54 hrs.	9.4 mg/L	3.1 mg/L	0.33
120 hrs.	9.2 mg/L	3.1 mg/L	0.34

When zinc is present in solution, the aluminum concentration is reduced by roughly a factor of three. This reduction may be attributed to the anodic behavior of zinc; zinc will catholically shield corrosion of many other metals.

4.4.2 Theme 4 pH Analysis

Series 4.1 had an initial chemistry identical to Series 2.1, which includes 220 millimolar boric acid and 10 millimolar TSP, which naturally settles at a pH value near 7.3. The measurements for the final pH for Series 4.1 are shown in Figure 56.

Figure 56. Theme 4 final pH

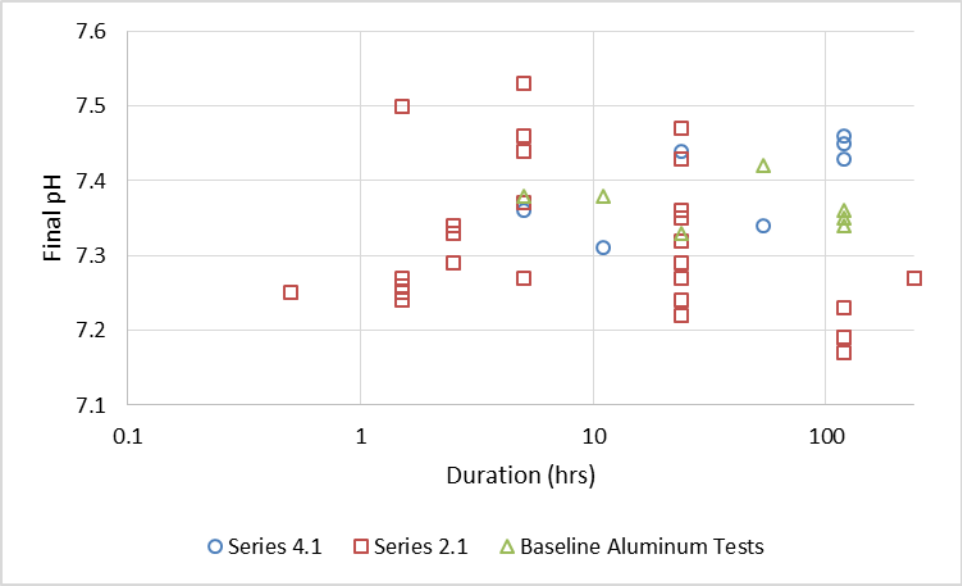

The pH measurements from Series 4.1 do not exhibit any unusual behaviors. The pH for all three sets of testing solutions remains within the bounds of pH measurements made with the Series 2.1 tests, and within 0.1 pH unit of the baseline aluminum tests.

4.5 Theme 5: Chemical Descaling Methods to Quantify Scale Layer

The fifth testing theme studied the effectiveness of various descaling methods applied to zinc source coupons after testing in buffered, borated solution. Select coupon samples tests from Series 2.1 were descaled, and these efforts were collected into Series 5.1-5.4. Four descaling methods were applied, and are detailed in Table 24.

Table 24. Theme 5 testing matrix and descaling chemical composition

Series	Descaling Chemical	Descaling Solution Composition	Descaling Solution Temperature	Exposure Duration
5.1	Ammonium persulfate	100 g/L	22°C	5 min.
5.2	Ammonium chloride	100 g/L	70°C	5 min.
5.3	Ammonium acetate	100 g/L	70°C	5 min.
5.4	Hydrochloric acid	1% by weight	22°C	10 sec.

Descaling the zinc source coupon is a technique that has been applied to more accurately quantify the amount of scale that develops on a surface; these techniques are not intended to be applied to containment materials following a LOCA.

Four techniques are employed to validate effectiveness of zinc-source surface descaling: (1) zinc content in the descaling solutions to quantify the amount of zinc removed; (2) coupon mass change before and after descaling to connect the mass change of the coupon to the amount of zinc removed by the first technique; (3) EDS analysis to determine the effectiveness at removing scale layers by measuring surface elemental composition; and (4) SEM imaging to qualitatively assess surface cleanliness.

Reference SEM images are shown in Figure 57. These images provide a baseline image of a clean, untested surface, and a surface that has been tested, but not descaled.

Figure 57. Theme 5 baseline SEM images

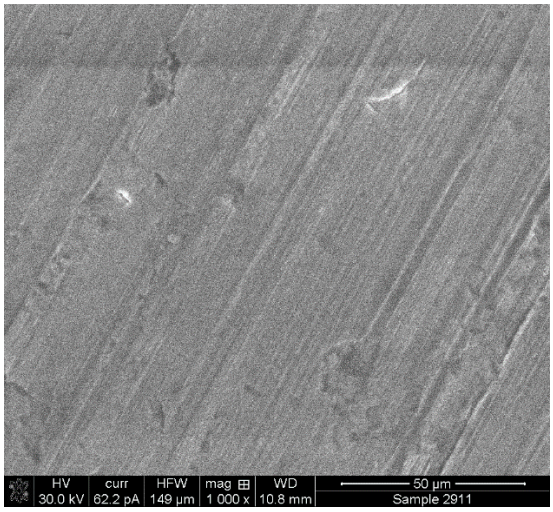

Pure zinc, clean

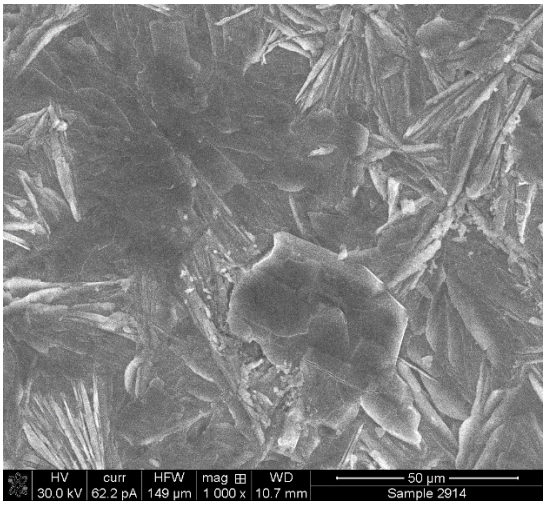

Pure zinc, 24 hrs. tested at 10 mM TSP

4.5.1 Series 5.1 (Ammonium Persulfate) Analysis

The mass lost by a coupon and the amount of zinc removed through descaling for Series 5.1 are shown in Table 25. The descaling solution used was ammonium persulfate.

Table 25. Series 5.1 Total mass lost through descaling and zinc lost through descaling

Exposure Time to Borated and Buffered Testing Solution	Mass Lost From Coupon	Zinc Removed with Descaling Solution	% of Mass Loss Attributed to Zinc
1.5 hrs.	99 mg	80 mg	81%
5 hrs.	95 mg	79 mg	83%
24 hrs.	63 mg	48 mg	76%

There are two primary forms of zinc corrosion products in these tests: zinc oxide and zinc phosphate. Zinc oxide is approximately 80% zinc by mass, and zinc phosphate is

approximately 51% zinc by mass. The data available in Table 25 suggests that zinc oxide has been removed from the surface. This hypothesis may be tested through EDS analysis, which is shown in Table 26 for the twenty-four hour test. This EDS spectrum is compared with an analogous sample from Series 2.1, a coupon sample which was tested under the same conditions but not descaled.

Table 26. Series 5.1 (pure zinc) EDS spectral results in atomic percentage (%)

Sample Analyzed	Zinc	Oxygen	Phosphorus
Series 5.1 – 24 hr. Test	35.3	58.4	6.3
Series 2.1 – 24 hr. Test	39.6	52.4	8.0

The EDS spectral results have shown that surface composition does not significantly change with descaling. This invalidates the hypothesis that the descaling solution for Series 5.1 removes zinc oxide.

The final analysis, the qualitative SEM imaging, is provided in Figure 58.

Figure 58. Series 5.1 SEM image after descaling with ammonium persulfate

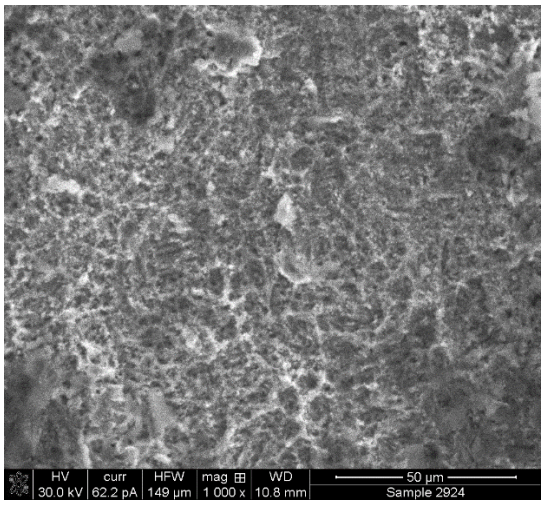

The SEM image of the descaled coupon has shown that the coupon surface is neither clean nor undamaged by the descaling solution. The descaling method has failed to remove zinc scale from the surface, confirmed by EDS analysis, the mass lost analysis has not conclusively determined what has been removed, and the SEM imaging does not support surface cleanliness. Therefore, ammonium persulfate is not an effective descaling solution for removing scale or for informing what was removed with the descaling solution.

4.5.2 Series 5.2 (Ammonium Chloride) Analysis

The mass lost by a coupon and the amount of zinc removed through descaling for Series 5.2 are shown in Table 27. The descaling solution used was ammonium chloride.

Table 27. Series 5.2 Total mass lost through descaling and zinc lost through descaling

Exposure Time to Borated and Buffered Testing Solution	Mass Lost From Coupon	Zinc Removed with Descaling Solution	% of Mass Loss Attributed to Zinc
1.5 hrs.	1.3 mg	0.46 mg	35%
5 hrs.	5.6 mg	0.58 mg	10%
24 hrs.	1.2 mg	0.71 mg	59%

The data available in Table 27 would lead to no conclusion about the identity of the removed scale layers, whether it was zinc oxide, zinc phosphate, or metallic zinc removed. A markedly reduced amount of both total mass and total zinc was removed with this cleaning method when compared with the first descaling method. EDS analysis is

necessary to determine the effectiveness of this descaling method; these results are shown in Table 28.

Table 28. Series 5.2 (pure zinc) EDS spectral results in atomic percentage (%)

Sample Analyzed	Zinc	Oxygen	Phosphorus
Series 5.2 – 24 hr. Test	35.1	56.1	8.8
Series 2.1 – 24 hr. Test	39.6	52.4	8.0

Similar to the results of the first descaling solution, the surface composition has not significantly changed with descaling. SEM imaging for this coupon sample in provided in Figure 59.

Figure 59. Series 5.2 SEM image after descaling with ammonium chloride

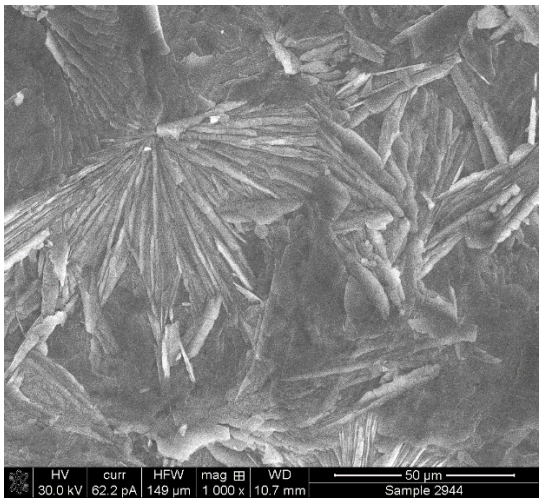

There are visibly zinc phosphate crystals in this SEM image. This indicates that the descaling solution was ineffective at removing zinc scale. The descaling method has failed to remove zinc phosphate from the surface, the mass lost analysis has not conclusively determined what has been removed, and the SEM imaging has confirmed that

zinc scale has not been removed. Therefore, ammonium chloride is not an effective descaling solution.

4.5.3 Series 5.3 (Ammonium Acetate) Analysis

The mass lost by a coupon and the amount of zinc removed through descaling for Series 5.3 are shown in Table 29. The descaling solution used was ammonium acetate.

Table 29. Series 5.3 Total mass lost through descaling and zinc lost through descaling

Exposure Time to Borated and Buffered Testing Solution	Mass Lost From Coupon	Zinc Removed with Descaling Solution	% of Mass Loss Attributed to Zinc
1.5 hrs.	0.4 mg	0.40 mg	100%
5 hrs.	None	0.74 mg	N/A
24 hrs.	1.6 mg	0.86 mg	54 %

The data available in Table 29 is inconclusive; the scale layers cannot be identified with this information. For the coupon tested for 1.5 hours before descaling, there are similar quantities of both zinc lost and total mass lost. This results would suggest that metallic zinc has been stripped from the coupon surface, rather than corrosion products.

There are competing factors in this analysis, such as scale removal and additional scale layering induced by the descaling solution. This is made clear by observing the results from the five-hour duration test. There was not a net mass change with the coupon, but zinc was definitely removed from the coupon, as evidenced by the Zinc Remove with Descaling Solution column.

Additional insights may be provided by the EDS spectral data. This information is presented in Table 30. The EDS spectral results have shown that the surface composition slightly shifts after exposure to the descaling solution. Relative compositional quantities of both zinc and phosphorus increase, while the relative oxygen decreases. However, in all cases, the surface remains within 17% of the original surface composition. SEM imaging is provided in Figure 60.

Table 30. Series 5.3 (pure zinc) EDS spectral results in atomic percentage (%)

Sample Analyzed	Zinc	Oxygen	Phosphorus
Series 5.3 – 24 hr. Test	42.0	50.4	7.6
Series 2.1 – 24 hr. Test	39.6	52.4	8.0

Figure 60. Series 5.3 SEM image after descaling with ammonium acetate

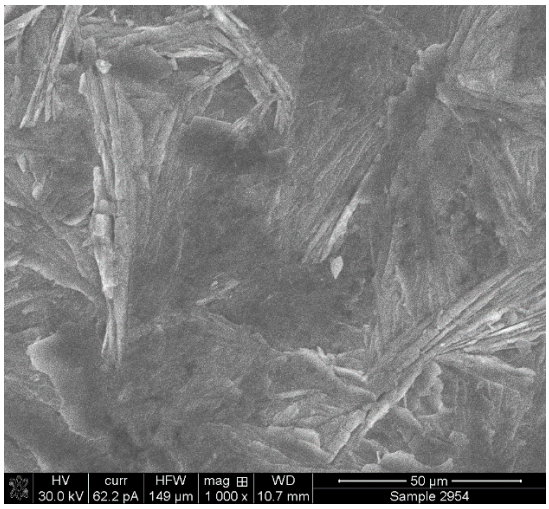

As with ammonium chloride in the previous section, ammonium acetate has not removed zinc phosphate crystals from the surface. These results have shown that phosphate scale is not effectively removed from the surface, the mass loss data is

inconclusive, and SEM imaging has confirmed the presence of scale on the coupon surface. Therefore, ammonium acetate is not an effective descaling solution for removing scale or for informing what was removed with the descaling solution.

4.5.4 Series 5.4 (Hydrochloric Acid) Analysis

The mass lost by a coupon and the amount of zinc removed through descaling for Series 5.4 are shown in Table 31. The descaling solution used was hydrochloric acid.

Table 31. Series 5.4 (pure zinc) Total mass lost through descaling and zinc lost through descaling

Exposure Time to Borated and Buffered Testing Solution	Mass Lost From Coupon	Zinc Removed with Descaling Solution	% of Mass Loss Attributed to Zinc
1.5 hrs.	0.6 mg	0.34 mg	57%
5 hrs.	1.0 mg	0.81 mg	81%
24 hrs.	10 mg	4.9 mg	49%

For the coupons tested for 1.5 and 24 hours before descaling, there is a similar value for the percent of total mass lost which is attributed to zinc. This mass lost percentage is also similar to the mass percent composition of zinc phosphate (51%).

To confirm the identity of the removed scale layers, the EDS spectral results are necessary. These results are provided in Table 32. The EDS spectral results reveal a clean surface on the zinc coupon after applying the descaling solution. The SEM imaging for this coupon is provided in Figure 61.

Table 32. Series 5.4 EDS spectral results in atomic percentage (%)

Sample Analyzed	Zinc	Oxygen	Phosphorus
Series 5.4 – 24 hr. Test	100	0	0
Series 2.1 – 24 hr. Test	39.6	52.4	8.0

Figure 61. Series 5.4 SEM image after descaling with 1% hydrochloric acid

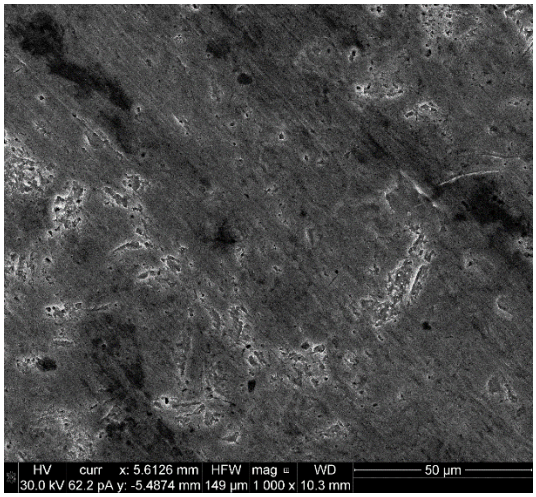

This image reveals no distinguishable signs of phosphate scale. There is considerably more surface wear on this coupon than there was on the un-tested sample; however, this may be inherent to the nature of testing and not due to the descaling method.

The EDS spectral information, along with the corresponding mass analysis information and SEM imaging, confirms that the mass lost has the same mass composition as zinc phosphate, and the surface is cleaned of all traces of both oxygen and phosphate. Therefore, hydrochloric acid is an effective descaling solution for removing scale and for informing what was removed with the descaling solution.

CHAPTER 5: DISCUSSION AND CONCLUSIONS

5.1 Theme 1 Discussion

The prompt release behavior of zinc sources has been investigated in Theme 1. All three sources of zinc exhibited a consistent trend of linear dissolution, as measured by ICP, and are functions of both temperature and the source of zinc. Pure zinc and galvanized steel surfaces were tested for durations long enough to detect dissolved zinc concentration saturation limits, which was shown to be a function of temperature, but not a function of the zinc source. These results exhibited the retrograde solubility of dissolved zinc.

Temperature-dependent saturation equations were developed for Series 1.3, 1.4, and 1.5, and were used to determine the saturation properties of Series 1.6. There is not enough experimental data to confirm the calculated saturation properties for Series 1.6; however, the calculated values were within the limits established by experimental measurements.

EDS spectral measurements showed that zinc oxide scale growth on galvanized steel coupons corresponded to the achievement of dissolved zinc solution saturation. The sampling time that preceded the sampling time corresponding to saturation was achieved revealed a zinc oxide scale in all series with galvanized steel. Zinc oxide scale formation may be the mechanism through which dissolved zinc is removed from solution to maintain the saturation limit as release and precipitation compete in equilibrium.

Qualitative SEM analysis has shown that with shorter exposure times to the testing solution, zinc from galvanized steel was released from the surface in organized clusters,

leaving behind surface pitting. As zinc continued to release from the coupons, these pitting clusters grew into larger pits, and eventually culminated in the destruction of surface structure. In a few cases, hexagonal pitting formations were observed; metallic zinc is known to have a hexagonal close-packed (HCP) metallic crystal structure, and this is likely the cause for this observation.

5.2 Theme 2 Discussion

Theme 2 testing series have several valuable findings. A solubility limit for dissolved zinc under these conditions has been established to be 0.8 mg/L of total dissolved zinc. The minimum solubility agrees well with the thermodynamic equilibrium modelling prediction for zinc solubility under these conditions (Section 2.1.2), and is approximately 0.1 mg/L. Early in the testing for all applicable series, a regular increase in dissolved zinc concentration—attributed to zinc releasing from the source—was observed. In Series 2.2, where a lower operating temperature was used, the dissolved zinc concentration grew more rapidly than the tests which used the baseline temperature, which displays the retrograde solubility behavior of zinc. Slight adjustments to the pH did not result in a significant response to measurable results such as zinc concentration.

Turbidity measurements showed that with a sufficiently large sampling size, the dissolved zinc concentration is accurately predicted by turbidity, but only for tests that had a pure zinc coupon for the zinc source; this trend was not observed with galvanized steel surfaces as the source of zinc. This is attributed to the presence of iron in tests that used galvanized steel zinc sources.

The EDS spectral measurements have confirmed that zinc phosphate scale develops on the surfaces of the coupons. The amount of measured phosphate tends to increase with time, which suggests zinc phosphate scale growth. Qualitative SEM imaging confirmed that zinc phosphate scale develops and accumulates over time, growing to cover more of the zinc source surface with longer exposure times.

5.3 Theme 3 Discussion

Theme 3 tests have displayed the unique behavior that zinc phosphate precipitation exhibits when exposed to trisodium phosphate under a range of conditions. Within the first two series of tests, TSP was introduced to the testing solution gradually over the course of an hour, at different rates for each series. EDS spectral results and qualitative surface imaging confirmed that zinc phosphate scale layer deposition on the zinc coupon occurred sooner for the series with a lower rate of TSP addition (Series 3.2). This result has been attributed to the high sensitivity to three early conditions during the period where TSP was introduced: (1) the pH remained lower for longer in Series 3.2, which promoted more rapid zinc dissolution, (2) the total inventory of released zinc was greater—3.0 mg/L in Series 3.2 versus 2.5 mg/L in Series 3.1—and (3) the development of a passive oxide layer on Series 3.1 samples, which delayed zinc phosphate precipitate deposition.

In Series 3.3, 3.5, 3.7, and 3.9, when zinc remained below a particular threshold concentration, as defined in Section 4.3.1, the release and precipitation mechanisms remained in competition with each other. However, above the given threshold, precipitation tended to dominate over continued release. For the series at temperatures

85°C and 25°C (Series 3.3 and 3.9), the presence of the zinc source coupon promoted even more zinc phosphate precipitation than when the coupon was not present in the corresponding series without the coupon (Series 3.4 and 3.10).

For experiments which contained galvanized steel, zinc phosphate tended to precipitate and accumulate in surface voids that were created during the prompt release phase of the testing, showing preference to the voids over the relatively smooth non-pitted surface areas. Zinc phosphate surface depositions occurred sooner in tests that were operated at higher temperatures, as shown in the EDS spectral measurements.

5.4 Theme 4 Discussion

Theme 4 testing has shown that the presence of a zinc surface in the same vicinity as an aluminum surface has a marked impact on the release and passivation response of the aluminum surface. The measured dissolved aluminum concentration for all experimental durations was reduced by a factor of three when zinc was present, while all other experimental conditions were maintained the same as the reference tests which only contained aluminum surfaces. This reduction in released aluminum is attributed to the electrochemical cathodic shielding that zinc contributes.

Conversely, the release rate, saturation limit, and other measureable responses of the zinc surfaces show that aluminum does not impact zinc behavior in a quantifiable manner for these tests.

5.5 Theme 5 Discussion

Tests within Theme 5 experiments have conclusively shown that three ammonium-based salts—persulfate, chloride, and acetate—are ineffective at removing zinc phosphate scale in a repeatable and quantifiable manner. To arrive at this conclusion, four techniques were applied to these salts, including a benchtop measurement of mass change, a concentration analysis by ICP, and surface analyses by EDS and SEM.

One descaling solution was found to be effective at clearing zinc phosphate scale from a pure zinc coupon exposed to borated and TSP-buffered solution. This solution consisted of one-percent by weight hydrochloric acid, with an exposure time of ten seconds, performed at room temperature.

There are shortcomings to these experiments that are worth mentioning. Due to the nature of the experimental process, it was necessary to use benchmark samples for each phase of testing. Separate testing samples were used for (1) a baseline scaling quantification and (2) descaling effectiveness. There may be slight differences between the scale layer that developed on the tested coupon and the baseline coupon, and this is not quantifiable.

There is no spectral EDS information available for tests with durations of 1.5 hours or five hours, which restricts the analyses to coupons which were exposed to the testing solution for twenty-four hours.

5.6 Conclusions

Numerous experiments have been performed which involved examining the chemical effects that zinc contributes to a post-LOCA environment. Galvanized steel, IOZ, and pure zinc surfaces have been tested in chemical environments similar to those expected during a LOCA. Boric acid representative of the dissolved boron in reactor coolant comprised the primary testing solution. To this solution, chemicals were added including trisodium phosphate, aluminum, hydrochloric acid, and sodium hydroxide to test the effects of phosphate buffering, secondary metal interactions, and pH responses to phenomenology such as dissolution and precipitation. A range of experimental temperatures were used to show the competition between precipitation and retrograde solubility characteristics of zinc.

Experiments were divided by a specific set of conditions into five distinct Themes of testing. The first three themes were designed around the interaction of zinc-bearing surfaces with coolant, including before, during, and after trisodium phosphate buffer is expected to dissolve and contribute to post-LOCA chemistry. The fourth experimental testing theme included the coupled effects of aluminum and zinc sources, and the response each source has on the other. A final testing theme was designed to test the effectiveness of descaling solutions, which were designed to help quantify the zinc phosphate scale layer development on zinc surfaces that had exposure to borated, buffered testing solution.

Among the most important finding of this body of research is the detection of zinc phosphate scale formation. Discovering chemical precipitates and scale formation is a key focus of the GSI-191 chemical effects experimental work, because such products may

interact with the ECCS sump debris bed, resulting in restricted flow and potential damage to ECCS capabilities during a LOCA. In several tests, zinc phosphate scale was observed growing on the coupon sample surfaces in a crystalline form, which showed development over time. Zinc phosphate precipitate deposition and scale growth began with small isolated crystals which, over time, grew to cover a majority of the coupon surfaces.

The dissolution and release of zinc was found to be greatest under non-TSP-buffered conditions, and by a significant margin. The dissolved zinc concentration in buffered experiments remained within the range of 0.1 to 0.8 mg/L TSP for all tests with durations ranging from thirty minutes through ten days; this result agrees with thermodynamic modelling simulations (Chapter 2). In testing solutions which did not contain any TSP buffer, the concentration of dissolved zinc reached as high as 120 mg/L; the maximum release expected is 124 mg/L at twenty-six hours of exposure to unbuffered solution at 25°C. The prompt release of zinc in unbuffered tests was found to be linear until a temperature-specific saturation limit was achieved, which followed the retrograde solubility behavior of dissolved zinc. A zinc oxide layer development on the surface of coupons corresponds with the achievement of a dissolved zinc saturation limit in all prompt-release tests for which this data exists.

Zinc was found to be an effective sacrificial electrode when paired with iron and aluminum. Iron release from the edges of galvanized steel was passivated at a value roughly four times lower than expected (Section 4.1.1). The release of aluminum from an aluminum coupon was reduced by a factor of three while zinc was present (Section 4.4.1), and the saturation limit of dissolved aluminum was likewise reduced by a factor of three.

There was no observed effect on the release of zinc, which means that zinc effectively protects against greater amounts of iron and aluminum release.

The pH-buffering capabilities of phosphate were shown for all tests which included TSP. For any such given testing conditions, a range of plus-or-minus 0.2 pH units or less was observed, indicating that the pH is buffered while phosphate is present. A significantly more dramatic response was observed in the pH trends of non-TSP-buffered tests, which was attributed to the consumption of dissolved hydronium through the oxidation of metals, which resulted in an increase in pH.

To quantify scale layer development, four techniques were employed. Three ammonium salts (persulfate, chloride, and acetate) and one strong acid (HCl) were used to test whether any of the methods could successfully remove zinc phosphate scale from the surface of the coupons with the objective of quantifying the amount of zinc phosphate that had developed during testing. The application of the strong acid hydrochloric acid was found to be effective at removing scale layers, and the ammonium-based salts were not effective or reliable. None of the methods were able to quantify scale layers.

This body of research has shown that zinc contributions to the post-LOCA chemical environment are significant. Zinc phosphate readily forms, and may transport to interfere with ECCS sump operations. Dissolved zinc may be generated in large quantities during the early-stages of a LOCA. The concentration of dissolved zinc has been shown to increase with a decreasing temperature, suggesting that the natural cooling of containment in a post-LOCA will promote additional zinc dissolution, further compounding the impact of ECCS operations. The presence of zinc may be beneficial in particular instances, where its presence has been shown to reduce aluminum and iron corrosion.

5.7 Future Work

There is a need to determine the transportability of dissolved zinc and zinc-based corrosion products through the containment building during post-LOCA operations. Zinc phosphate scale deposition and growth on zinc surfaces has been confirmed through this research, but the stability of scale layers should be quantified. If zinc phosphate scale can be shown to remain on the zinc surface under a range of flow conditions, then the impact of scale transport to the ECCS is minimized. However, if zinc phosphate scale is easily sheared from the surfaces on which they develop, the impact on ECCS operations may be very significant. Previous research has shown that sump head loss effects correspond with zinc phosphate development under specific conditions. A controlled environment with zinc isolated from other metals is necessary to determine the impact that zinc phosphate scale may have on sump head loss.

Additional work may also be necessary in TSP-buffered conditions in a variety of temperatures. A majority of the research presented herein involving TSP buffer was done at 85°C. Series 2.2 testing had an operating temperature of 60°C, and the resulting dissolved zinc concentration measurements revealed that the release was marginally greater at this lower temperature. The scope of Series 2.2 was limited, and was not long enough to capture the saturation limit at that temperature. Additional tests at other temperatures should be performed, and the durations should be extended to allow for observing the saturation limits. Zinc has shown retrograde solubility, so it would be expected that the solubility limit of dissolved zinc at lower temperature s should exceed the limit of 0.8 mg/L observed in Theme 2 testing (85°C).

REFERENCES

[1] D. Lochbaum, *Pressurized Water Reactor Containment Sump Failure,* Washington D.C., 2003.

[2] A. Ali, *Filtration of Particulates and Pressure Drop in Fibrous Media in Resolution of GSI-191,* Anaheim, CA: Transactions 2014 American Nuclear Society Winter Meeting, 2014, 2014.

[3] A. W. Serkiz, *Containment Emergency Sump Performance*, Washington , D.C.: U.S. Nuclear Regulatory Commission, NUREG-0897, Rev. 1, 1985.

[4] B. W. Sheron, *Summary of Activities Releated to The Generic Safety Issues Program,* U.S. NRC, SECY-12-0105, 2012.

[5] W. J. Dircks, *Resolution of Unresolved Safety Issue A-43, "Containment Emergency Sump Performance"*, Washington, D.C., 1985.

[6] U. S. NRC, *NRC Bulletin 96-03: Potential Plugging of Emergency Core Cooling Suction Strainers by Debris in Boiling Water-Reactors*, Washington, D.C., 1996.

[7] U. S. NRC, *Potential Impact of Debris Blockage on Emergency Recirculation During Design Basis Accidents At Pressurized-Water Reactors,* Washington D.C., 2004.

[8] C. Shaffer, *Knowledge Base for the Effect of Debris on Pressurized Water Reactor Emergency Core Cooling Sump Performance,* Washington, D.C.: U.S. NRC, NUREG/CR-6808, 2003.

[9] G. Zigler, *Parametric Study of the potential for BWR ECCS Striner Blockage Due to LOCA Generated Debris,* Washington, D.C.: U.S. NRC, NUREG/CR-6224, 1995.

[10] J. Dallman, *Integrated Chemical Effects Test Project: consiolidated Data Report,* Washington, D.C.: U.S. NRC, NUREG/CR-6914, 2006.

[11] M. M. Benjamin, *Water Chemistry,* New York, NY: McGraw Hill, 2000.

[12] J. P. Gustafson, *Visual MINTEQ,* www.lwr.kth.se/English/OurSoftware/vminteq/index.html.

[13] H. Kryk, *Influence of Corrosion Porcesses on the Head Loss Across ECCS Sump Strainers,* Munich, Germany: Kerntechnik, 2011.

[14] S.-J. Kim, *CHLE-019 Test Results for Chemical Effects Tests Simulating Corrosion and Precipitation (T3 & T4),* Albuquerque, NM, 2013.

[15] J. Dallman, *Integrated Chemical Effects Test Project: Test #1 Data Report,* Washington, D.C.: U. S. NRC NUREG/CR-6914, 2006.

[16] J. Dallman, *Integrated Chemical Effects Test Project: Test #2 Data Report,* Washington, D.C.: U. S. NRC NUREG/CR-6914, Vol. 3, 2006.

[17] J. Leavitt, *CHLE-014 T2 MBLOCA Test Report,* Albuquerque, NM, 2013.

[18] S.-J. Kim, *CHLE-020 Test Results for a 10-day Chemical Effects test Simulating LBLOCA Conditions (T5),* Albuquerque, NM, 2013.

[19] J. Leavitt, *CHLE-004 CHLE Equipment Description and Specifications,* Albuquerque, NM, 2012.

[20] R. C. Johns, *Small-Scale Exeriments: Effects of Chemical reactions on Debris-Bed Head Loss,* Washington, D.C.: U.S. NRC, NUREG/CR-6868, 2005.

[21] J. Piippo, *Corrosion hehavior of Zinc and Aluminum in Simulated nuclear Accident Environments,* Helsinki, Finland: Finnish Centre for Radiation and Nuclear Safety, STUK-YTO-TR 123, 1997.

[22] P. V. M. Mokaddem, *The Anodic Dissolution of Zinc and Zinc Alloys in Alkaline Solution. I. Oxide Formation on Electrogalvanized Steel,* Electrochemica Acta 7867-7875, 2010.

[23] D. Gimenez-Romero, *EQCM and EIS Studies of Zinc Electrochemical Reaction in Moderated Acid Medium,* Journal of Electroanalytical Chemistry 25-33, 2003.

[24] G. Borbely, *Removal of Zinc and Nickel Ions by Compelxation-membrane Filtration Process from Industrial Wastewater,* Desalination 218-226, 2008.

[25] M. Bethencourt, *Inhibitor Properties of "Green" Pigments for Paints,* Progress in Organic Coatings 280-287, 2003.

[26] A. C. Bastos, *Comparative electrochemical Studies of Zinc Chromate and Zinc Phosphate as Corrosion Inhibitors for Zinc,* Progress in Organic Coatings 339-350, 2005.

[27] K. Aramaki, *Preparation of Self-Healing Protective Films on a Zinc electrode Treated in a Cerium (III) Nitrate Solution and Modified with Sodium Phosphate and Cerium (III) Nitrate,* Corrosion Science 1564-1579, 2004.

[28] L. Mitchell, *CHLE-SNC-006 Bench Test Results for Series 2000 Tests for Vogtle Electric Generating Plant,* Albuquerque, NM, 2013.

[29] D. Pease, *CHLE-SNC-007 Bench Test results for Series 3000 Tests for Vogtle Electric Generating Plant,* Albuquerque, NM, 2014.

[30] D. Pease, *CHLE-SNC-015 CHLE Bench Test 2600 Series,* Albuquerque, NM, 2014.

[31] D. Pease, *CHLE-SNC-016 2800 Series CHLE Bench Test,* Albuquerque, NM, 2014.

[32] D. Pease, *CHLE-SNC-017 2900 Series CHLE Bench Test,* Albuquerque, NM, 2014.

[33] D. LaBrier, *CHLE-SNC-018 2700 Series CHLE Bench Test: Investigation of Prompt Zinc Surrogates,* Albuquerque, NM, 2014.

[34] D. Pease, *Risk-informed Resolution of GSI-191: Zinc Chemical Effects during a PWR LOCA Event,* Anaheim, CA: Transactions 2014 American nuclear Society Winter Meeting, 2014.

[35] D. Pease, *Corrosion and Solubility in a TSP-Buffered Chemical Environment Following a Loss of Coolant Acident: Part 2 - Zinc*, Submitted to Nuclear Engineering and Design (2015).

[36] L. Mitchell, *CHLE-SNC-001 Bench tetst Results for Series 1000 Tests for Vogtle Electric Generating Plant*, Albuquerque, NM, 2013.

[37] D. Pease, *CHLE-SNC-007 Bench Tests Results for Series 3000 Tests for Vogtle Electric Generating Plant*, Albuquerque, NM, 2014.

[38] S. J. Kim, *An experimental study of the corrosion and precipitation of aluminum in the presence of trisodium phosphate buffer following a loss of coolant accident (LOCA) scenario,* Nuclear Engineering and Design 282, 2015.

[39] A. Lane, *Evaluation of Post-Accident Chemical Effects in Containment Sump Fluids to Support GSI-191*, Pittsburgh, PA: Westinghouse Electric Company LLC, WCAP-16530, 2008.

[40] ASTM, *Annual Book of Standards Volume Section 3 03.02 Corrosion of Metals; Wear and Erosion*, ASTM International, 2008.

[41] K. Howe, *Corrosion and Solubility in a TSP-buffered Chemical Environment Following a Loss of Coolant Accident: Part 1 - Aluminum*, Nuclear Engineering and Design (Article in Press), 2015.

[42] C. H. Delegard, *Final Report - Evaluation of Chemical Effects Phenomena in Post-LOCA Coolant*, U.S. NRC, NUREG/CR-6988, 2008.